2013-02-14

Regulation of Higher Order Chromatin at GRIN2B and GAD1 Genetic Loci in Human and Mouse Brain: A Dissertation

Rahul Bharadwaj
University of Massachusetts Medical School

REGULATION OF HIGHER ORDER CHROMATIN AT GRIN2B AND GAD1 GENETIC LOCI IN HUMAN AND MOUSE BRAIN

A Dissertation Presented

By

RAHUL BHARADWAJ

Submitted to the Faculty of the
University of Massachusetts Graduate School of Biomedical Sciences, Worcester
in partial fulfillment of the requirements for the degree of

DOCTOR OF PHILOSOPHY

FEBRUARY 14, 2013

INTERDISCIPLINARY GRADUATE PROGRAM

REGULATION OF HIGHER ORDER CHROMATIN AT GRIN2B AND GAD1 GENE LOCI IN HUMAN AND MOUSE BRAIN

A Dissertation Presented By

Rahul Bharadwaj

The signatures of the Dissertation Defense Committee signifies completion and approval as to style and content of the Dissertation

Schahram Akbarian, Ph.D., Thesis Advisor

Kensuke Futai, Ph.D., Member of Committee

Gilles Martin, Ph.D., Member of Committee

Theodore Rasmussen, Ph.D., Member of Committee

Charles Sagerström, Ph.D., Member of Committee

The signature of the Chair of the Committee signifies that the written dissertation meets the requirements of the Dissertation Committee

Paul Gardner, Ph.D., Chair of Committee

The signature of the Dean of the Graduate School of Biomedical Sciences signifies that the student has met all graduation requirements of the School

Anthony Carruthers, Ph.D.
Dean of the Graduate School of Biomedical Sciences

Interdisciplinary Graduate Program
February 14, 2013

COPYRIGHT INFORMATION

ACKNOWLEDGEMENTS

The following collaborators made data contributions to this thesis work: Catheryne Whittle, Winfried Krueger and Theodore Rasmussen (Figures 3.3, 3.4, 4.7, 4.8), Yin Guo and Yan Jiang (Figure 3.6), Cyril Peter (Figure 4.10), Aslihan Dincer and Juerg Straubhaar (Figure 3.1, 4.1).

I would like to thank my advisor, Schahram Akbarian, for all his patience and support with standardization of novel technology. He has developed my scientific presentation skills and has given me many opportunities to represent the Akbarian Lab in front of distinguished scientists at international conferences which I have benefitted from greatly. He has also been instrumental in pioneering our bids to successfully obtain clinical samples from brain banks across the country.

Special thanks to the Dekker Lab and Nynke VanBerkum, Amartya Sanyal, Brain Lajoie and Natasha for all their advice and support in regards to my 3C assays and bioinformatics information. I am grateful to Job Dekker for allowing me to learn the 3C technique at his lab which was a critical step for my thesis project to materialize.

I thank the Gardner Lab for their support with luciferase enhancer assays and Paul Gardner for his mentoring throughout my research right from my qualifying examination to my defense.

Thanks to the Futai Lab for help with the activity-dependent cell culture system and Wenjie Mao for taking the trouble to grow the incredible difficult mice neuronal cells for me.

I must mention Cathy for all her help with the neuronal differentiation assays and thank the Rasmussen Lab, University of Connecticut, Storrs, for sharing this critical assay development protocol with us which has significantly improved my thesis data impact. Thanks to Subroto Ghose and Carol Taminga from the University of Texas, Southwestern Medical Center for all the clinical samples and background data. Thanks to Cyril for generating cell lines and helping with Western Blotting data.

Thanks to all members of my Committee (Paul Gardner, Daniel Kilpatrick, Job Dekker) for their intellectual support and belief in my project through all the meetings and progress reports. Thanks to my Dissertation Committee (Paul Gardner, Charles Sagerstrom, Kensuke Futai, Gilles Martin) for stepping up and agreeing to mentor and participate in my thesis examination.

I cannot forget all the help and support given to me by other members of the Akbarian Lab, both past and present and will always keep you in mind in a professional and personal capacity.

Isaac Houston, Nikolaos Mellios, Iris Cheung, Yin Guo – thanks for all the special moments we have shared.

I dedicate this thesis to my wife, Rujuta Narurkar for all her patience and persistence that she has transferred to me that made me get this far. Thanks to my family (mom, dad, uncles &

grandparents who have kindly assisted in many ways) and thanks to my immediate uncle and aunt and my little nephew Kishore for constantly providing me with warmth.

Jeetesh, Kartik, Ashish, Saurav….always my inner circle of trust.

I would especially like to thank all the families of patients whose samples I have processed to generate clinical data. I sincerely wish you the best and hope that research can do good for patients in future and that the Heavens offer you kindness and comfort in the memory of those whom you have lost.

ABSTRACT

Little is known about higher order chromatin structures in the human brain and their function in transcription regulation. We employed chromosome conformation capture (3C) to analyze chromatin architecture within 700 Kb surrounding the transcription start site (TSS) of the NMDA receptor and schizophrenia susceptibility gene, GRIN2B, in human and mouse cerebral cortex. Remarkably, both species showed a higher interaction between the TSS and an intronic sequence, enriched for (KRAB) Krueppel associated Box domain binding sites and selectively targeted by the (H3K9) histone 3 lysine 9 specific methyltransferase ESET/SETDB1. Transgenic mice brain cortical nuclei over-expressing Setdb1 showed increased heterochromatin-protein 1 signal at the interacting regions coupled with decreased Grin2b expression. 3C further revealed three long distant chromatin loop interactions enriched with functional enhancer specific (H3K27Ac) histone 3 lysine 27 acetylation signal in GRIN2B expressing tissue (human cortical nuclei and Human Embryonic Kidney - HEK cells). Doxycycline-induced SETDB1 over-expression decreased 2 out of 3 loop interaction frequencies suggesting a possible SETDB1-mediated transcription repression. We also report a specific looping interaction between a region 50Kb upstream of the (GAD1) Glutamic Acid Decarboxylase – 1 gene TSS and the GAD1 TSS in human brain nuclei. GAD1 catalyzes the rate limiting step in (GABA) gamma amino-butyric acid synthesis and is quintessential for inhibitory signaling in the human brain. Clinical studies in schizophrenia brain samples reveal a decreased looping interaction frequency in correspondence with a decrease in gene expression. Our findings provide evidence for the existence of transcription relevant higher order chromatin structures in human brain.

TABLE OF CONTENTS

LIST OF TAB.LES

LIST OF FIGURES

CHAPTER I

INTRODUCTION TO CHROMATIN STRUCTURE AND THE CONCEPT OF HIGHER ORDER CHROMATIN

General structure and function of chromatin

DNA is made up of nucleotides, the building blocks of life, and does not functionally exist in a naked state inside the cell nucleus. Nuclear DNA is wrapped around a histone protein octameric core, specifically, 146 base pairs of DNA are wrapped around a single histone octamer to constitute the unit nucleosome. The histone core associated with the nucleosome consists of 8 histone proteins including 2 subunits each of histone 2A, histone 2B, histone 3 and histone 4. Histone 1 is not part of the nucleosome and is the largest of the histone proteins, serving as a linker protein between nucleosomal units through its binding with other histone 1 proteins, thus offering a range of structural hierarchy options. The nucleosomal unit provides a 100-fold compaction of DNA. Specific histone amino acid residues are target sites of enzymatic modification by regulatory proteins in the nucleus. Chemical charge largely forms the basis for DNA-histone associations. Histones harbor an overall positive charge due to the presence of basic amino acid residue side chains (lysine, arginine) while DNA has a negative charge due to the phosphate residues of nucleotides (each nucleotide = sugar + nitrogen base + phosphate residue). DNA and histones interact directly with many regulatory protein complexes and together, form chromatin. Chromatin consists of two types of proteins: non-histone proteins and the histones. The cell has the daunting task of accommodating roughly 2-meters of DNA into a 2-micron diameter nucleus necessitating a $10^{\wedge 6}$ degree of

compaction! As mentioned above, the degree of compaction offered by nucleosomal units are only 1000-fold. Chromatin still needs to be 1000-fold more compacted which can only be achieved by further structural constraints. However, random folding is not an option due to the necessity for specific regulation of gene expression. Only 1% of the genome is expressed and transcriptional protein machinery needs access to the gene transcription start sites (TSS) in order for a gene to be transcribed (International Human Genome Sequencing Consortium., 2004). Furthermore, induced gene expression makes transcription regulation even more complex and involves many groups of protein factors and co-factors that functionally integrate to activate or repress the expression of a single gene. Besides gene expression, there is the essential function of gene replication and segregation into daughter cells that requires a high degree of packaging and compaction in a very short temporal frame. These structural and functional roles make chromatin a highly dynamic ensemble.

Post-translational modifications on histone proteins influence chromatin structure

Chromatin exists in different structural states depending on specific biochemical modifications made to DNA nucleotides, histones and the regulatory protein complexes (Gavin DP, Akbarian S, 2012). Chemical modifications include the transfer to or removal of methyl, acetyl and phosphoryl groups on specific amino acid residues of histone protein tails. The general mechanistic change that these modifications achieve are the addition or removal of charges that alter the degree of chemical association between histones and DNA rendering specific sites on DNA or along the genome more accessible through local dissociation of the DNA-histone complex or less accessible through

stronger association of the DNA-histone complex. Chromatin that is involved in active or induced transcription is called euchromatin while chromatin that is involved in very little or no transcription is called heterochromatin and is highly condensed with specific heterochromatin proteins. Heterochromatin proteins are enriched at specific histone modification sites, for example, Heterochromatin Protein 1 (HP 1) at histone 3 lysine 9 tri-methyl (H3K9me3) residues (Schultz DC et al., 2002). Chemical histone modifications are capable of altering the electrovalent DNA-histone associations. For example, histone acetylation adds a negative charge ($-CH3COO^{-1}$) and de-acetylation removes one negative charge whereas the methylation of basic amino acid side chains (lysine, arginine) neutralizes the positive charge on histones. To illustrate different histone modifications and their association with transcriptional activation and silencing, below are two figures providing a mechanistic and functional correlation between histone modifications, chromatin state and gene expression **(Figures 1.1, 1.2)**

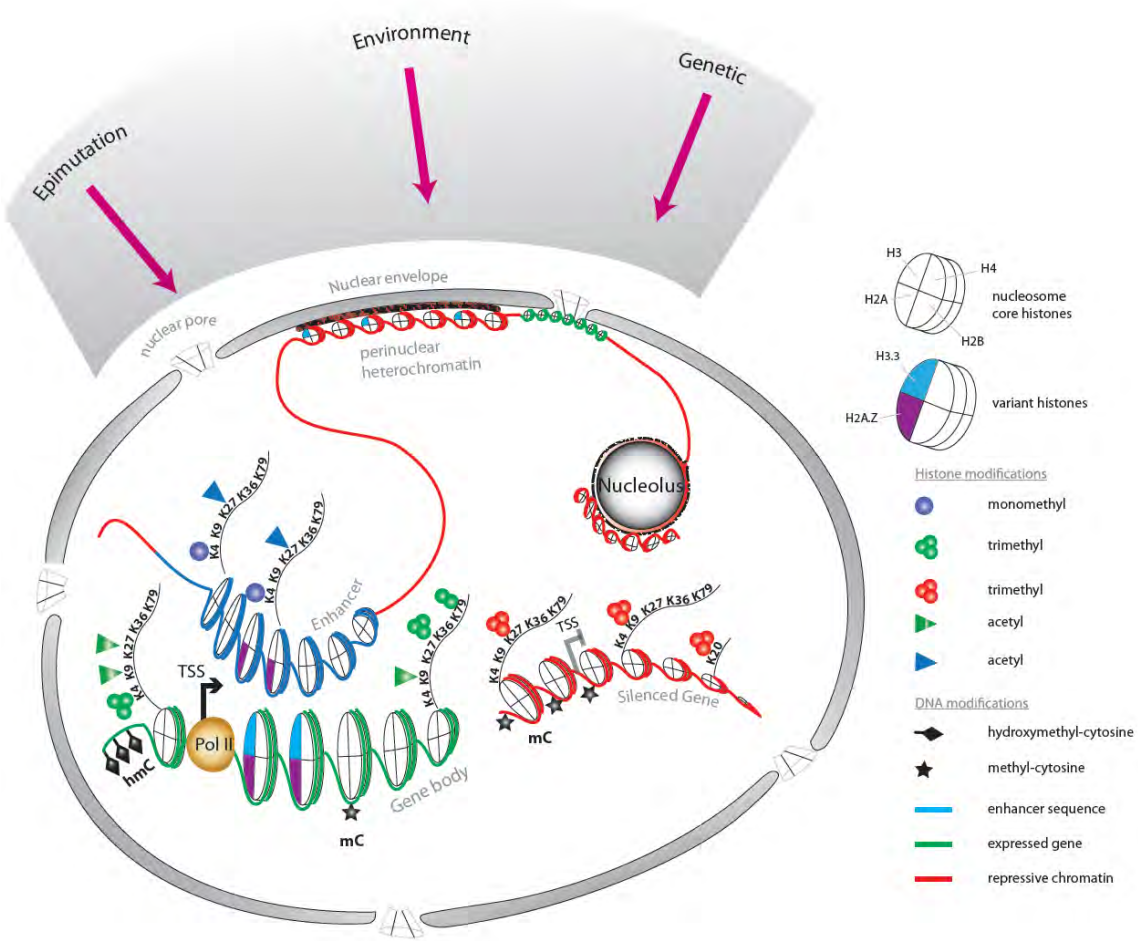
Environment
Epimutation
Genetic
Nuclear envelope
nuclear pore
perinuclear
heterochromatin
Nucleolus
Enhancer
TSS
Pol II
hmC
mC
Gene body
Silenced Gene
H3
H4
H2A
H2B
nucleosome
core histones
H3.3
H2A.Z
variant histones
Histone modifications
monomethyl
trimethyl
trimethyl
acetyl
acetyl
DNA modifications
hydroxymethyl-cytosine
methyl-cytosine
enhancer sequence
expressed gene
repressive chromatin

Fig.1.1 Overview of the nucleosome structure, histone modifications and signaling - induced gene expression regulation
The figure is a simple representation of the nucleosome structure on the top right followed by a list of histone modifications and DNA modifications. The figure shows the many histone lysine (K) modifications at specific positions and the association of these modifications with an expressed gene (green) or a silenced gene (red). Gene expression or silencing is inducible and can occur as a consequence of signaling pathways activating downstream regulatory protein complexes.

Bharadwaj et al., 'Epigenetics in the Nervous System', (2012)

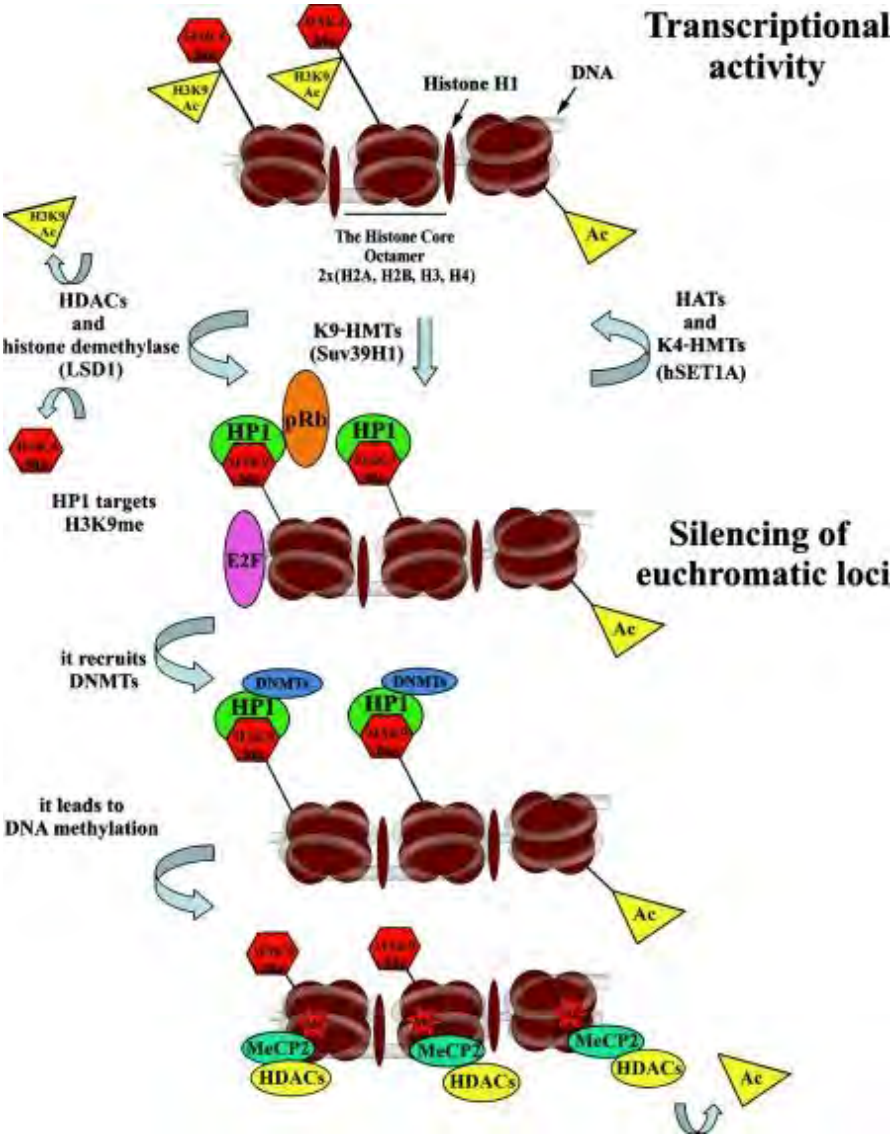
Transcriptional activity
Histone H1
DNA
H3K9 Ac
H3K9 Ac
Ac
The Histone Core Octamer 2x(H2A, H2B, H3, H4)
HDACs and histone demethylase (LSD1)
K9-HMTs (Suv39H1)
HATs and K4-HMTs (hSET1A)
HP1
pRb
HP1
HP1 targets H3K9me
E2F
Silencing of euchromatic loci
Ac
it recruits DNMTs
DNMTs
DNMTs
HP1
HP1
it leads to DNA methylation
Ac
MeCP2
HDACs
MeCP2
HDACs
MeCP2
HDACs
Ac

Fig1.2. Interplay between histone modifications and transcriptional states
The figure nicely describes the model of transitioning from transcriptionally active chromatin to silenced chromatin via the action of specific groups of histone modifying enzymes that generate histone modifications associated with these different chromatin states in the context of gene regulation. (Ac – Acetylation), HP1 – Heterochromatin Protein1, H3K9 – Histone 3 Lysine 9, HMT – Histone Methyl Transferase, DNMT – DNA methyl transferase, MeCP2- methyl CpG binding protein -2, HDAC – Histone De-Acetylase.

Eva Bártová, et al, 2008.

(H3K9Ac) Acetylated Histone 3 Lysine 9 and (H3K4me3) trimethyl Histone 3 Lysine 4 associate with the transcriptionally active chromatin state of the mammalian genome. Histone acetylation is brought about by histone acetyl transferases (HATs) while histone deacetylases (HDACs; classes I, II, III) de-acetylate histones. H3K4 methylation is facilitated by specific histone methylases while de-methylation is done by histone demethylases, which leads to the activation of (K9-HMT) Lysine 9- Histone MethylTransferase which mediates H3K9 methylation. The chromodomain of the HP1 recognizes H3K9(me)3 and renders chromatin silenced. Transcriptional co-repressors, such as retinoblastoma protein pRb, tend to stabilize HP1 binding to regional H3K9 methylation. In the final step below, DNA methyltransferases (DNMTs) are activated, leading to DNA methylation of 5-cytosine residues. Methylated DNA is consequently recognized by methyl-DNA-binding proteins, such as MeCP2, which can combine with HDAC activity to increase methylation and decrease acetylation on histones.

There are many classes of histone modifying enzymes and there can be a redundancy in the enzymes that modify a specific histone target but generally, histone modifying enzymes have very specific target histone residues. Histone residues are stable and can be maintained in isolated nuclei from tissue or cells (Huang HS et al., 2006). Using a combination of techniques such as flow cytometry and chromatin immunoprecipitation, it is possible to identify specific histone modifications from specific cell populations and the gene promoters they are present at. This extends the biological significance of associating transcriptionally active or repressed chromatin states with histone modifications to a clinical context where it is possible to identify and semi-quantify the

histone modification signals at specific disease candidate genes from diseased tissue samples and compare against matched normal tissue samples to achieve mechanistic insight into disease from a diagnostic standpoint. Matching chromatin states with gene expression levels in response to drug treatment can also help identify possible genetic targets for epigenetic drugs (Huang HS et al., 2007, Dong E et al., 2007).

The study of the regulation of gene expression is complex and involves understanding the integration of a multitude of signaling pathways. There are many regulatory protein complexes that operate as downstream effectors of signaling. These protein complexes vary in composition and number and are capable of a multitude of functions such as the recognition of specific DNA sequence binding motifs, the recruitment of other proteins that function as co-factors and the recruitment of histone modifying enzymes, all of which play significant roles in the regulation of mammalian gene expression.

Long range chromosomal interactions and their impact on gene expression

Basically speaking, one might think of the gene promoter or transcription start site (TSS) as the penultimate location that the gene expression regulatory mechanisms target. This is true to some extent. Transcription initiation is facilitated via the integrated actions of protein transcription factors, effectors and mediators interacting with transcription protein machinery to facilitate stable assembly of the transcription initiation complex. This is followed by the synthesis of messenger RNA transcript complementary to the DNA sequence of the coding strand. There are many regulatory elements with specific DNA binding sequence motifs for transcription factor protein complexes present within a few (kilobase pairs) Kb of the gene TSS and generally located upstream. In recent times, with

the advent of technologies seeking to probe chromatin structure, researchers have also reported the existence of regulatory elements that can either enhance or repress specific gene transcription levels and are located several hundreds of Kb away from the TSS (Dekker, 2008). It has been shown that these elements are in physical contact with the gene TSS (Vakoc CR et al., 2005). This physical interaction between any element and gene TSS is thought to be brought about by transcription factors with binding motifs located within the element and the gene TSS and the remaining in-between non-interacting part of chromatin looping out. If one takes a step back to envision a specific regulatory element interacting with the gene TSS in the context of higher order chromatin packaging structure within the nucleus, this is obviously a daunting task and demands a high level of specificity. Add on the complexity brought forth by induced gene expression and the fact that many of these structures are transient by nature and we can only start to guess the complex protein machinery that needs to be involved to enable this type of highly specific but transient chromatin dynamics. The first step would be to capture these chromatin structures as they are in nature and the next step would be the functional analysis of these structures from a transcription regulation and an epigenetic characterization angle. Capturing these structures also makes it tricky since they are transient and it may be very hard to obtain a cell culture population where all the cells in a petri-dish have the same structure at the same time at the same genetic location. Therefore, purely qualitative approaches, even with a tremendous attention to detail and specificity will still make it very tedious to identify these structures and couple this identification with gene expression or epigenetic analysis. A great approach that can

actually render results, albeit in a semi-quantitative manner, is the technique called chromosome conformation capture (3C) **(Figure 1.3)** that can measure the physical interaction frequency between any two regions across the genome simultaneously matching these interaction frequency maps to gene expression and epigenetic characterization of cells or tissue in the same batch or sample. An illustration of the yeast genome generated on the basis of 3C results across the genome gives an idea of the power of this technique **(Figure 1.4)**.

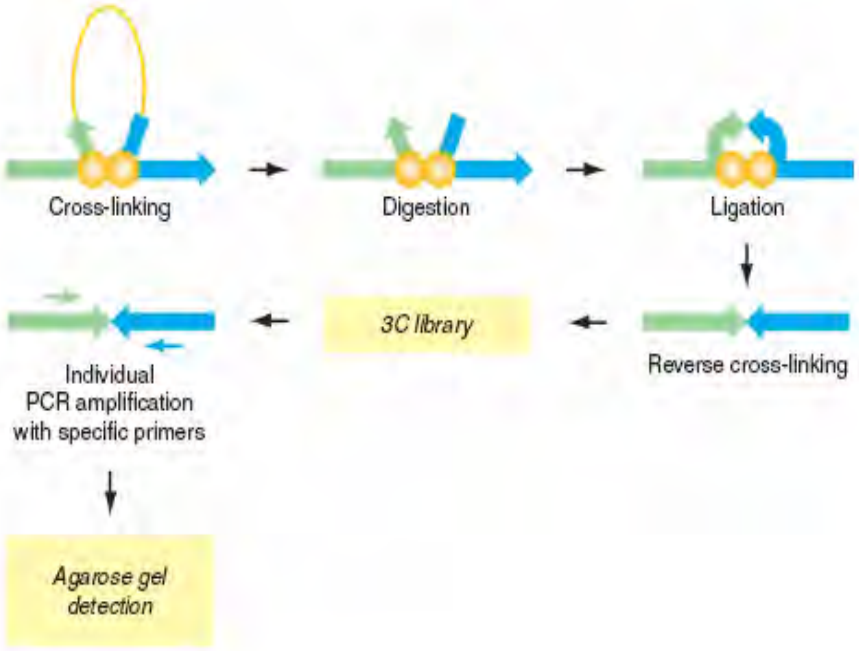
Cross-linking
Digestion
Ligation
Reverse cross-linking
3C library
Individual
PCR amplification
with specific primers
Agarose gel
detection

Fig1.3. Overview of the chromosome conformation capture technique
The technique basically involves 4 steps: (i) Cross-linking and harvesting of cells or tissue material for analysis (ii) Restriction digestion of cross-linked chromatin (iii) Ligation of the restriction fragments at low sample concentrations to promote higher levels of ligation between interacting restriction fragments along the genome (iv)Reverse cross-linking followed by isolation of the ligated fragments to obtain a 3C library.
The quantification part of the technique involves 3 steps: (i) Design of 3C-PCR primers with specific parameters (protocols section) (ii) PCR detection of interacting fragments amplified across ligation junctions on a gel (iii) Quantification of specific PCR product bands using imaging software followed by plotting pixel intensity (interaction frequency) versus genomic location of primers on a graph to determine higher interaction frequency (peak) signals at primer specified genomic locations.

Dostie J, Dekker J, 2007

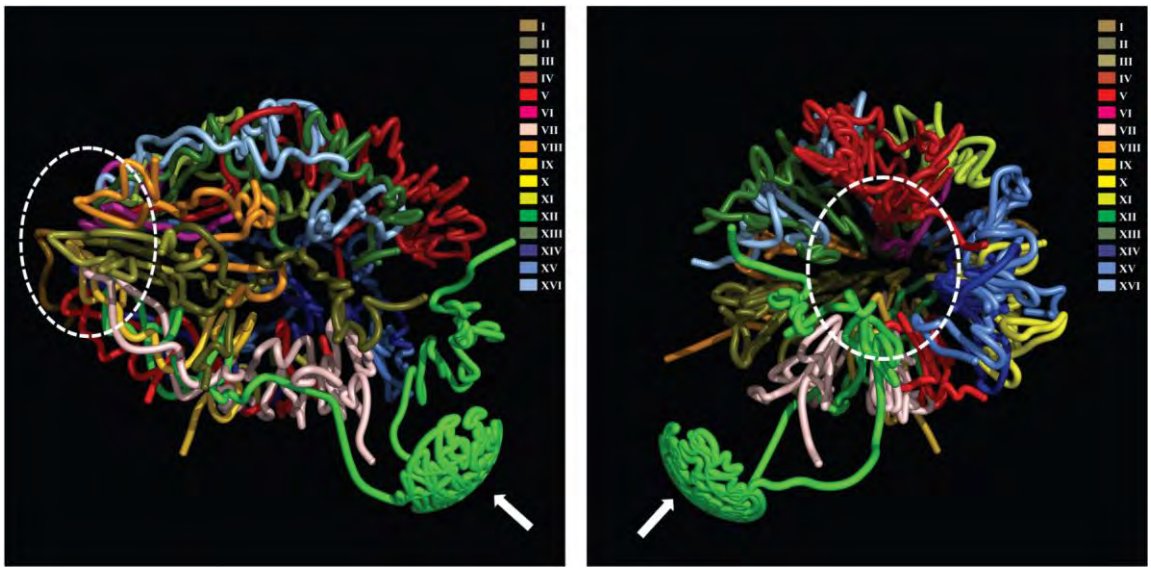
I
II
III
IV
V
VI
VII
VIII
IX
X
XI
XII
XIII
XIV
XV
XVI

Fig1.4. Three-dimensional model of the yeast genome using the 3C technique
Chromosomal color code is as indicated in the upper right of each figure. All chromosomes cluster via centromeres at one pole of the nucleus indicated by the dashed oval region to give a structured array of chromosomes at one end of the yeast nucleus (Duan.Z et al., 2010). The structured array has to allow for the functional expression of genes which makes specific gene TSS the centers of activity. Little is known about the higher order structure of the mammalian genome and research has only just begun to understand the functional implications of these chromatin structures. These structures, that are proposed to generate the chromosomal loops, can potentially span several hundred kilobases (Kb) of genetic material.

Duan.Z et al., 2010

Molecular approaches to probing chromatin architecture

Presently, the area of epigenetics is growing rapidly with techniques like chromosome conformation capture (3C) and high throughput deep sequencing that enable scientists to associate complex chromatin structures with specific genetic sequences that are known targets of regulatory protein complexes. 3C data provide a semi-quantitative measure of interaction frequencies between any two regions across the genome. Interaction frequency maps, spanning hundreds of Kb, are constructed for specific genomic co-ordinates and are used to generate a three dimensional map explaining the physical architecture of specific regions of the genome. This structure probing capability of 3C has helped it evolve as a leader in technology focused on understanding complex chromatin structures and the mechanism by which they regulate gene expression. In an attempt to functionally characterize the molecular regulators of chromatin remodeling and thereby, gene expression, technologies combining (ChIP) Chromatin Immunoprecipitation, deep sequencing and microarray hybridization, have identified sequence specific binding sites across the genome for many regulatory protein complexes. These binding site sequences are dispersed throughout the genome and are of considerable interest from transcription regulation and clinical diagnostic standpoints. My research has sought to use a combination of the above techniques to understand how histone modification signals at distant sequences can influence gene transcription via complex or higher order chromatin structures that brings these distant sequences together in close interaction with the gene TSS to influence gene transcript levels. The table **(Table.1.1)** below is an overview of some techniques used routinely to probe chromatin structure and function.

Table 1.1 Overview of techniques used routinely to probe chromatin structure and function

NAME OF TECHNIQUE	APPLICATIONS
DNA Sequencing Based Approaches	
Bisulfite sequencing	Methylated cytosine (C) residues in DNA are converted by bisulfite treatment to uracil (U) providing a chemical basis for distinguishing between methylated versus non-methylated C residues via sequencing analysis. Barring limitations such as the incomplete chemical conversion of methylated C and DNA degradation during the chemical process of hydrolytic amination, bisulfite sequencing is a standard qualitative test to identify methylated cytosine, which is known to affect gene transcription regulation. (Clark SJ et al., 1994)
Hydroxymethyl cytosine sequencing	Immunoprecipitation of hydroxy-methyl cytosine residues coupled with sequencing identifies DNA sequences previously thought to have methylated cytosines. Biological and functional significance of hydroxymethyl cytosine residues are being unraveled and are generally centered around chromatin remodelling and gene regulation. Interestingly, higher levels of hydroxymethyl cytosine are found in CNS neurons. (Münzel M et al., 2010)
Chromatin Immunoprecipitation Based Approaches	
Native or Cross linked ChIP (Chromatin	Cross-linking ChIP is used to

Immunoprecipitation) combined with PCR / Sequencing / microarray chip.	identify DNA sequences from across the genome that are associated with specific proteins (e.g. transcription factors or co-factors) and employs a cross-linking agent such as formaldehyde to fix protein-protein and protein-DNA interactions. (Min-Hao Kuo, C.David Allis,1999) Native ChIP analyzes DNA sequences associated with specific protein modifications (e.g. histone methylation, acetylation and other post-translational chromatin protein modifications) and is coupled with enzymatic (e.g. micrococcal nuclease) digestion to facilitate downstream sequencing analysis. ChIP data generate a better understanding of (i) transcription factor and co-factor target sites across the genome, (ii) genomic locations of specific histone modifications and their relation to transcription regulation and chromatin structure and (iii) identification of putative regulatory regions located hundreds of Kb away from the promoter in intronic or intergenic sequences. (Thorne AW et al., 2004)
Chromosome Conformation Capture Based Approaches	
3C (Chromosome Conformation Capture)	3C semi-quantitatively measures physical interaction frequency between any two regions of the chromosome giving an idea of higher order chromatin structures that may influence transcription

	regulation or play a structurally supportive role in chromatin organization. Technique is adapted for analysis of chromatin architecture over distances ranging from 20 - 500 Kb. (Miele A, Dekker J, 2009)
5C (Chromosome Conformation Capture Carbon Copy)	5C is an extension of the 3C technique, where the 3C library is amplified using universal PCR followed by high throughput sequencing enabling measurement of interaction frequencies at longer ranges across the genome. 5C analysis can identify more global order chromatin structures such as transcription regulation factories. Dostie J, Dekker J, 2007
ChIA-PET (Chromatin interaction analysis with paired-end tag sequencing)	ChIA-PET is a technique that couples chromatin immunoprecipitation with 3C technology followed by deep sequencing thereby quantifying interaction frequencies between specific protein associated regions across the genome. This is very useful for analysis of higher order chromatin structures associated with and/or mediated by histone modifications or chromatin proteins immunoprecipitated. (Li G et al., 2010)

Chapter II

SCHIZOPHRENIA: A NEED FOR MOLECULAR MARKERS

Inhibitory neurotransmission in the mammalian brain

Gamma amino-butyric acid (GABA) is the principal inhibitory neurotransmitter in the adult mammalian brain (Akbarian.S et al., 2006). GABA inhibits the post-synaptic neuron from generating an action potential thereby facilitating inhibitory chemical signaling in the brain. GABA is also implicated in neurodevelopment (Represa, A, Ben-Ari Y, 2005; Tozuka, Y et al., 2005; Ge, S et al., 2006). Given the all important role played by GABA in inhibitory signaling in the mammalian brain, it follows that there are deleterious consequences of GABA level changes in neurodevelopment, behavior and thereby, nervous system function. One can better appreciate this by considering the role played by cortical inhibition in the mammalian brain. Cortical inhibition broadly refers to the inhibitory activity of GABAergic interneurons present in the cortex. They attenuate the activity or firing of other neurons and promote the firing of specific neurons to bring about a particular output. Taken in a very simplified context, in order to perform a specific task and focus, the brain has to inhibit responses to other stimuli and promote the activation of a specific group of neurons that are involved in or necessary for executing a particular task. This is a very basic example of the role of inhibitory signaling function in the mammalian brain. Extrapolating from this example, cortical inhibition plays a role in many functions, examples of which include attenuating excitatory neurotransmission thereby preventing seizures, facilitating neural plasticity to promote learning of new skills and applications thereof and in performing newly learnt tasks and drawing on experience

to perform them more effectively with time as in memory, to name a few. Deficits in learning and memory and attention span due to a lack of cortical inhibition are observed in nervous system disorders including schizophrenia and bipolar affective disorder (Daskalakis et al. 2007). Strong evidence implicating a lack of cortical inhibition in schizophrenia came from studies showing a 15 – 20% decrease in cortical interneuron cell counts (interneurons form a majority of the inhibitory neuronal population in cortical layers II – IV; Benes and Beretta, 2001) in postmortem schizophrenic brain. Another strong basis supporting a decrease in the inhibitory interneuronal population in the cortex of schizophrenic brain has been inferred from the decrease in reelin in cortical layers I and II. Reelin is a protein secreted by the Cajal Retzius interneurons and is thought to play a role in cortical lamination and influences synaptic plasticity and neuronal migration. In a recent study done to evaluate the levels of reelin mRNA in the schizophrenia cortex, hippocampal and thalamic regions, the left prefrontal area of schizophrenia patients revealed a decreased expression of reelin-mRNA of 29.1% in the white ($p = 0.022$) and 13.6% in the gray matter ($p = 0.007$) compared to the control group. None of the other regions examined showed any statistically significant differences and the sample size was small (12 schizophrenic cases compared to 13 normal samples, (Habl, G et al. 2012). Another indirect mechanism of decreasing cortical inhibitory modulation implicated in schizophrenia involves the shift of inhibitory dopaminergic input from excitatory pyramidal neurons to inhibitory interneurons in the cortex (Benes et al., 1997). Therefore, inhibition of inhibitory interneurons results in greater cortical excitability overall. Lastly, the biological significance of cortical

inhibition and GABAergic signaling is evident in the role that it plays in neural plasticity, a key process necessary for adaptation and survival. Latent cortical connectivity is modulated based on environmental cues that an individual experiences and this modifies the individual's response accordingly, to the local environmental stimuli. Support for this theory stems from the finding that GABAergic antagonist administration to rats resulted in a reorganization of cortical layers and enhanced intracortical connectivity thereby greatly reducing the relaying of information through the cortex and limiting the ability of the animal to respond to external stimulus compared to normal rats (Jacobs et al.1991).

Schizophrenia – symptoms and possible associated brain regions

Schizophrenia is a complex genetic disorder with multiple risk gene candidates. There is evidence for an epigenetic basis with the association of copy number variants and single nucleotide polymorphisms at specific genetic loci and schizophrenia occurrence. The prevalence is 1% with an age of onset ranging from the early teens to late twenties. Schizophrenia is characterized by a variety of symptoms broadly classified into positive, negative and cognitive symptoms. Positive symptoms of schizophrenia include auditory and visual hallucinations, delusional beliefs, thought and consequently speech disorganization and dysfunction and lastly, movement disorders, which could either be repetitive movements or in certain rare cases, 'catatonia', which is a total loss of movement and response to stimulus. Negative symptoms of schizophrenia are generally prolonged, lasting from months to years and significantly impair an individual's lifestyle and ability to function in a society. They include a variety of behavioral and emotional disruptions and overlap with symptoms associated with depression. Symptoms include a

lack of pleasure associated with everyday life (anhedonia), a lack of ability to carry out planned or complex activities, apathetic speech and facial expression and a neglect of self with regards to hygiene or health. Cognitive symptoms are very hard to notice and are often estimated with the help of tests that focus on gauging the cognitive abilities of a normal individual. They include decreased attention span and a problem with focusing, decreased ability to learn information quickly and apply it (working memory deficit) and a general decrease in 'executive functioning' and decision making capability. Negative and cognitive symptoms associated with schizophrenia make it difficult to lead a normal and functional life and cause great emotional distress to the individual. Due to a lack of absolute association of molecular biomarkers with the disease, diagnosis is based upon behavioral and cognitive tests as stipulated in the (DSM-IV) Diagnostic and Statistical Manual of Mental Disorders, making the process of diagnosis of this disorder difficult clinically and emotionally painful for the patient and immediate family. There is definitely a need for research into disease mechanism and the establishment of molecular markers with the occurrence of schizophrenia. However, the complexity in understanding schizophrenia persists with the possibility of the association of many different brain regions being involved. The proposal for the involvement of specific brain regions is based on performing imaging techniques and matching the results with specific symptoms. For example, (PET) Positron Emission Tomography scans performed in individuals experiencing visual and auditory hallucinations have revealed that there is a general activation of the thalamic and striatal nuclei and of the orbitofrontal cortex, the cingulate cortex and the hippocampus (Silbersweig et al., 1995). Functional

neuroanatomical imaging studies have also shown that the basal ganglia receive input from and project to the inferotemporal and frontal cortex, thus potentially playing a role in higher order visual processing. This evidence fits nicely with the fact that patients receiving L-Dopa treatment frequently experience visual hallucinations as a side effect (Middleton et al., 2002). Since the basal ganglia receive input from widespread areas of the cerebral cortex, including the frontal, parietal and temporal cortices, input from these regions as well could contribute to some of the positive symptoms of schizophrenia.

Some schizophrenia symptoms may be associated with dopaminergic transmission

Another theory that implicates specific neural circuitry in the possible pathology of schizophrenia is based on the use of antipsychotics, typical and atypical, in the treatment of positive symptoms of schizophrenia. General antipsychotics prescribed are dopaminergic receptor antagonists, therefore implying that the excessive stimulation of dopaminergic pathways may account for some of the symptoms seen in schizophrenia. Besides, it must be noted that typical antipsychotics have affinity for dopamine receptor class D2 (inhibits adenylyl cyclase downstream) while the atypical antipsychotics have affinity for classes D3 and D4 (inhibit adenylyl cyclase downstream). There is a difference in the distribution of these classes of receptors in the brain. Notably, a couple of dopaminergic systems, the meso-cortical system, mainly projecting to the pre-frontal cortex (brain region associated with motivation, planning, attention and social behavior), and the meso-limbic circuit, projecting to different components of the limbic system including the amygdala, the hippocampus, entorhinal cortex, medial frontal cortex and anterior cingulate cortex (areas involved in emotions and memory processing), are

thought to be playing a significant role in causing schizophrenia symptoms (Weinberger et al., 1987). The meso-cortical system seems to play a more significant role in negative symptoms while the meso-limbic circuit is more likely to play a role in positive symptoms associated with schizophrenia. Interestingly, typical antipsychotics are effective in allaying the positive symptoms of schizophrenia while the atypical antipsychotics are more effective in treating the negative and cognitive symptoms of schizophrenia. Other antipsychotic targets include inhibiting many steps of the dopamine signaling pathway, including the inhibition of tyrosine hydroxylase and interference with the vesicular storage of dopamine. Due to the complexities arising from the number of brain regions and neuronal circuits that could possibly be involved in schizophrenia etiology, there are also a number of molecular targets that function in signaling between different groups of neurons within and across these brain regions and neuronal systems. Hence, there is a great need for a more robust establishment of clinical biomarkers to assist in the diagnosis of schizophrenia, currently performed with the help of criteria as specified by the DSM – IV.

Epigenetic alterations in psychiatry: focus on schizophrenia

Schizophrenia is a major psychiatric disorder affecting 1% of the general population, often with onset in young-adult years but at least in some patients subtle, cognitive and neurological deficits precede the full blown syndrome for many years (Jarskog LF et al., 2007). The disease is viewed as highly heterogeneous in terms of genetics, and is primarily defined by partially independent symptom complexes as described in the section on symptoms. Currently prescribed antipsychotics, which are mainly aimed at

dopaminergic and/or serotonergic receptor systems, exert therapeutic effects on psychosis in approximately 75% of patients but often do not adequately address the cognitive impairment which is a potentially disabling feature of schizophrenia . Currently there are no established pharmacological treatments for this symptom complex. Cognitive dysfunction is an important predictor for long-term outcome, and therefore this area is considered a high priority in schizophrenia research and gave rise to cross-institutional initiatives such as (*Measurement and Treatment Research to Improve Cognition in Schizophrenia*) MATRICS (Ibrahim HM et al., 2010).

Autism is primarily a disorder of social communication and interaction with onset in early childhood often prior to age 3, and occurs with or without deficits in speech and language, repetitive behaviors and a host of other neurological symptoms. Treatment is largely symptomatic, and the social core deficits are poorly addressed by current psychoactive drugs (Canitano R., 2011). Schizophrenia and autism show similarities in their genetic risk architecture, including a significant overlap in certain copy number and other rare structural DNA variants that carry high disease penetrance (Cichon S et al., 2009; Sebat J et al., 2009; Weiss LA et al., 2009). The etiology of both schizophrenia and autism is complex but defects in pre- and early postnatal neurodevelopment, including adverse influences such as maternal infection and malnutrition are thought to play an important role in a substantial portion of cases (Brown AS et al., 2010). Furthermore, according to some studies, there is a striking contribution of 'environmental' factors, as evidence by a highly significant shared risk even in dizygotic twins, which is only slightly less than the shared disease risk in monozygotic twin pairs (Hallmayer J et al.,

2011).

Epigenetic studies in postmortem brain tissue of subjects with schizophrenia

Given the prominent role of neurodevelopmental theories in the etiology of schizophrenia, it seems not too surprising that the early wave of epigenetic studies in schizophrenia postmortem brain was focused on candidate genes with a critical role in neurodevelopment such as the glycoprotein REELIN important for migration and positioning of young neurons (Abdolmaleky HM et al., 2005), the transcription factor SOX10, which orchestrates transcription in myelin-producing oligodendrocytes (Iwamoto K et al., 2005) and the 67 Kda glutamic acid decarboxylase (GAD67/GAD67) GABA synthesis enzyme that is essential for proper formation of inhibitory neuronal circuitry. These studies, taken together, indeed suggest that some subjects on the psychosis spectrum are affected by subtle DNA methylation and histone acetylation and methylation changes at the promoters of these and various other genes. Moreover, the DNA methylation and histone modification markings at REELIN, GAD67, BDNF (brain derived neurotrophic factor) and other genes with key regulatory roleS during development are highly regulated in human cerebral cortex during the course of development and aging, including positive correlations between age and DNA methylation (REELIN, GAD67) (Straub RE et al., 2007) and a decline in GAD67-associated histone acetylation in older brains (Tang B et al., 2011). Consistent with such wide windows of epigenetic vulnerability, robust differences in the trajectories of age-associated DNA methylation and histone modifications emerge when disease versus control groups are compared, even with fairly limited cohort sizes of a few dozen brains

or less. Indeed, some of the observed epigenetic changes in schizophrenia postmortem brain may have little to do with the etiology of disease but simply could reflect differences in lifestyles and diet or medication effectS, because it becomes increasingly clear that exposure to alcohol, nicotine, psychostimulant and antipsychotic drugs, and many other external and internal factors affect brain DNA methylation and histone modifications.

Complicating matters further, many of the observed epigenetic alterations in chromatin surrounding the aforementioned candidate gene studies in cerebral cortex of subjects with schizophrenia are comparatively subtle, with only a small subset of CpG dinucleotides (or nucleosomes in case of histone modifications) at specific gene promoters showing significant changes on the group level. These are unlikely to be experimental artifacts related to the idiosyncrasies of postmortem brain with its hosts of confounds related to autolysis process or cause of death etc., because promoter DNA methylation changes in hippocampus of rats exposed to different rearing conditions are equally selective for specific sets of CpGs of, for example, the aforementioned *GAD67* gene (Zhang TY et al., 2010). Similarly, more extensive genome-wide surveys for differential DNA methylation at thousands of CpG islands revealed approximately 100 loci with differential methylation between subjects on the psychosis spectrum and controls, but the magnitude of change was comparatively subtle, such as 17% vs. 25% for the *WD Repeat Domain 18* (*WDR18*) as one of the most significantly changed genes (Mill J et al., 2008). These changes in chronic neuropsychiatric disease then appear much more subtle when compared to the several fold (>100%) increases (or decreases) in

DNA methylation at tumor suppressors and other genes epigenetically implicated in gliomas , neuroectodermal tumors (Alaminos M et al., 2005) and many other cancers in the CNS or peripheral tissues. Given the subtle nature of the observed epigenetic changes on the group level (patients versus controls), the uncertainties whether such type of alteration is 'state or trait' and related to the disease process as opposed to some unrelated and perhaps even irrelevant environmental factor, the reader may start to wonder at this point whether there is indeed any scientific merit to study epigenetics in diseased (brain) tissue!

To answer such skepticism, we would argue that chromatin studies in human brain, when combined with genetic approaches, are likely to provide very meaningful insights into the mechanisms of disease of individual cases and may offer a way forward from current approaches in the field that are merely based on uncovering significant differences on the group level. Notably, DNA methylation analyses in blood chromatin collected across 3 generations from the same pedigrees provided evidence that at some loci, more than 92% of the differences in methylcytosine load between alleles is explained by haplotype, suggesting a dominant role of genetic variation in the establishment of epigenetic markings, as opposed to environmental influences (Gertz J et al., 2011). Furthermore, in the human cerebral and cerebellar cortices, methylation of several hundred CpG enriched sequences is significantly affected by genetic variations, including single nucleotide polymorphisms (SNPs) separated from the CpG site by more than one megabase and an even larger number of SNPs 'drive' between-subject gene expression differences in the prefrontal cortex (Colantuoni C et al., 2011). Extrapolating

from these general findings then, it is very likely that genotype is a critical variable in the context of epigenetic (dys)regulation and gene expression changes in schizophrenia brain. Therefore, we predict that the intersection between epigenetic dysregulation and genetic variation will turn out to be very important for a large number of psychiatric susceptibility genes. An early example is provided by the proximal promoter of the already mentioned GAD67 gene (encoding the 67 Kda glutamic acid decarboxylase GABA synthesis enzyme). There is evidence that the decline in GAD67 RNA and protein—which has been reported in ~20 postmortem studies on cerebral cortex of subjects with schizophrenia and related disease (Costa E et al., 2004)— is accompanied by a deficit in GAD67 promoter-associated open chromatin-associated histone methylation, including H3K4me3. However, these features appear not to be consistently present in all the clinical samples, but instead may occur mainly in conjunction with a specific haplotype, comprised of multiple SNPs, spanning ± 3Kb from the GAD67 transcription start site (Huang HS et al., 2007). Interestingly, subjects with schizophrenia biallelic for the risk haplotype not only show decreased H3K4me3, but also an increased level of H3K27me3 (Huang HS et al., 2007), a mark regulated by repressive Polycomb group chromatin remodeling complexes associated with inhibition of transcription. Furthermore, some of the same polymorphisms around the GAD67 promoter were previously associated with schizophrenia and accelerated loss of frontal lobe gray matter and emerged as genetic determinants for cognitive performance in an epistatic interaction with common variants of the Catechyl-O-Methyltransferase (COMT) gene, which regulates monoamine metabolism and signaling (Marenco S et al., 2010). Therefore, at

least 3 layers of epigenetic regulation emerge for the GAD67 promoter (i) a developmentally regulated increase during the extended course of prefrontal maturation for the first 2 decades of postnatal life, (ii) common polymorphisms around the GAD67 promoter, which in susceptible individuals diagnosed with schizophrenia are associated with a shift in open and repressive chromatin-associated histone modifications and (iii) a subset of antipsychotic and mood-stabilizer drugs, including clozapine and valproate, up-regulate transcription-associated histone methylation and acetylation at the *GAD67* promoter (Huang HS et al., 2007) . Thus, as illustrated by the *GAD67* example, which probably is representative for the large pool of 'common variant, small contribution to disease risk' schizophrenia candidate genes, a complex pathophysiology exists with multiple, independent determinants converging on the same epigenetic phenotypes in diseased brain tissue.

One possible molecular basis

As mentioned before, there is a suggestive link between a decrease in cortical inhibition and some symptoms associated with schizophrenia. Evidence has also been published to suggest that GABAergic activity is decreased in the schizophrenic brain (Lewis D.A. 2000). Are there any molecular biomarkers that are known to function in cortical inhibition and be associated with schizophrenia? The GABAergic pathway has many molecular components that could contribute in part to the decrease in GABAergic activity and consequently, cortical inhibition. Of the many proteins that function in the GABAergic pathway, GAD is an attractive candidate since the enzyme catalyzes the rate limiting step in the process of GABA synthesis via the decarboxylation of glutamate to

GABA. It should be noted that GABA is synthesized by two isoforms of GAD; GAD67 (67kDa) and GAD65 (65kDa). GABA that is present in neuronal vesicles and functions as a neurotransmitter, is thought to come from cytoplasmic 2-oxoketoglutarate, an intermediate molecular product of the TCA (Tri-Carboxylic Acid) cycle. 2-oxoketoglutarate is converted to glutamate and decarboxylated to GABA by GAD. It has already been established from animal studies that GAD67 is an exclusive marker of GABAergic neurons (Esclapez, M. et al., 1994), catalyzing the rate limiting step in GABA synthesis accounting for ~85% of GABA synthesized in the mouse brain (Asada H et al., 1997). GAD65 is the only other enzyme synthesizing GABA. Studies suggest that, although, GAD65 helps in maintaining GABA levels in the cell it cannot substitute for GAD67 as demonstrated from deletion studies in mice underscoring the importance of GAD67 in GABA synthesis. Moreover, GAD67 deletion is lethal whereas GAD65 deletion increases the occurrence of seizures in mice brain (Asada H et al. 1997) and compromises synaptic plasticity, therefore suggesting that Gad65 has an important but not biologically essential role in the synthesis of GABA and nervous system functionality. Clinically speaking, genetic studies have linked GAD67 to abnormal neurodevelopment and early (childhood)-onset schizophrenia (Addington et al., 2005) and bipolar disorder (Lundorf et al., 2005). If GAD67 is to be established as one of the GABAergic pathway molecules in a possible direct association with schizophrenia, there should be a change noted in the levels of GAD67 mRNA and protein from postmortem schizophrenic brain tissue. This theory follows from the findings that GAD67 expression is regulated by neuronal activity and that there is hypoactivity, primarily in the prefrontal

cortex and other cortices of schizophrenic brain (Goff and Evins, 1998). Postmortem brain analyses probing this question have repeatedly shown decreased levels of GAD67 mRNA and protein in the prefrontal and temporal cortices (Akbarian, S, Huang HS, 2006) of individuals with schizophrenia. Altogether, 10 studies that used postmortem tissue from five different brain banks have revealed decreased GAD67 mRNA expression in the prefrontal and other neocortical association areas of schizophrenics. This finding is of great interest validating further research since, although a number of molecular mechanisms have been hypothesized to alter GAD67 mRNA levels, none of them have been definitively linked to the underlying disease etiology of schizophrenia. It should be noted that while there have been reports of increased GAD67 transcript and protein in schizophrenic prefrontal cortices studied from one brain bank, the majority of research studies strongly suggest a decrease in GAD67 mRNA and protein levels based on replication of these findings from different groups that have conducted this study across different brain banks (Akbarian et al., 2006). Taking a safe stand, several scientific groups will agree that altered GAD67 mRNA and protein has been associated with schizophrenic prefrontal cortex. Besides, the general consensus finding that there is not much neurodegeneration attributed to these disorders goes to implicate a possible molecular or cellular mechanism responsible for the altered GAD67 expression. Amongst the many mechanisms such as the level of sensory or excitatory input, decreases in neurotrophic factors like BDNF and receptor Trk B (Tyrosine kinase B), brain injury and molecular deficits that lead to disordered connectivity that have been scientifically proven to have an effect on GAD67 expression, the presence of single nucleotide

polymorphisms in and around the GAD67 promoter region and their association with schizophrenia, is most interesting from an epigenetic transcription regulation standpoint of GAD67 and its clinical significance as a potential molecular factor in schizophrenia.

Single Nucleotide Polymorphisms around the GAD67 genetic locus show significant association with schizophrenia occurrence

Addington (Addington et al., 2005) has reported the presence of a number of adjacent (single nucleotide polymorphisms) SNPs surrounding the proximal promoter and transcription start site of GAD67 that conferred genetic risk for childhood-onset schizophrenia and an increased rate of frontal gray matter loss. This study reports the statistically significant association of 3 SNPs in the 5' upstream region (non-transcribed) of GAD67 with the childhood onset of schizophrenia (COS). Magnetic resonance imaging (MRI) studies have associated these same SNPs with gray matter loss in the frontal cortex. Studies have also, successfully delineated a single allele with a SNP in the 5' (UTR) Untranslated Region of GAD67 that shows statistically significant association with decreased GAD67 mRNA and protein levels in the prefrontal cortex of schizophrenic brain. Another comprehensive study has established the statistical significance of GAD67 promoter proximal SNP association with schizophrenia occurrence. Statistically significant SNPs include rs1978340 located around 3Kb upstream of the GAD67 TSS and SNPs rs2356236, rs3762556 and rs3749035 located within 1.8Kb upstream of the GAD67TSS, the last three of which are only associated significantly with the male offspring of the particular schizophrenia family based study

conducted (Straub RE et al., 2005).

SNPs around the GRIN2B genetic locus show significant association with schizophrenia occurrence

(GRIN2B) Glutamate Receptor Ionotropic 2B is one of the subunits of the (NMDA) N-Methyl D-Aspartate receptor channel. As discussed in Chapter IV, GRIN2B has tremendous biological relevance for the process of learning and memory. Clinically, NMDA receptor blockade like that with phencyclidine (PCP or 'angel dust') results in hallucinations, resembling one of the psychotic symptoms experienced by schizophrenic individuals. Certain anti-psychotic drugs also enhance the flow of ions across the NMDA channels and this has led to the idea that NMDA receptor defects may be involved in schizophrenia occurrence. Furthermore, there is also the presence of SNPs in and around the GRIN2B genetic locus. Some of these SNPs (rs2160519) are also associated with cognitive dysfunction and working memory defects from population studies (Need AC et al., 2009). GRIN2B is a large gene (418 kb) with 12 intronic regions, including intron 1 spanning 113kb, upstream of the translation start site. There is definitely a possibility for the presence of regulatory elements in these non-coding regions and the presence of SNPs in these regions also strengthens the clinical significance of transcriptional regulation mapping across the genetic locus.

CHAPTER III

CHARACTERIZATION OF A SINGLE HIGHER ORDER CHROMATIN LOOP STRUCTURE 50KB UPSTREAM OF THE GAD67 TRANSCRIPTION START SITE IN HUMAN AND MOUSE CORTEX

Introduction

Cognitive defects and other symptoms of psychosis in schizophrenia can be related to the molecular and cellular defects in the cortical GABAergic system, affecting widespread areas of the cerebral cortex and other brain regions and compromising orderly synchronization of neuronal circuitries and other functions that critically depend on inhibitory neurotransmission (Daskalakis ZJ et al., 2007). The empirical framework for this hypothesis is based, among others, on a large body of postmortem literature reporting altered expression of various molecular markers defining the GABAergic phenotype, including down-regulated RNA and protein levels for the rate limiting GABA synthesis enzyme, 67Kda glutamic acid decarboxylase (GAD67), in multiple subtypes of cortical interneurons (Akbarian and Huang, 2006; Fung et al., 2010; Schmidt and Mirnics, 2012). The emerging view is that a sizeable portion, perhaps 30 or 40% of subjects with schizophrenia, are affected by a robust deficit in GABAergic gene expression, including GAD67 RNA, together with select transcription factors including Lhx6, neuropeptides including somatostatin and the Ca^{2+}-buffering protein parvalbumin (Volk et al., 2012). Importantly, single nucleotide polymorphisms (SNPs) in the proximal GAD67 promoter are associated with genetic risk for schizophrenia, and accelerated loss of gray matter and

impairments in working memory (Addington et al., 2005; Straub et al., 2007), and altered expression of key modulators of postsynaptic, $GABA_A$ receptor currents, including the cation/chloride co-transporters NKCC1/KCC2 (Hyde et al., 2011). Therefore, GAD67 dysregulation could play a part in the pathophysiology of disease both in pre- and postsynaptic structures in the inhibitory circuitry of cortex, thereby providing an important rationale to gain deeper insight into the molecular mechanisms associated with decreased GAD67 expression in the affected brains.

Indeed, a significant amount of information points to defects in the process of gene expression. Thus, decreased GAD67 expression in schizophrenia has been associated with altered chromatin structures at the proximal GAD67 promoter, including a shift from open to repressive chromatin-associated histone modifications and abnormal DNA methylation signatures (Huang and Akbarian, 2007;Tang et al., 2011). However, transcriptional regulation in the human genome goes far beyond simple epigenetic decoration and proximal promoter activity, which typically is explored within a few hundred basepairs surrounding gene transcription start sites. Instead, a picture is emerging with a three-dimensional genome being packaged in non-random fashion inside the cell nucleus, thereby enabling regulatory non-coding DNA to bypass, or 'loop around' many kilo- or even megabases of interspersed sequence, in order to physically interact with a distant promoter target for transcriptional regulation (Dekker J. 2008). To date, however, nothing is known about genome architecture and higher order chromatin in the human or animal brain, particularly in the context of schizophrenia and other psychiatric disease.

Here, we employ chromosome conformation capture (3C) assays encompassing 200Kb surrounding the GAD67 gene (2q31) in the prefrontal cortices PFC of subjects with schizophrenia and in controls, together with RNA-seq-based transcriptome profiling and chromatin immunoprecipitation, cell culture and animal models to dissect the role of development and disease as opposed to antipsychotic medication. Specifically, we identify a regulatory DNA element positioned 50Kb upstream of the GAD67 transcription start site (TSS) that by multiple lines of evidence bears the hallmark of an enhancer and that physically interacts via loop formation with GAD67 TSS in the PFC. This type of GAD67 higher order chromatin was absent in skin fibroblasts and stem cells but emerged, in parallel with increased GAD67 gene expression, when these non-neuronal cell types differentiated into neurons. Adult subjects with schizophrenia affected by low levels of GAD67 transcript in the PFC showed a decrease in physical interactions between the GAD67 enhancer and the GAD67 TSS. Remarkably, sequences in the mouse genome that showed homology to human GAD67 enhancer physically interacted with GAD67 TSS in mouse cerebral cortex, indicating that GAD67-associated higher order chromatin is conserved across mammalian lineages. Antipsychotic drug treatment did not alter the chromosomal loopings at the murine GAD67 gene. Our findings provide first insights into higher order chromatin structures surrounding the GAD67 locus and draw a connection between developmental mechanisms to the alterations observed in specific cases with schizophrenia.

Results

First reports of GAD67 expression-specific higher order chromatin looping in human brain

Deep sequencing of RNA extracted from adult PFC specimens revealed that within 200Kb surrounding the GAD67 TSS on chromosome 2q31.1, the only sequences transcribed were from the annotated GAD67 gene body (**Figure 3.1**). However, examination of the local chromatin landscape revealed multiple positions, some of which outside of GAD67, decorated with various types of histone modifications associated with open chromatin and active gene expression. For example, Histone H3 trimethylated at lysine 4 (H3K4me3)— a mark often enriched at CpG dense sequences associated with transcriptional regulation--showed two sharp peaks in neuronal chromatin from PFC, one that overlapped with the GAD67 TSS, with a second peak positioned 50 Kb further upstream of the GAD67 TSS.

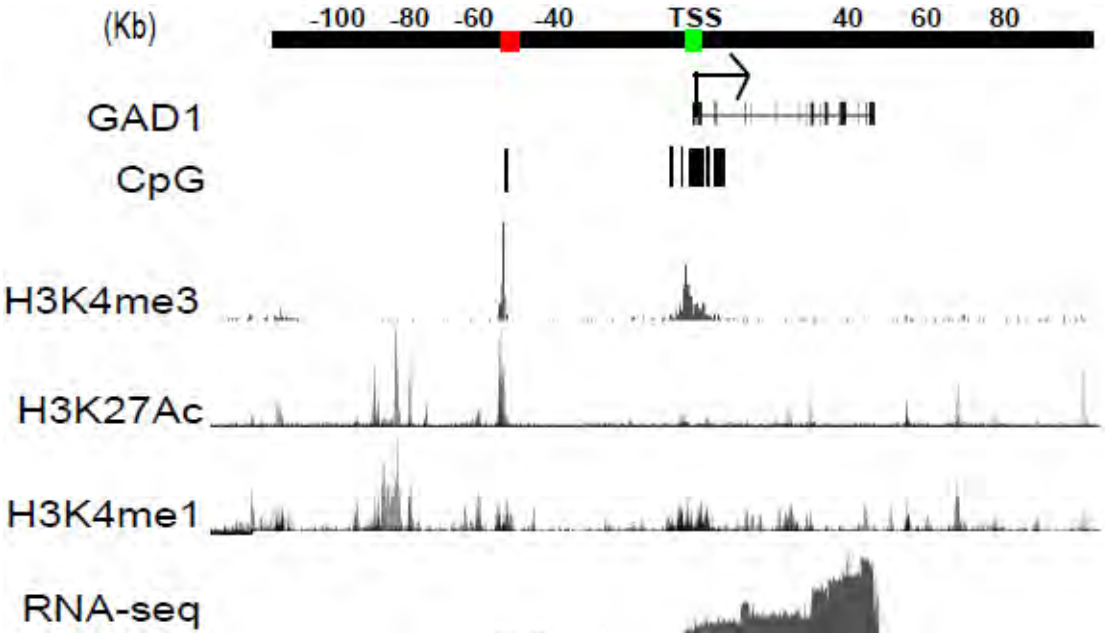
(Kb)
-100
-80
-60
-40
TSS
40
60
80
GAD1
CpG
H3K4me3
H3K27Ac
H3K4me1
RNA-seq

Fig.3.1. Epigenetic modification signals at the human GAD67 (Glutamic Acid Decarboxylase-1) gene in a region -100 Kb upstream of the GAD67 TSS to +80 Kb downstream of the GAD67 TSS

On top is a black horizontal bar drawn to scale for the region 100Kb upstream of the human GAD67 Transcription Start Site (TSS) to 80Kb downstream of the human GAD67 TSS. Specific regions of interest are indicated by colored boxes [GAD67 TSS region – green box, enhancer signal enriched region - red box]. Below is the GAD67 transcript with exons shown as vertical lines and introns in between the exons. GAD67 TSS is indicated by the arrow mark just below the green box. Tracks below indicate CpG island concentrations, Brain neuronal nuclei specific ChIP-sequence signals for histone 3 lysine 4 tri-methyl (h3k4me3) open chromatin mark, cell line specific ChIP-sequence signals for acetylated histone 3 lysine 27 (h3k27Ac) active enhancer mark, cell line specific ChIP-sequence signals for mono-methyl histone 3 lysine 4 (h3k4me1) enhancer enriched mark and RNA sequencing signal from brain neuronal nuclei (UCSC Genome Browser data).

Furthermore, the same -50Kb sequence (red box in **Figure 3.1**) matched to various cell lines explored by the Encyclopedia of DNA Elements (ENCODE) consortium (Melgar et al., 2011). In particular, these sequences overlapped with sharp peaks for histone H3 acetylated at lysine 27 (H3K27ac) and mono-methylated at lysine 4 (H3K4me1) (**Figure 3.1**), two epigenetic markings that in combination frequently define enhancer sequences (Ong and Corces, 2012). Therefore, in order to search for regulatory DNA elements in 2q31.1 that could play a role in GAD67 transcription, we interrogated 200Kb of sequence surrounding the GAD67 with 3C assays, centering the anchoring primer on the TSS (green box in **Figure 3.2)**. Indeed, in PFC from controls (N=4), the 3C interaction frequency between the GAD67 TSS and the Hind III fragment containing the above mentioned sequence defined by a unique 'triple-tagging' with H3K27ac/H3K4me3/H3K4me1, at -50Kb from GAD67 TSS, was several-fold higher, when compared to surrounding Hind III fragments. Furthermore, this interaction was much higher in PFC, when compared to skin fibroblast cultures from a healthy donor (**Figure 3.2**). Of note, in contrast to robust GAD67 RNA expression in PFC, GAD67 transcript levels in fibroblasts were essentially indistinguishable from background (**Figure 3.2**). Therefore, we asked whether the GAD67 higher order chromatin, including the looping between the -50Kb sequence with the GAD67 TSS (red and green boxes in **Figure 3.2**), which essentially was absent in skin fibroblasts (**Figure 3.2**), would emerge if the fibroblasts are converted to neurons.

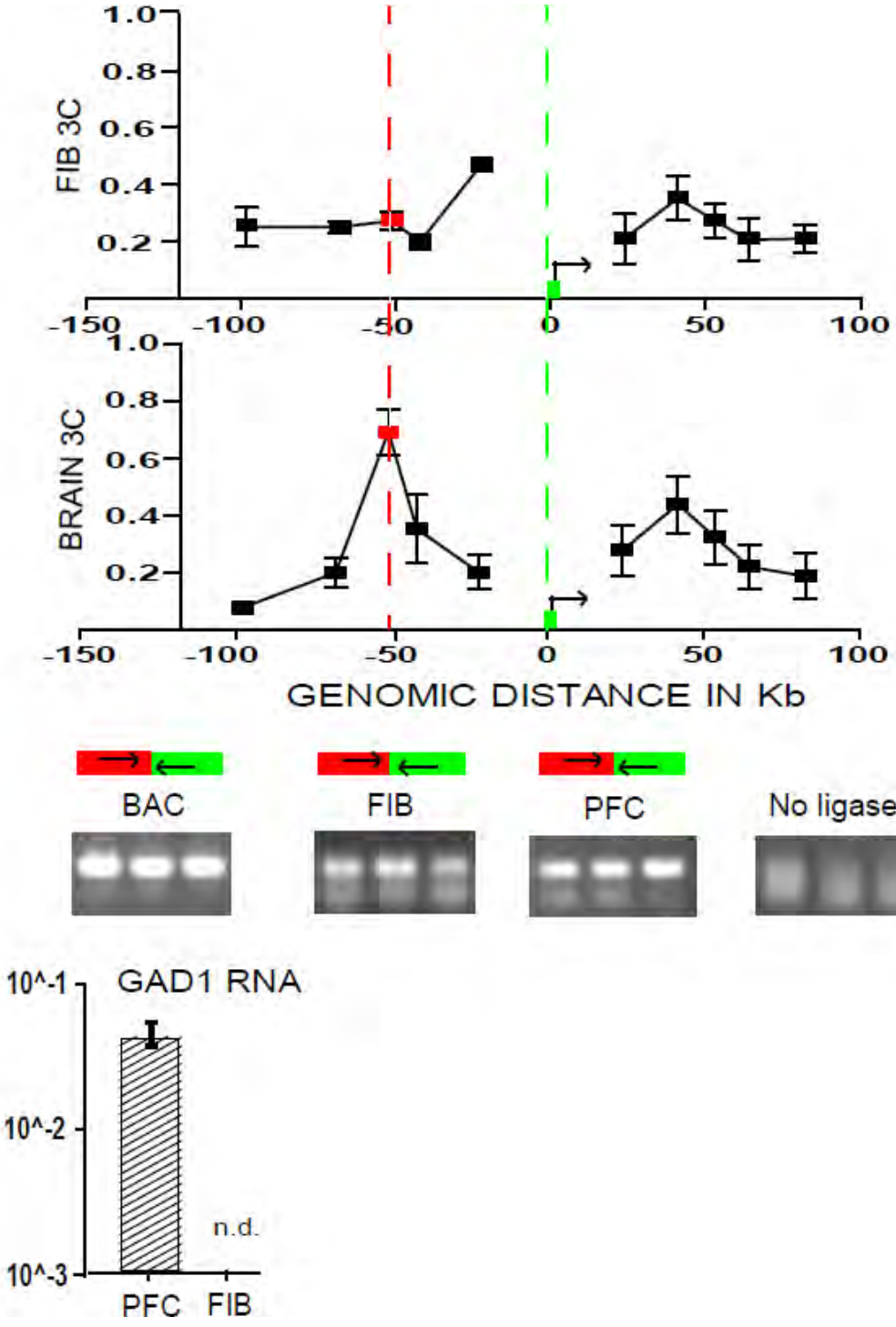
FIB 3C
1.0
0.8
0.6
0.4
0.2
-150
-100
-50
0
50
100
BRAIN 3C
GENOMIC DISTANCE IN Kb
BAC
FIB
PFC
No ligase
GAD1 RNA
10^-1
10^-2
10^-3
n.d.
PFC
FIB

Fig.3.2. Chromosome Conformation Capture (3C) at the human GAD67 (Glutamic Acid Decarboxylase-1) gene reveals a transcription-specific significant physical interaction in human brain PFC nuclei

3C interaction frequency maps for FIB (human keratinocyte-derived fibroblasts) and PFC (prefrontal cortical nuclei) of human brain subjects. Note the striking increase in interaction frequency in human PFC nuclei at active enhancer-enriched h3k27Ac mark located 50Kb upstream of the GAD67 TSS. All interaction frequencies are represented by square data points (mean +/- SEM, N=4 – PFC, N=2 FIB) and are measured by the average PCR product pixel intensity (n=3) for primers amplifying across the ligation junctions of the specific interacting fragment (red data point) with the TSS fragment (green data point). Each data point is an average of interaction frequency measures from 4 human brain PFC and from 2 FIB 3C libraries that have been normalized for primer pair efficiency and for ligation efficiency variations between 3C libraries. PCR products for the peak interaction point are shown in the gel below for PFC, FIB and BAC – Bacterial Artificial Chromosome (positive control 3C library for primer pair efficiency normalization). Panel on the lower left shows GAD67 RNA levels (N=3 PFC, N=2 FIB; mean +/- SD) normalized to 18S RNA for both PFC and FIB (undetectable).

GAD67 chromatin looping emerges during the course of neuronal differentiation

We induced pluripotent stem cells (iPS) from donor skin fibroblasts by lentiviral transduction with OCT4, SOX2, KLF4 and c-MYC transcription factors (Dhar et al., 2008) and then differentiated towards the neuronal lineage, as defined by neuronal morphology and immunoreactivity for microtubule-associated protein 2 (MAP-2) (**Figure 3.3**).

Indeed, these differentiated cultures showed, in comparison to the fibroblast-derived iPS, a several-fold increase in GAD67 RNA and at least a doubling of the 3C interaction between the -50Kb fragment and the GAD67 TSS (**Figure 3.4**). From this, we draw two conclusions. First, physical interactions between the -50Kb putative enhancer element with the GAD67 TSS are, at least in part, linked to the process of gene expression because these interactions were much higher in PFC and cultured neurons. This is because in these tissues and cells, GAD67 RNA levels and chromosomal loopings were increased, compared to skin fibroblasts and stem cells (**Figures 3.2 and 3.4**). Second, higher order chromatin structures at GAD67 are subject to dynamic epigenetic regulation, because cells derived from the same donor showed increased chromosomal looping after neural differentiation, when compared to their undifferentiated precursors or the fibroblasts from which the stem cells were induced (**Figure 3.3 and 3.4**).

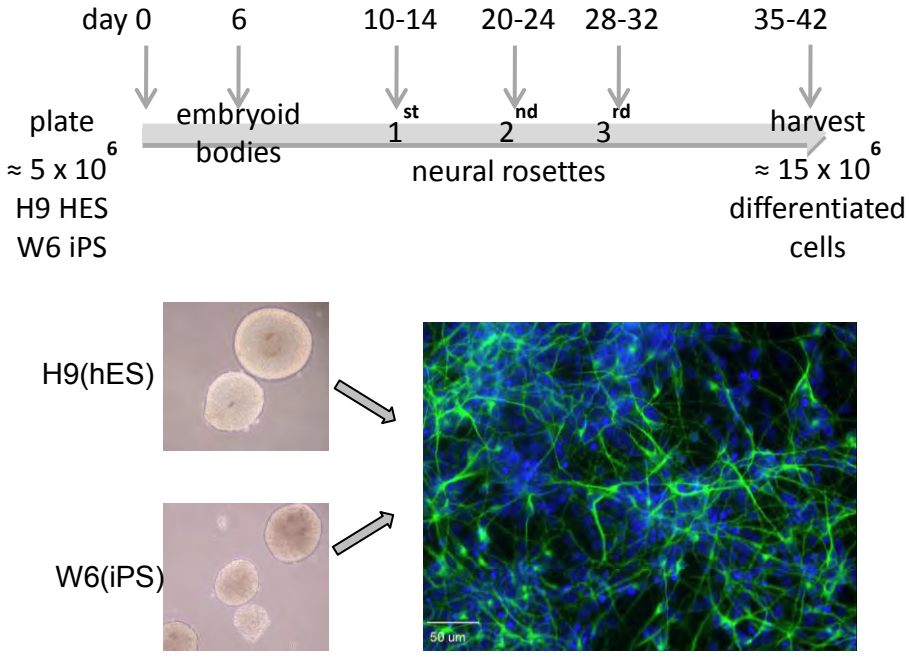

Cathy Whittle, Akbarian Lab

Fig.3.3. Cellular neurodevelopment model involving iPS (induced Pluripotent Stem) cells to Neurons

On top is a schematic showing the timeline for the differentiation of iPS cells into neurons in culture. Below is an image depicting iPS cells in their embryoid body stage (day 6) followed by a fluorescence image of differentiated neuronal culture staining post 42 days; MAP-2 stained neuronal nuclei (green) counterstained against DAPI (blue). Presence of neuronal nuclei indicates successful differentiation (60 – 85%) although the types of neuronal nuclei present were not estimated in the differentiation assay. Samples were harvested from iPS, H9 HES and from neurons and processed for RNA quantification and 3C interaction data as mentioned in the protocols section.

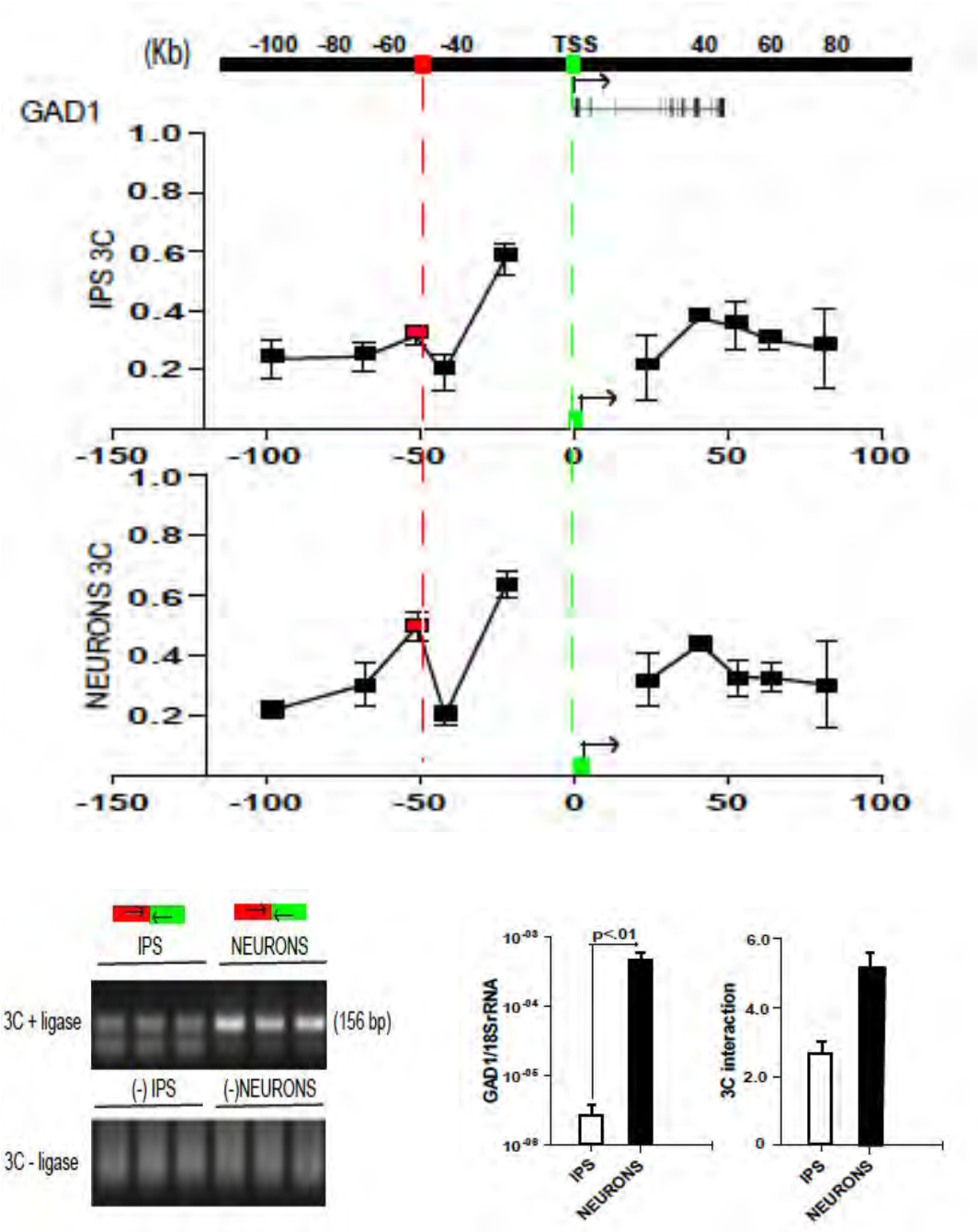
(Kb)
-100 -80 -60 -40 TSS 40 60 80
GAD1
IPS 3C
NEURONS 3C
1.0
0.8
0.6
0.4
0.2
-150 -100 -50 0 50 100
IPS
NEURONS
3C + ligase
(156 bp)
(-) IPS
(-)NEURONS
3C - ligase
p<.01
GAD1/18SrRNA
3C interaction
6.0
4.0
2.0
0
IPS
NEURONS

Fig.3.4. 3C interaction pattern at GAD67 locus shows an increase in interaction frequency correlating with GAD67 mRNA up-regulation in mature neurons but not in their iPS counterparts

3C interaction pattern at GAD67 locus (examined previously in Fig.3.2) in the iPS cells and their differentiated neurons. Note the increase in interaction frequency at the peak region enriched with enhancer signal (as in Figure 3.1) in neurons but not in the iPS cells. Interaction pattern is mapped with respect to the GAD67 TSS as anchor (green box region). Upper gel with 3C PCR products run in triplicate from iPS cells (lanes 1-3 from the left) and their neuronal counterparts (lanes 3-6 on the right); lower gel on the bottom with no ligase control in the same lane arrangement as the upper gel. Characteristic 156 bp PCR product (sequence confirmed) indicative of a positive interaction is absent in the no ligase control.

Bar graph (mean +/- SEM; N=3; statistics were performed (student t test) to check for a significant difference between means) below shows GAD67 mRNA normalized to 18S rRNA for iPS cells and their differentiated neuronal counterparts. Bar graph (mean +/- SEM, N=3) on the right shows the interaction frequency change between iPS cells and their differentiated neurons between GAD67 TSS with the enhancer signal enriched positive peak interaction (green GAD67 TSS fragment with red control fragment).

Characterization of the single higher order chromatin loop at the GAD67 locus

In an attempt to experimentally determine if the H3K4me3 signals are in fact enriched at the 50Kb upstream interacting region and at human GAD67 TSS in PFC nuclei and if these regions interact with each other, we next performed the ChIP-3C combination technique **(Figure 3.5)**. We immunoprecipitated chromatin with anti-H3K4me3 to obtain an enriched cross-linked fraction of H3K4me3 associated genome. Then we proceeded to generate a 3C library from this enriched H3K4me3 part of the genome and probed this library for our specific looping interaction at the GAD67 genetic locus **(Figure 3.2)**. As a background, we checked for interaction between fragments devoid of H3K4me3 signal.

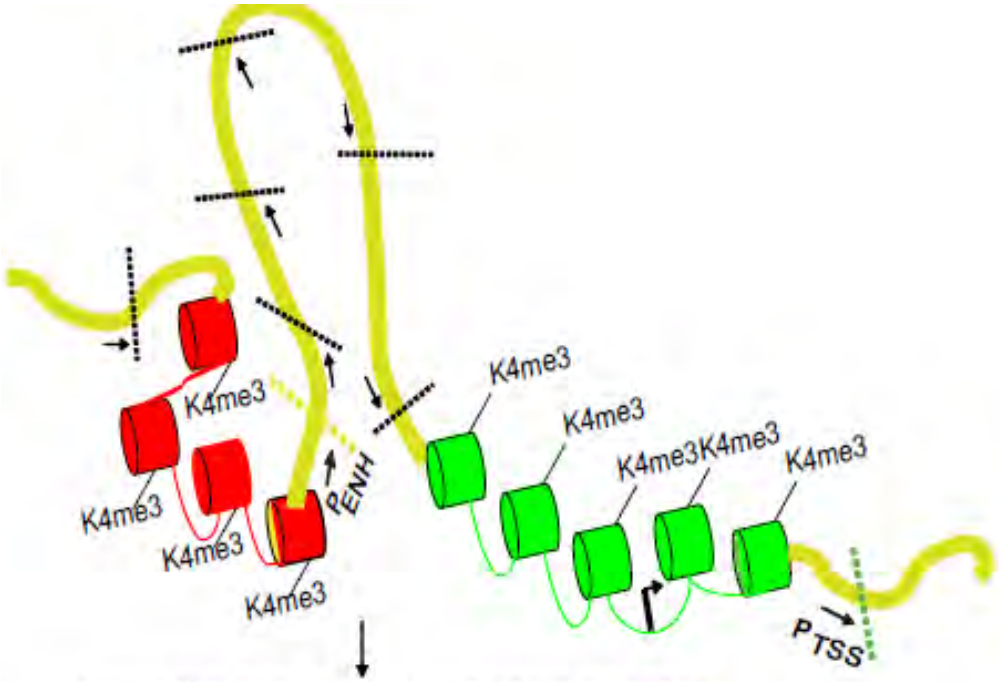

Cross link followed by restriction digestion

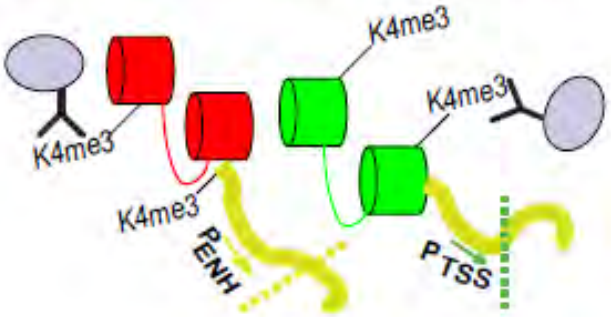

4C library

Fig.3.5. Diagrammatic representation of the (ChIP-3C) ChIP coupled with Chromosome Conformation Capture technique shows H3K4me3 enrichment at the peak and GAD67 TSS fragments

(Detailed stepwise protocol with materials and methods included in the protocols section.) Red nucleosome structures with methylated lysine tails (K4me3) represent the peak interacting fragment from previous figures and green nucleosome structures with methylated lysine tails (K4me3) represent the GAD67 TSS fragment. Hind III restriction sites in between are shown as dotted lines drawn across the chromosome (thick yellow thread-like structure) and 3C primers are shown as arrow heads in the same 5' to 3' orientation. Following cross-linking and restriction digestion as in the 3C protocol, anti - H3K4me3 antibody (Abcam, 1:1000 dilution for primary) shown as Y, was used to pull down brain nuclei chromatin followed by ligation of interacting fragments on the beads, shown as grey blips. Ligated DNA fragments were then eluted and purified by ethanol precipitation. Results are the presence of a comparatively intense PCR product amplified across the ligation junction of the GAD67 TSS (green) and peak fragment (red) from the H3K4me3 fraction compared to the IgG fraction. No ligase control showed no product.

We did not obtain any interaction frequency in this case. This was actual evidence of the existence of a higher order chromatin interaction coupled with high H3K4me3 signal at these interacting regions, suggestive of a 3C interactome associated with specific histone modifications. Next, we looked at the mouse GAD67 genome map to try and see if there could be a possible conserved 3C loop interaction in mouse cortical nuclei. From the Encode H3K4me3 ChIP-seq track, we found that there was a H3K4me3 peak at a region 55Kb upstream of the GAD67 TSS in mouse brain nuclei. Encouraged by our results from the H3K4me3 enriched peak interaction **(Figure 3.4)** in human brain, we decided to probe the mouse GAD67 region for 3C interactions. Interestingly, there was an increase in interaction frequency between the 55 Kb upstream region and the GAD67 TSS **(Figure 3.5).** This suggested conservation of the H3K4me3 epigenetic modification and higher order chromatin loop at the GAD67 genetic locus between human and mouse. Finally, we were eager to see if this interaction was specific to neuronal nuclei since GAD67 is a GABAergic neuronal marker. For this, we used transgenic mice that expressed a Gad65 driven Histone 2 B – Green Fluorescence Protein (GFP) fusion which facilitated GFP+ neuronal nuclei sorting. The 3C looping interaction was only detectable in the GFP nuclei-sorted fraction indicating neuronal enrichment of the looping interaction and there was no interaction obtained from the non-neuronal fraction sorted **(Figure 3.6)**.

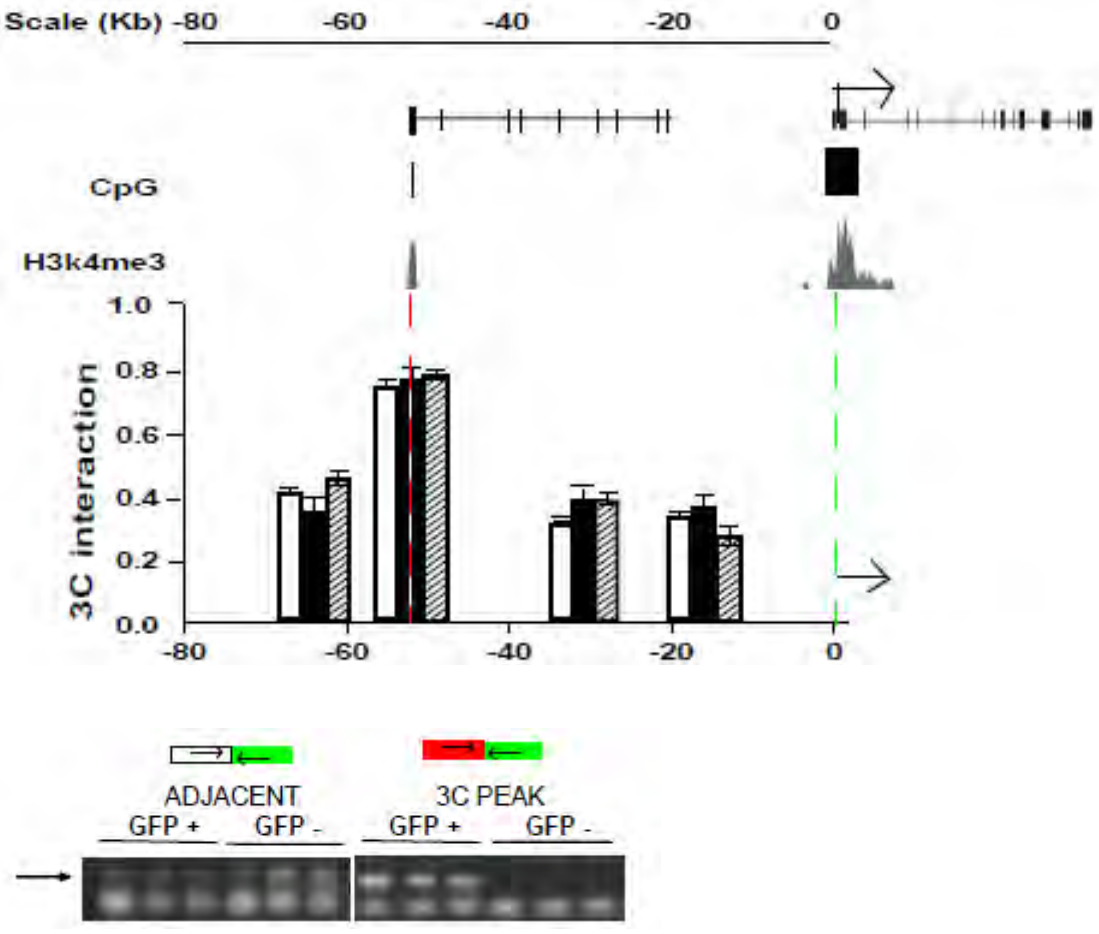
Scale (Kb) -80
-60
-40
-20
0
CpG
H3k4me3
3C interaction
1.0
0.8
0.6
0.4
0.2
0.0
-80
-60
-40
-20
0
ADJACENT
GFP +
GFP -
3C PEAK
GFP +
GFP -

Fig.3.6. Characterization of the 3C interaction frequency in mouse brain nuclei and conformation of the enrichment of this interaction in mouse neuronal nuclei

On top is the scale of the mouse genome in Kb with the mouse GAD67 TSS at the 0Kb mark. Below is the UCSC transcript track showing two transcripts, the first is a non-coding transcript and the second with the TSS arrow highlighted is GAD67. Below are tracks for CpG islands and mouse brain specific H3K4me3 signals that are both high at the 5'end of both transcripts. 5'end transcript of the non-coding transcript is located 55Kb upstream of the mouse GAD67 TSS. Below is the 3C interaction fold change map for mouse brain nuclei (white bars – clozapine treated, black bars – haloperidol treated, shaded bars – wild-type; bars are mean +/- SEM; N=3 individual 3C libraries) that shows a 2-fold increase in interaction frequency in 3/3 libraries tested for drug treated and wild-type mouse brain nuclei indicating no drug inflicted change in 3C interaction at the peak region and GAD67 TSS. Furthermore, there is evidence to support the notion that this interaction is neuron enriched as seen in the gel pictures. Both gels are PCR products run in triplicate from sorted neuronal nuclei (GFP +) and non-neuronal nuclei (GFP -) as indicated by the bars drawn above the lanes. Gel on the left is for adjacent fragments while the gel on the right is for the peak fragment with the GRIN2B TSS. Note there is no PCR product detectable from GFP- non-neuronal nuclei only for the 3C peak interacting product.

Sequences within the GAD67 Higher Order Chromatin harbor enhancer potential for GAD67 Transcription

Since the upstream interacting region shows chromatin architecture conservation for both the H3K4me3 signal and the interaction with the GRIN2B TSS across human and mouse species, we thought of evaluating the enhancer potential of the upstream interacting region in a luciferase reporter gene expression assay **(Figure 3.7)**. Interestingly, there is an increase in H3K27Ac signal within this region across several cell lines **(Figure 3.2)**, which goes to suggest that this region may harbor active enhancer elements (Chen CY et al., 2012). The interacting upstream restriction fragment however, is several Kb in length which would make it difficult to clone and also to pinpoint what specific sequences could have enhancer potential within this fragment. In order to obtain a general idea of the transcription factor binding sites present in this fragment; we performed a transcription factor scan of the fragment using MATCH (TRANSFAC - Biobase) available on the biotools.umassmed.edu website. We found an increased density of (AP-1) Activator Protein-1 sites among some others within this fragment and proceeded to clone this particular sequence into a luciferase reporter gene expression vector system to evaluate enhancer potential. We focused upon a 115-base pair sequence with the AP-1 binding sites concentrated in the middle. AP-1 binding sites (TGAGTCA) are for the Fos and Jun family of early stage developmental transcription factors and are known to play a role in induced transcription regulation (Buttice et al., 1991). The reporter gene assay showed a 10-fold increase in luciferase activity with the cloned (3C peak; chr2:171622200-171622300) sequence compared to the control (chr2:171645000-171645125) sequence.

The control sequence is located just upstream of the human GAD67 transcript in between the interacting upstream region and the GAD67 TSS and is devoid of AP-1 binding sites. These results increased the significance of our findings thus far. Due to the clinical implication of GAD67 in schizophrenia occurrence as mentioned in Chapter II of this thesis, we proceeded to evaluate this enhancer containing interacting region's frequency (between this fragment and the GAD67 TSS fragment) in select schizophrenia brain samples compared to matched normal brain samples.

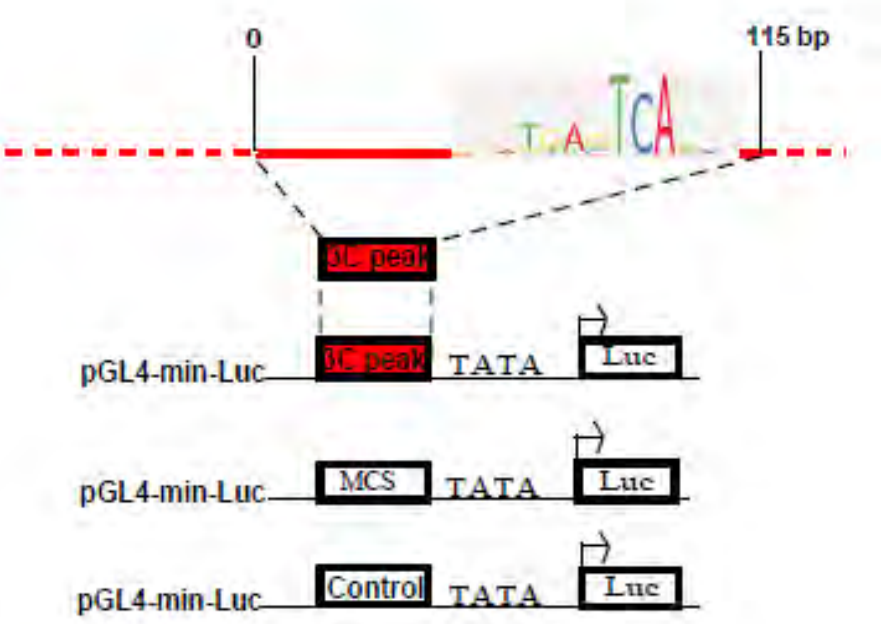
0
115 bp
3C peak
pGL4-min-Luc
3C peak
TATA
Luc
pGL4-min-Luc
MCS
TATA
Luc
pGL4-min-Luc
Control
TATA
Luc

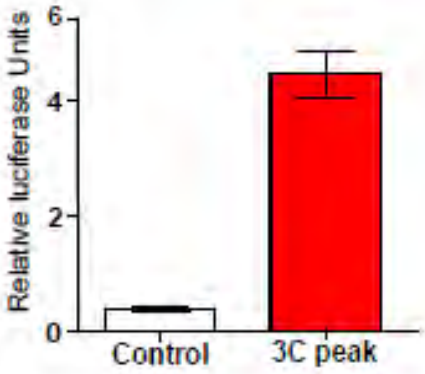
Relative luciferase Units
6
4
2
0
Control
3C peak

Fig.3.7. Luciferase reporter gene expression assay confirms enhancer potential of GAD67 upstream peak interacting region

Luciferase reporter gene assay schematic with the 116-bp sequence within potential enhancer region 3 that is cloned into pGL4-min-Luc vector. Three clones were generated: 3C peak, empty vector and Control shown in order from the top to bottom. 3C peak region cloned has AP-1 transcription factor sites enriched in that sequence with the consensus binding site sequence for AP-1 represented in the cartoon above the 120bp red bar. Transfections were performed in HEK cells using the lipofectamine transfection kit (Invitrogen). Selective medium (200 ug/ml hygromycin) was used to propogate transfected cells which were harvested after 48 hrs using the lysis protocol as described in the Promega luciferase assay kit. Firefly luciferase units were measured in a luminometer for each of the 3 clones. In addition, the renilla luciferase vector was co-transfected into every experimental cell batch and renilla luciferase units were used for normalization in accordance with the Promega luciferase kit protocol. Luciferase units estimated were normalized for transfection efficiency and were normalized against the minimum TATA box driven luciferase to obtain relative luciferase units plotted on the Y-axis of the bar graph (B) for control region and 3C peak region clones. Relative Luciferase Units are luciferase activity units plotted relative to the minimal promoter driven luciferase vector. Negative controls employed were a random plasmid vector with no luciferase gene and untransfected cell lysate (data not shown).

Higher order chromatin loop at the GAD67 gene locus shows a significant change in interaction frequency in schizophrenia PFC brain nuclei

We attempted to perform an appropriate evaluation of the general chromatin architecture at the GAD67 genetic region that takes into consideration the H3K4me3 signal and the interacting loop region, in clinical samples. This 50Kb upstream region had high H3K4me3 signals and interacted at a high frequency with the GAD67 TSS **(Figures 3.2 & 3.4)** in human cortical nuclei. Since this region did demonstrate enhancer potential **(Figure 3.7)** with the interacting loop existing only in GAD67 expressing tissue **(Figure 3.2)**, we evaluated this interaction in schizophrenia cases that had decreased GAD67 expression simultaneously showing a decrease in H3K4me3 signals compared to their matched normal samples **(Table 3.1)**. We first checked to see if there was a general decrease between the normal subjects compared to the schizophrenia cases in accordance with the decreased GAD67 expression and HEK4me3 TSS signal. We did see a significant decrease in the schizophrenia case mean interaction frequency (10 cases) compared to the normal case mean interaction frequency **(7 cases, Figure 3.8).**

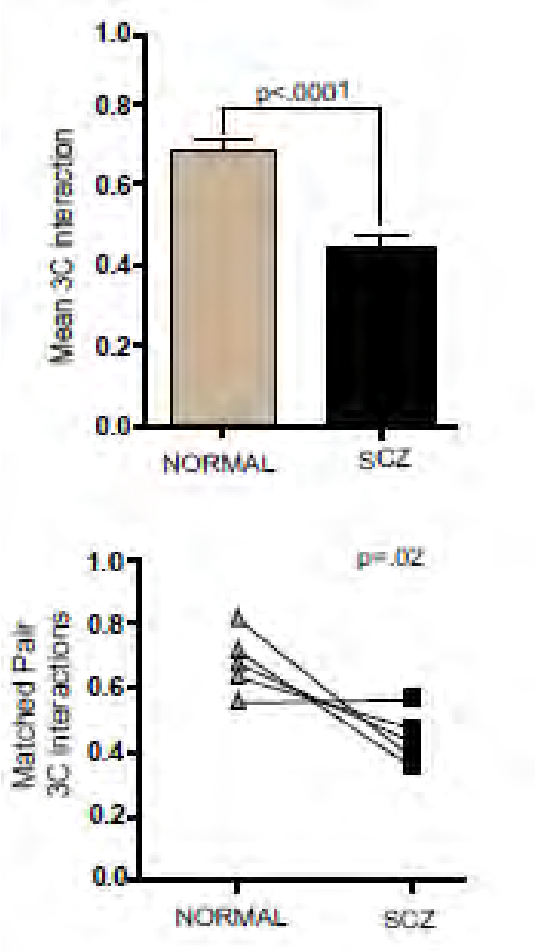
1.0
0.8
0.6
0.4
0.2
0.0
Mean 3C interaction
p<.0001
NORMAL
SCZ
1.0
0.8
0.6
0.4
0.2
0.0
Matched Pair
3C interactions
p=.02
NORMAL
SCZ

Fig.3.8. 3C interaction frequency for enhancer region 50Kb upstream of GAD67 is decreased in schizophrenia brain samples with decreased GAD67 expression and decreased H3K4me3 signal

Mean 3C interaction frequency bar graphs (mean +/- SEM) plotted for 10 schizophrenia cases (SCZ) and for 7 normal cases. Decrease in mean interaction frequency is significant and is calculated using simple t test, two tailed ($p<.0001$).

Below is a graph drawn to show the change in interaction frequency on the Y axis for the same peak interacting enhancer region 50Kb upstream of GAD67 between 5 normal cases (gray triangles) and their matched schizophrenia cases (black squares).

We proceeded to then do a matched case by case evaluation between each schizophrenia and normal subject, chosen for acceptable pairings of post-mortem interval, age, pH and RNA integrity number (RIN) criteria. We obtained a decrease in interaction frequency in 4/5 matched cases evaluated with one matched pair showing no significant change in interaction frequency **(Figure 3.8).**

Discussion

Previous studies focused on the transcription regulation of GAD67 have identified regulatory elements, located immediately upstream of the human GAD67 promoter (Kobayashi, T et al., 2003). In spite of this, researchers have failed to accurately replicate the expression of human GAD67 at all GABAergic centers, known in the murine brain (Katarova, Z et al., 1998; Kobayashi, T et al., 2003). This implies that there are regulatory elements upstream of the GAD67 promoter. Our work is a first attempt to identify where these regulatory elements might be located within a 180 Kb region surrounding the human GAD67 TSS. Ours is also the first study to explore transcription regulation in the context of chromatin architecture in human brain using 3C, a technology that has been already established robustly, in yeast and mammalian cell cultures (Miele A et al., 2006), but with no results reported yet, in the human brain. Besides the novelty of technology application to answer a biologically relevant question, we have also tried to explore a clinical angle for our chromatin structure findings. From Figures 3.1 and 3.2, it is clear that there is a single human brain specific chromosomal loop within the GAD67 genetic region mapped. This finding is exciting, since it is absent in the GAD67 non-

expressing fibroblasts, suggesting that this may one of many GAD67 expression-specific chromosomal loop structures in the human brain. This result clearly does not imply a neuron specific looping structure though, and it is also be important to look for this looping interaction in other tissues that express low levels of GAD67, such as kidney, to evaluate if there is any gradation observable in the level of interaction frequency across these tissues. This would give a clearer idea as to the robustness of 3C quantification done in human brain. While Figures 3.3 and 3.4 offer evidence for the possible enrichment of GAD67 chromosomal looping in neurons as compared to non-neuronal cells, it still does not clearly argue that the GAD67 chromosomal loop is neuron specific and only demonstrates that this loop may be developmentally up-regulated in correlation with the increase in GAD67 RNA. The ideal experiment should include a cell sorting experimental design followed by probing the neuronal and the non-neuronal fractions for GAD67 RNA levels, HEK4me3 signals and 3C interactions at the GAD67 genetic region to clearly answer the underlying question of neuronal specificity. However, the cross-linking part of the technique confounds the process of cell sorting, whereas, cell sorting without cross-linking may not preserve all the relevant chromatin architecture. Nevertheless, this approach should now be tried to see if these results can be duplicated. Figure 3.5 is a nice technique to explore chromosomal loopings specifically associated with a histone modification across the genome. In this case, it serves as a good qualitative method of confirming the presence of HEK4me3 signals at the regions involved in chromosomal looping. Other lower interacting regions were probed for and turned up negative from the 3C-ChIP libraries, proving the existence of H3K4me3 associated

higher order chromatin. It would be interesting to probe this library for two regions with H3K4me3 peaks that are known to be non-interacting as a confirmatory proof of concept for the 3C-ChIP approach. Figure 3.6 moves closer towards establishing the conserved loop in murine brain tissue as neuron specific. While this is sufficient evidence, there is still a need to achieve more robust background signals since the presence of an interaction does not automatically translate into the presence of a peak interaction, since a peak interaction is gauged relative to the background signal of interaction frequencies. Figure 3.7 is a shorter way of achieving the status of potential enhancer for the interacting region sequence cloned into the reporter gene assay, but needs much more experimentation before anything conclusive can be said about the interacting region being an enhancer relevant to GAD67 gene expression. Firstly, there are AP-1 sites enriched in the cloned region from the interacting peak co-ordinates, but AP-1 factor is not active in neurons only and can also be active in HEK cells. Also, the presence of AP-1 binding motifs in the sequence needs to be backed up with a chromatin immunoprecipitation experiment demonstrating the occupancy of AP-1 within the peak interacting region, around the AP-1 binding motifs. Lastly, if the peak interacting region acts as an enhancer, there is a strong possibility of detecting AP-1 signal in the GAD67 TSS region too. Once these experiments are conducted, we can start to better understand the role that this region plays as an enhancer and if AP-1 is the transcription activator mediating enhancer function. This also then opens up new experimental avenues, including identifying binding partners for AP-1, or knocking down AP-1 to see if there is a decrease in GAD67 expression, which would have to be done in a neuronal cell culture.

There are hardly any known transcription factors or signaling pathways implicated conclusively in the transcriptional regulation of GAD67 and these would be important findings towards advancing this area. Further characterization of a transcription factor for GAD67 expression opens up the possibility of a clinical angle as well, since a change in transcription factor function, or a mutational change in the regulatory DNA element motif, would definitely be able to account as a mechanism of decreasing GAD67 expression, which is commonly seen in the prefrontal, temporal and parietal cortices of schizophrenia subjects (Huang HS et al., 2006). Finally, the clinical data shown in Figure 3.8 does explore a novel diagnostic area of clinically relevant chromatin signatures, with some serious additional factors that need to be considered, before anything can be concluded. Firstly, we need to perform these results in a greater number of schizophrenia samples to achieve better significance, and we need to establish a timeline in terms of the appearance of chromatin that can influence GAD67 RNA levels later. This finding would only then be of true diagnostic significance with clinical chromatin serving a preventative purpose, since it may be manifest much earlier than the decrease observed in GAD67 RNA levels. Secondly, schizophrenia is a polygenic illness, with many genes implicated in its etiology; therefore GAD67 cannot be proposed as a single marker despite its biological role as a rate limiting enzyme, catalyzing the synthesis of GAD67 from GABA (Akbarian and Huang, 2006; Fung et al., 2010; Schmidt and Mirnics, 2012). Lastly, while these studies have evaluated the prefrontal cortical tissues of schizophrenia case and control subjects, there is a need to check and see if this finding is also manifest in other brain regions including the temporal and parietal cortices and the hippocampus, where

GAD67 RNA levels are also known to be decreased in schizophrenia subjects (Heckers et al., 2002). The results presented in this study here are novel and innovative, setting a nice platform to explore chromatin architecture in the context of transcription regulation and clinical significance. There is also a dearth of appropriate disease models when it comes to schizophrenia and many other polygenic illnesses like some cancers, but the complexity of a cognitive disease is special in that it is nearly impossible to design a disease model capable of simulating the cognitive makeup and connectivity resembling the human brain. The closest animal disease model to explore would be primates, which is difficult to handle and treat and process, for emotional, technical and data validity reasons. In the absence of the right disease models and protein pathological hallmarks, the best way to explore transcription regulation mechanism based diseases might be cellular developmental models as presented here, in this study, with confirmation of the results in diseased tissue. At this point in time, the results of such a study can purely have an impact on diagnosis and not cure, but can biologically give insight into disease mechanism and may shed some light by way of preventative care.

Summary

This is the first study of its kind performed to evaluate chromatin architecture at the GAD67 genetic region in brain cortex. Significance of these findings includes a possible specificity to GABAergic nuclei in human brain **(Figure 3.6)** based on the findings of the looping interaction in sorted neuronal nuclei only. It is also safe to conclude that this looping interaction is not influenced by the action of antipsychotic medication and that it has a significant relation to GAD67 transcription on account of its absence in non GAD67 expressing human fibroblasts. The study also advances the notion that epigenetic modifications combine with higher order chromatin to influence gene regulation. This is in addition to many previous studies that have shown a decrease in H3K4me3 signal at the GAD67 TSS correlated with a lower level of GAD67 RNA (Huang H S et al., 2007). Our results here also show that there is a strong possibility that there could be an extension of histone modifications to distant regulatory elements that come in physical contact with the gene TSS region or that histone modifications occur at regulatory elements located at distant sites from the gene TSS. This makes us wonder if there could be pre-determined epigenetic signals at specific regulatory elements or if the regulatory elements are in constant interaction with gene TSS upon transcription and therefore is subject to histone modifications by virtue of the spatial proximity. In addition, what decides which regulatory elements come in contact with the gene TSS and what conformations are more favorable in the cell nucleus at a specific genetic region? The redundancy of regulatory elements makes this a complicated question to answer. We must first start to map regulatory elements that play a functional role in gene transcription

using chromatin techniques like 3C, ChIP-seq and RNA quantitation. Next, we should confirm enhancer potential of these elements in reporter gene assays. This is always complicated when it comes to negative regulatory elements. Once the most significant regulatory elements have been identified, targeted deletion studies must be performed to confirm the relevance or exclusivity of a particular element/s for a given gene. Identification of significant elements is critical since these may hold the key to epigenetic diagnostic tests for disease susceptibility. The presence of SNPs within any of these functional regulatory elements is also an added degree of clinical relevance to any regulatory element mapped especially with respect to a candidate risk gene such as GAD67. These are exciting times in the field of chromatin dynamics analysis and understanding the relevance of higher order chromatin in a transcriptional and clinical context.

CHAPTER IV

TRANSCRIPTIONAL AND CLINICAL SIGNIFICANCE OF LONG DISTANCE CHROMATIN LOOPINGS AT THE HUMAN GRIN2B GENE LOCUS

The NMDA Receptors: GRIN2B (Glutamate Receptor Ionotropic, subunit 2B) is one of the protein subunits of the NMDA (N-Methyl D-Aspartate) ligand gated ionotropic receptors. Glutamate receptors can be broadly divided into ionotropic and metabotropic receptors, with the ionotropic receptors allowing the flow of ions directly through them and the metabotropic receptors indirectly activating ion channels via secondary messengers. Ionotropic glutamate receptors are divided into NMDA receptors and non-NMDA receptors: AMPA (ά-amino 3-hydroxy 5-methylisoxazole 4-propionic acid) receptors and kainate receptors, named after the agonists that bind to them. NMDA receptors function in the transmission of excitatory signals in the central nervous system. They are multimeric protein channels and are typically made up of a hetrotetrameric combination of 2NMDA R1 subunits and 2 NMDA R2 subunits. The NMDA R1 subunits bind the co-agonist glycine while the NMDA R2 subunits bind glutamate.

Biological & Clinical Significance: A characteristic feature of the NMDA receptor channels is the blockade by Mg ions that results in a delayed contribution of NMDA receptors to an excitatory post synaptic potential (EPSP). Another feature that is unique to NMDA receptors is their permeability to Ca ions. This combination ensures that NMDA receptors are activated only upon repeated multiple depolarizations that depolarizes the membrane enough to expel the Mg ion blocking the pore followed by an

influx of Ca and Na ions that lead to rapid depolarization of the membrane. The inflow of Ca ions is biologically relevant since it activates many enzymes that are Ca dependent, including some protein kinases that are key regulators of cellular signaling and gene expression modulation. This leads to long term changes in the protein machinery of the neuron. This mechanism is thought to be largely responsible for the basis of learning and memory that requires reinforcement and long term molecular changes. Thus NMDA receptors definitely have an undisputed biological significance that goes way beyond their involvement in excitatory neurotransmission and into activity dependent synaptic modification through gene expression change. Clinically, NMDA receptor blockade like that with phencyclidine (PCP or 'angel dust') results in hallucinations, resembling one of the psychotic symptoms experienced by schizophrenic individuals. Certain anti-psychotic drugs also enhance the flow of ions across the NMDA channels and this has led to thinking that NMDA receptor defects may be involved in schizophrenia occurrence. Glutamate at higher concentrations is toxic to neurons and is theorized to play a role in the death of neurons after stroke, multiple seizures or degenerative disorders like Huntington's chorea. Hence, there is clinical interest in NMDA receptor blockers that could protect neurons against glutamate excitotoxicity.

Setdb1 and its role in chromatin remodeling

Setdb1 (Set domain, bifurcated – 1)/ ESet/ Kmt1e is a histone 3 lysine 9 specific methyl transferase converting non-methylated residues to tri-methyl forms. Posttranslational histone modifications (including acetylation, phosphorylation, and methylation) on specific amino acid residues are known to be associated with the epigenetic regulation of

gene expression. Relatively less information is available on gene expression regulation associated with methylation. While the methylation of H3K9 residues is thought to play a part in transcription repression, the larger mechanistic role of histone methyl transferases like Setdb1 in regulating neuronal gene expression is still unclear (Cedar & Bergman, 2009; Gupta et al., 2010). Setdb1 has been postulated to function as part of a chromatin remodeling complex based on its physical association with KAP-1 (KRAB associated protein-1, a conserved transcriptional co-repressor that binds to KRAB – Kruepel associated box elements) (Schultz DC et al., 2002). It has also been reported that Heterochromatin Protein-1 (HP-1) is enriched at H3K9me3 sites, a finding that further suggests the involvement of SETDB1 in repressive chromatin remodeling (Schultz DC et al., 2002). A good approach towards understanding the larger role of SETDB1 in repressive chromatin remodeling would be to identify the binding sites of SETDB1 and thereby get an idea of the possible genetic targets or elements that are subject to SETDB1 mediated H3K9 methylation. It is obvious that looking for binding sites for SETDB1 across any mammalian genome in its entirety is a daunting task.

Where does SETDB1 bind to in the mouse genome?

Previous studies have identified a region in mouse chromosome 16 showing synteny to the human genetic locus 22q11.2. This region in humans has microdeletions that are linked to affective disorder and psychosis (Mukai et al., 2008). Therefore, mouse chromosome 16 was an attractive candidate region to begin to look for SETDB1 target sites since it would be interesting to map repressive chromatin remodeling at specific sites here in relation to the locations of microdeletions to see if there could be an

epigenetic connection. Chromosomes 6 and 8 were also added to the list of interesting chromosomes to scan for SETDB1 target sites due to the increased number of ionotropic glutamate receptors present across these 3 chromosomes. An Affymetrix (genomic DNA) tiling array (chip-chip) covering murine chromosomes 6, 8, and 16 excluding repeats was used to identify SETDB1 binding sites and any potential gene targets based on the location. Table.1.2 shows a detailed genetic location and proximity to genes for SETDB1 location with specific distance downstream (+) or upstream (-) of the gene transcription start site.

Table 1. Gene hits from anti-myc ChIP-chip

Gene symbol	Setdb1 occupancy [a]	[b]	Gene name
Angpt2	+10.9	Int 1	Angiopoietin 2
Ano2	+96.1	Int 6	Anoctamin 2
Cadm2	+462.4	Int 1	Cell adhesion molecule 2
Cblb	+162.6	Ex 17	E3 ubiquitin-protein ligase Casitas B-lineage lymphoma B
Clec1a	+11.1	Int 1	C-type lectin domain, family 1, member A
Cntn4	+563.3	Int 5	Contactin-4
Cntn4	+703.4	Int 6	Contactin-4
Csmd1	+1610.4	Int 52	CUB and sushi domain-containing protein 1 precursor
Eps8	+27.0	Int 1	Epidermal growth factor receptor pathway substrate 8
Gm156	−5.6	5′	Gene model 156
Gpm6a	+97.7	Int 4	Neuronal membrane glycoprotein M6-a
Grid2	+40.9	Int 1	Grid2 glutamate receptor, ionotropic, delta 2
Grin2a	+289.3	Int 5	Glutamate receptor, ionotropic, NMDA2A
Grin2b	+31.4	Int 3	Glutamate receptor, ionotropic, NMDA2B
Il15	+13.4	Int 1	Interleukin-15
Kcnd2	+143.3	Int 1	Potassium voltage-gated channel, Shal-related family, member 2
Klra1	−1.4	5′	Killer cell lectin-like receptor, subfamily A, member 1
Klra14	−11.4	5′	Killer cell lectin-like receptor, subfamily A, member 14
Klra9	+85.7	Int 6	Killer cell lectin-like receptor, subfamily A, member 9
Klrk1	+2.4	Int 1	Killer cell lectin-like receptor, subfamily K, member 1
Lmo3	+204.8	Int 4	Lin11, Isl-1, Mec-3 domain only 3
Mcph1	+134.9	Int 12	Microcephalin
Mtmr7	+1.9	Int 1	Myotubularin-related protein 7
Olfr203	−1.6	5′	Olfactory receptor 203
Pik3c2g	+232.4	Int 18	Phosphatidylinositol 3-kinase, C2 domain containing, γ polypeptide
Ptprz1	+154.4	Int 17	Protein tyrosine phosphatase, receptor type Z, polypeptide 1
Robo2	+239.9	Int 2	Roundabout homolog 2 precursor
Styk1	+6.0	Int 3	Serine/threonine/tyrosine kinase 1
Tmem39a	−1.5	5′	Transmembrane protein 39A

Int, Intron; Ex, exon; 5′, 5′ upstream of TSS. All p values are ≤0.00001; $n = 3$ *CK-Setdb1* and, as negative control, 3 wild-type littermates.

[a] The length from gene hits to TSS (5′ to 3′; in kilobases).

[b] The length range of gene hits is from 624 to 1000 bp.

Table 4.1. Setdb1 target sites across mouse chromosomes 6, 8 and 16 with precise location and distance of these sites from the gene transcription start site.

Setdb1 ChIP-chip results revealed that Setdb1 target sites are <1% of annotated genes. Interestingly, the genes showing Setdb1 occupancy did include a majority of the glutamate receptor genes present on the 3 chromosomes probed. Genes in the red box represent 3 out of 4 glutamate receptor genes present in the region that remarkably show SETDB1 target sites, all located within the transcribed region. These included the two sole NMDA receptor genes, Grin2A (Glutamate Receptor Ionotropic 2A) and GRIN2B (Glutamate Receptor Ionotropic 2B), present on chromosomes, 6 and 16. Besides this striking association of Setdb1 with glutamate receptor chromatin, there were other genes included in Table 4.1. However, there were no target sites for Setdb1 in the syntenic regions of mouse chromosome 16. The next step was to check and see the expression levels of these genes since Setdb1 is associated with repressive chromatin modeling and therefore could mediate transcription repression, which would add some functional significance to the presence of a target site located within the transcribed region of a gene.

CamKII (Calcium/ Calmodulin dependent protein Kinase II) CK-Setdb1 over-expressing transgenic mice

CK-Setdb1 mice over-expressing Setdb1 in neuronal forebrain nuclei of mice were generated to see if the expression of these Setdb1 targeted genes (including the 3 glutamate receptors) was changed in neurons, based on the clinical significance of these findings for affective disorders. Results showed that only 11/28 target genes showed a significant decrease in RNA and protein levels in neuronal cells and furthermore, only GRIN2B and Grid2 were the glutamate receptors downregulated. This finding was

nevertheless exciting since we had a mouse model to explore the functional validity of the hypothesis that Setdb1 functions in transcription repression chromatin remodeling. The next step was to explore the chromatin architecture of the Setdb1 target site and the gene TSS to see if there was any molecular mechanism that could begin to account for the decrease in gene expression. Since this was a novel study and could potentially involve a lot of molecular biology techniques from mouse brain tissue, we picked GRIN2B due to the greater clinical significance attributable to the NMDA glutamate receptor family as already explained earlier. Mouse GRIN2B had the Setdb1 target site in the intron 3 region, 31Kb downstream of the GRIN2B TSS. The goal was to use chromatin structure probing techniques like 3C and ChIP to highlight significant changes in chromatin architecture that could potentially play a role in transcription repression of the GRIN2B gene. Setdb1 is thought to function as part of a protein complex and is known to physically interact with Kap-1 protein. The figure (**Figure 4.1)** below shows the binding patterns of both, Setdb1 and Kap-1, in the region 10Kb upstream of the GRIN2B TSS to 35Kb downstream of the TSS in CK-Setdb1 mouse brain nuclei. Also shown is the H3K4me3 signal (open chromatin histone modification often associated with active transcription start sites) to demonstrate active transcription of the mouse GRIN2B gene.

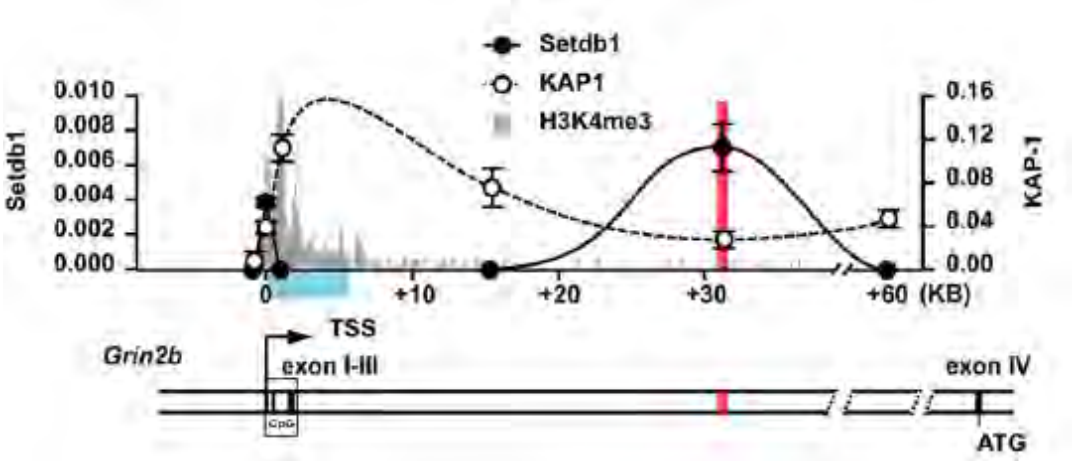

Jiang Y et al., 2010

Fig 4.1 Local chromatin profile of mouse GRIN2B region including GRIN2B Transcription Start Site and region 35Kb downstream.
Chip/Input signal for Setdb1 (black dots) on left Y axis and KAP-1 (white dots) on right Y axis as indicated by connecting lines across the mouse GRIN2B TSS and region upto 35Kb downstream in mouse forebrain nuclei. Data are expressed as the chip-to-input ratio (mean+/-SEM); n=3 chip experiments/antibody. Notice the big red bar corresponding to a heightened Setdb1 signal that indicates this region could be a potential target site for Setdb1. Gray H3K4me3 Chip-seq signal shading in the background is maximal at the TSS region indicating active transcription. Below is the mouse GRIN2B gene map with the TSS region and boxed CpG island region that include exons 1 – 3. Setdb1 target site indicated by red vertical line is in intron 3 region. Notice GRIN2B has a large 5'untranslated region with exon 4 positioned 127Kb downstream of the TSS corresponding to the translation start site indicated by ATG located to the right.

Setdb1 mediated chromatin architecture at the mouse GRIN2B gene and its possible role in transcription repression

The prior knowledge of physical interaction evidence between both proteins, Setdb1 and Kap-1, did not make sense with the observed binding patterns. Setdb1 peaked at a region 31Kb downstream of the GRIN2B TSS while Kap-1 was increased within 10Kb downstream of the GRIN2B TSS. How were they physically interacting then as part of the same complex, if at all? Bioinformatics based transcription factor site scans revealed a relative increase in the concentration of KRAB binding elements around 10Kb of the GRIN2B TSS and the location of the Setdb1 target site 31Kb downstream of the TSS. This finding, in addition to the results stated in the above figure, led us to test the possibility of a physical interaction between the GRIN2B TSS and the Setdb1 target site in the mouse genome that goes beyond the regular chromatin interaction landscape as we knew it. We initially looked at 3C interaction patterns from wild type mouse brain nuclei just to get an idea of what the normal 3C interaction pattern is and to go in unbiased when we look at CK-Setdb1 mice brain nuclei. 3C results in wild type mouse brain nuclei strongly supported the possibility of the existence of higher order chromatin at the GRIN2B gene (**Figure 4.2)**. The regions that interact with each other include the Setdb1 target site (pink fragment) and the GRIN2B TSS (blue fragment) and region with highest Kap-1 signals, suggesting that the physical interaction between Setdb1 and Kap-1 at this specific region could facilitate the coming together of these two genetic regions, 31Kb apart. The next step was then to check and see what happens to this looping physical

interaction when we over-express Setdb1 in the CK-Setdb1 mouse transgenic brain.

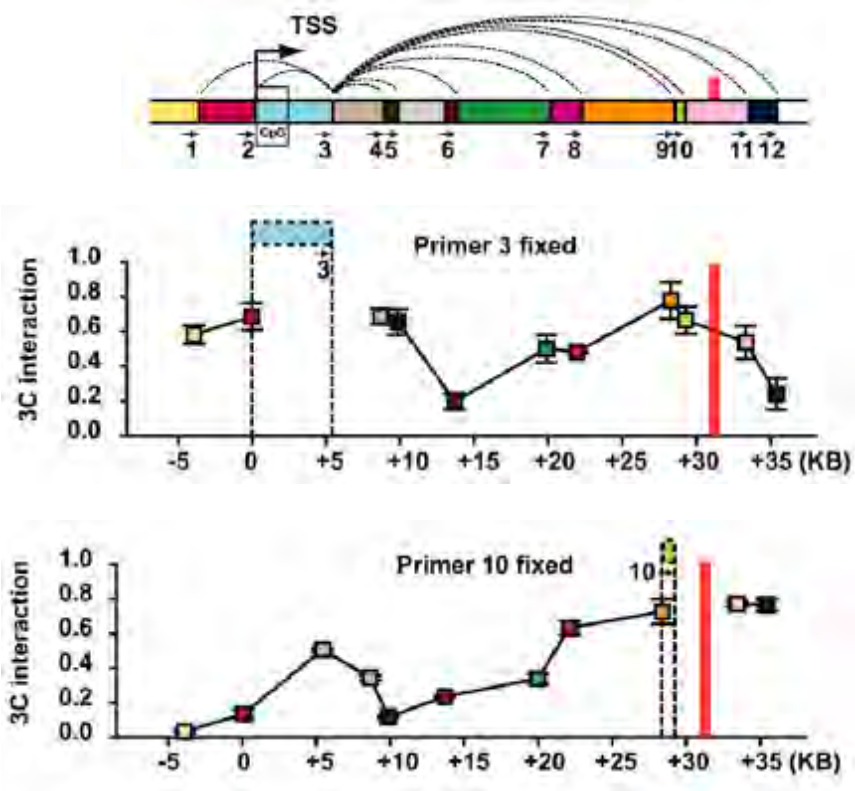

Jiang Y et al., 2010

Fig.4.2. 3C (Chromosome Conformation Capture) reveals a strong interaction between mouse GRIN2B TSS (blue restriction fragment) and Setdb1 target site (red vertical line that is part of pink restriction fragment).
3C profiles from adult mouse forebrain (wild-type) for proximal 35 Kb of GRIN2B; colored bars each represent a specific *Hin*dIII restriction fragment. The position and orientation of 3C primers 1–12 is as indicated. Each 3C profile is anchored on the TSS containing restriction fragment/primer as indicated by the blue colored horizontal bar in interaction map. The *y*-axes show the normalized pixel intensities (from agarose gel) for the specific PCR product from the anchoring primer and each of the remaining 11 primers as indicated by color code. Data are shown as the mean +/- SEM from two 3C libraries processed in triplicate. Notice that there are comparatively high levels of interaction between TSS fragment of mouse GRIN2B (blue) and fragments 30 kb farther downstream from the TSS. The Setdb1 target site is shown as a red line.

Hence, the evidence from wild type mouse brain nuclei, of a higher order chromatin loop existing at mouse GRIN2B fueled further efforts on our part to further explore higher order chromatin characterization in CK-Setdb1 mice **(Figure 4.3)** and to see if there is any change associated with the decrease in GRIN2B expression in neuronal nuclei from these mice?

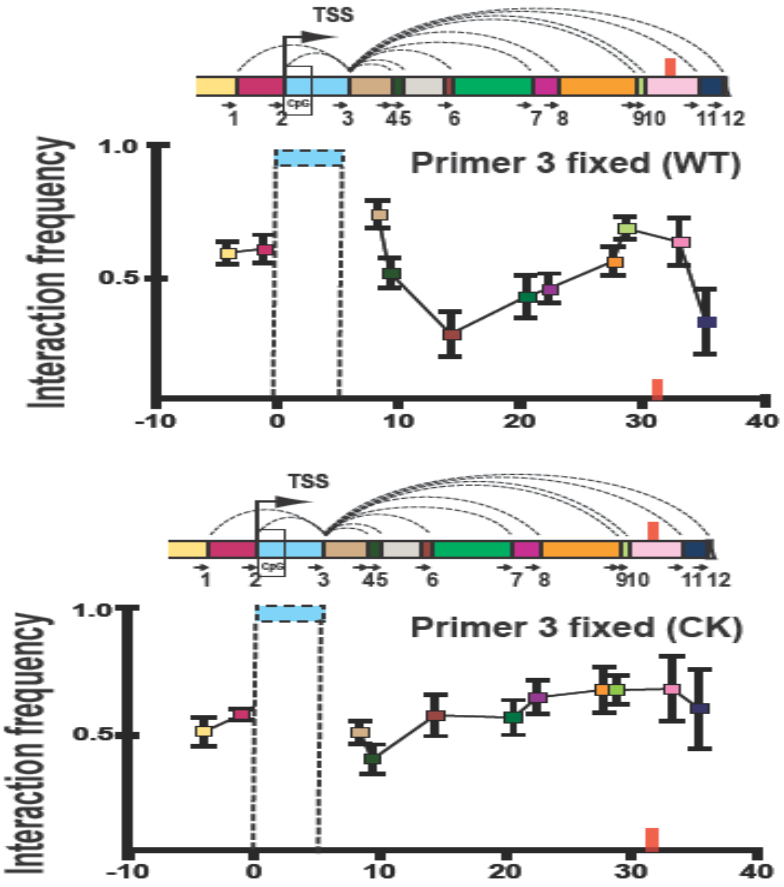
TSS
CpG
1
2
3
45
6
7
8
910
11
12
Primer 3 fixed (WT)
Interaction frequency
1.0
0.5
-10
0
10
20
30
40
TSS
CpG
1
2
3
45
6
7
8
910
11
12
Primer 3 fixed (CK)
Interaction frequency
1.0
0.5
-10
0
10
20
30
40

Fig.4.3 Comparative 3C interaction pattern for mouse GRIN2B region (-10Kb to +35Kb of the TSS blue fragment) between wild type adult forebrain nuclei (above) and Cam Kinase II driven Setdb1 adult forebrain nuclei (below).
Figure shows similar high interaction frequency between both, pink and green fragments adjacent to the Setdb1 target site (red vertical bar) and the blue TSS fragment. In addition, for the Setdb1 over-expressing transgenic mice below, the brown, green and violet fragments (fragments 6,7 and 8 respectively) also show an increase in interaction frequency suggesting that the entire 30Kb region comes in physical contact with the GRIN2B TSS upon Setdb1 over-expression.

As observed in the figure above, the higher order chromatin loop still exists in transgenic mice but the surrounding proximal region upstream of the Setdb1 target site now starts to interact at a higher frequency with the GRIN2B TSS. Whether this could be an overloading of Setdb1 protein onto the target site or the entire region or if this is some sort of a mechanism where these regions come together with the TSS to repress transcription of GRIN2B is debatable. Two findings can however start to help us understand what is happening in this region. One is to check and see if GRIN2B RNA and protein expression was actually downregulated and the other would be to quantify Heterochromatin Protein-1 signals at the TSS and Setdb1 target site to see if this is some sort of silencing process that is generally associated with this marker. Notably, adult CK-Setdb1 mice, compared to wild-type littermates, showed a highly significant, 20–50% reduction in GRIN2B mRNA and protein levels in hippocampus, and a similar tendency in prefrontal cortex. The lower level of GRIN2B in CK-Setdb1 brain could be attributable to transcriptional repression, because H3K9 methylation at GRIN2B's Setdb1 target site was significantly increased in the transgenic animals. Next we proceeded to quantify the levels of heterochromatin protein-1 from wild-type and CK-Setdb1 forebrain nuclei as shown below **(Figure 4.4)**. Our results have also been used to reconstruct a hypothetical model that tries to explain the possible mechanism of Setdb1 mediated transcription repression of GRIN2B in mouse brain neuronal nuclei.

A.

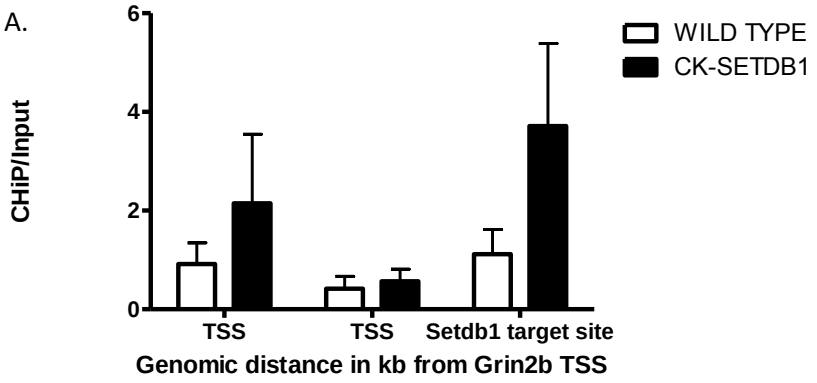
6
4
2
0
CHiP/Input
WILD TYPE
CK-SETDB1
TSS
TSS
Setdb1 target site
Genomic distance in kb from Grin2b TSS

B.

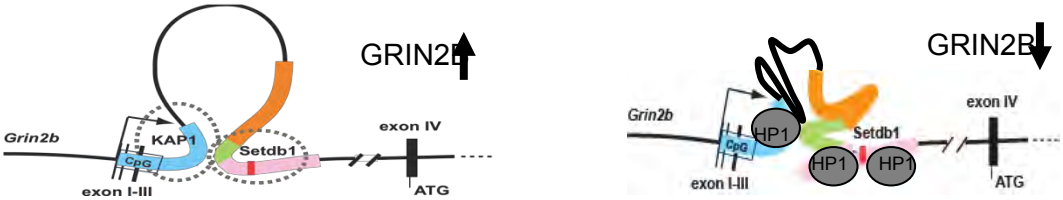
GRIN2B
Grin2b
KAP1
Setdb1
CpG
exon I-III
exon IV
ATG
GRIN2B
Grin2b
HP1
Setdb1
HP1
HP1
CpG
exon I-III
exon IV
ATG

Fig.4.4 Proposed chromatin folding model with Heterochromatin Protein-1 accumulation at transgenic mouse brain GRIN2B

A. ChIP-qPCR with anti-Heterochromatin Protein 1 (HP-1) from wild-type and CK-Setdb1 mouse forebrain nuclei data is plotted as ChIP/Input. There are a couple of primer pairs at the GRIN2B TSS and a single primer pair at the Setdb1 target site. Each bar graph is generated from 3 separate mice brains and results are recapitulated in 3/3 experimental tries. HP-1 is enriched 2-3 fold at mouse GRIN2B TSS and the Setdb1 target site located 31Kb downstream of the TSS.

B. Hypothetical model depicting chromatin folding and heterochromatin protein 1 accumulation that can potentially cause a decrease in GRIN2B expression in CK-Setdb1 transgenic mice forebrain nuclei.

The results above show heterochromatin protein-1 accumulation at the Setdb1 target site and to a lesser extent, at the GRIN2B TSS, in CK-Setdb1 transgenic mouse brain nuclei. This effect of accumulation is attributable to the over-expression of Setdb1 specifically in neurons over wild-type mice. Since Setdb1 and Kap-1 are conserved across species (Schultz DC et al., 2002), we checked if the Setdb1 target site had a homologous counterpart in the human genome. We did locate a 78% homologous sequence in the human genome to which, SETDB1 localized. Furthermore, there is also an increase in KRAB elements at the SETDB1 target site region (10Kb) in the human genome and this increase is about 40% greater than the surrounding 100Kb region. Due to cross species conservation of Setdb1 and the presence of a conserved SETDB1 target site in the human GRIN2B intron, 27 Kb downstream of the TSS, we proceeded to test the conservation of chromatin architecture between mouse and human species using a combination of 3C and ChIP techniques in the context of GRIN2B transcription regulation. The human GRIN2B gene spans 418Kb and has many large intronic regions with a large (117 Kb) intron before the translation start site. Our goal would be to identify other chromosomal loops that potentially play a role in transcription regulation of GRIN2B and analyze these loops in the context of SETDB1 expression in human brain cortex. This would be one of the first studies to provide concrete evidence of higher order chromatin structures in the human brain that seem to play a role in the transcription regulation of GRIN2B expression. Besides the biological significance of these findings, there is also the interesting possibility of testing the clinical significance of these structures. The study of the transcription regulation of GRIN2B is significant since there have been studies that

have identified schizophrenia associated SNPs (Single Nucleotide Polymorphisms) present in and around the human GRIN2B TSS. Interestingly, these SNPs were present in the non-coding part of GRIN2B, including upstream untranslated region and intronic regions (Martucci L et al., 2006) strongly suggesting the possibility of transcription regulation mechanism abnormality in disease occurrence. This is coupled with reports of changes in the levels of GRIN2B RNA and protein in postmortem brain samples of schizophrenic and bipolar disorder patients (Martucci L et al., 2006). It is an extremely exciting time for biological and clinical research in the field of chromatin remodeling in the context of gene expression.

Introduction to higher order chromatin architecture at the GRIN2B genetic locus

It has been generally recognized that there is a non-random spatial organization of interphase chromosomes **(Figure 1.4)** due to 'loopings' and other higher order chromatin structures that bring spatially separated DNA sequences from the entire genome into close physical contact with each other (Sanyal et al. 2011) . Specifically, many chromosomal areas are partitioned into megabase-scale topological domains which are defined by robust physical interaction of intra-domain sequences in and around transcription start sites and other regulatory sequences. Chromatin loopings, in particular, are among the most highly regulated 'higher order' or 'supranucleosomal' structures (nucleosomes as the elementary unit of chromatin are comprised of 146bp of DNA wrapped around a histone H2A/H2B/H3/H4 octamer) that are pivotal for the orderly process of gene expression, by enabling distal regulatory enhancer or repressor elements positioned ten to many hundred kilobases apart from a gene to physically interact with the gene promoter (Gaszner and Felsenfeld 2006; Wood et al. 2010). In spite of the growing importance of these higher order chromatin structures for transcriptional regulation, very little is known about their existence and role in the nervous system. For example, in mouse brain and cultured CNS cells, 3-dimensional architectures have been reported for the N-methyl-D-aspartate (NMDA) receptor subunit genes Grin1/Grin2a(b), including 40kb intron-transcription start site (intron-TSS) loopings involved in transcriptional repression (Jiang et al. 2010) and activity-regulated physical interactions with nuclear cytochrome c oxidase (COX) subunit genes (Dhar and Wong-Riley 2010).

It has been proposed that 3-dimensional regulation of genome organization could play a potential role in the neurobiology of psychiatric disorders such as, for example, depression, schizophrenia and autism (Houston et al. 2013). Therefore, it will be important to explore the "epigenome in 3D" in diseased human brain tissue since the correlations are more direct given the complexity of the brain as an organ and the fact that these and most other psychiatric ailments cannot be fully modeled in animals. However, it remains to be determined whether chromosomal arrangements above the nucleosomal level are amenable to analyses in human brain and whether such types of physical interactions between noncontiguous DNA elements indeed fulfill a regulatory function. Here, we employ chromosomal conformation capture (also known as '3C') to map loop formations across a 0.7Mb region in chromosome 12p31.1, encompassing the NMDA receptor gene *GRIN2B,* a candidate 'risk' gene associated with genetic (Ayalew et al. 2012; O'Roak et al. 2012; Talkowski et al. 2012) and epigenetic (Jiang et al. 2010) occurrence of mood, psychosis and autism spectrum disorders. We identify in the prefrontal cortex collected postmortem multiple loop formations spanning up to 500kb that are associated with active gene expression and reproducible in neural differentiation assays ex vivo. We also identify a DNA element in intronic sequences proximal to the *GRIN2B* TSS associated with conserved KAP-1/SETDB1-mediated repressive chromatin remodeling, thereby antagonizing the interaction of the TSS with putative enhancer elements positioned 3' from *GRIN2B*. Our results point to a complex and dynamic 3-dimensional organization of chromosome 12p13.1, with facilitative and repressive higher order chromatin loopings competing for interaction with the *GRIN2B* TSS.

GRIN2B expression specific higher order chromatin architecture in human brain

Cortical gray matter from the rostral frontal lobe of four adult postmortem specimens, ranging in (i) age from 58 - 81 years, (ii) postmortem interval 7 - 11 hours and (iii) tissue pH 6.1 - 7.2 was used to prepare 3C libraries from DNA ligase-treated HindIII digests, in order to map physical interactions of non-contiguous DNA elements by PCR (Protocols, chapter 2). Altogether we explored 27, or 13% of all Hind III fragments encompassing 700kb on chromosome 12 (bp 13,633,410-14,333,022 in HG19). These included the *GRIN2B* transcription start site (TSS), which is defined by a sharp peak of histone H3 trimethylated at lysine 4 (H3K4me3) in prefrontal neurons (green box in **Figure 4.5**)(Cheung et al., 2010), and at least three separate DNA elements (red boxes 1-3 in **Figure 4.5**) each defined by sharp peaks of histone H3 acetylated at lysine 27 (H3K27ac) in conjunction with a corresponding spike of histone H3 monomethylated at lysine 4 (H3K4me1) extracted from published ENCODE (Encyclopedia of DNA Elements Consortium) ChIP-seq tracks from three cell lines (H1 human embryonic stem cell (H1ESC), human umbilical vein endothelial cell (HUVEC) and K562 (erythroblastoid cell). Of note, DNA elements that are defined by sharp peaks of H3K27ac in conjunction with H3K4me1 often function as active enhancers and regulate gene expression at sites of promoters positioned further up- or downstream (Maston et al., 2012).

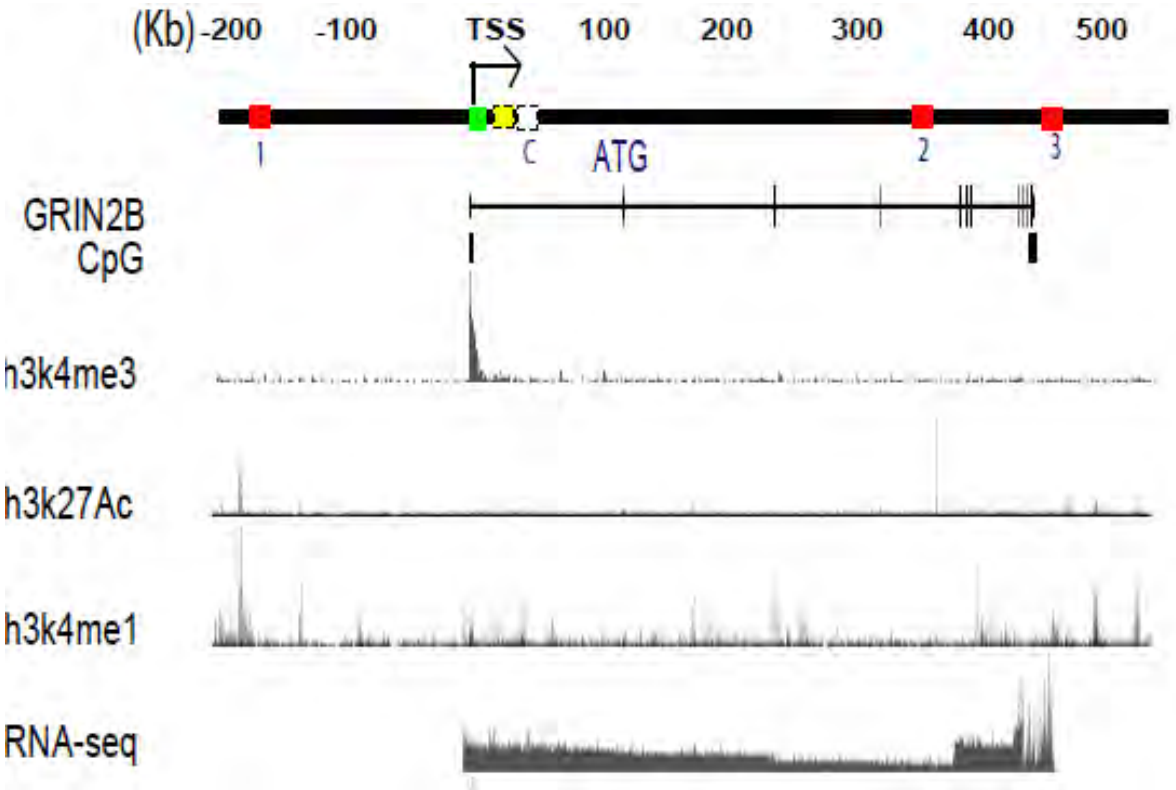
(Kb)
-200
-100
TSS
100
200
300
400
500
1
C
ATG
2
3
GRIN2B
CpG
h3k4me3
h3k27Ac
h3k4me1
RNA-seq

Fig4.5. Epigenetic modifications at the human GRIN2B (Glutamate Receptor Ionotropic – 2B) gene in a region -100Kb upstream of the GRIN2B TSS till +80Kb downstream of the GRIN2B TSS

On top is a black horizontal bar drawn to scale for the region 200Kb upstream of the human GRIN2B Transcription Start Site (TSS) to 550Kb downstream of the human GRIN2B TSS. Specific regions of interest are indicated by colored boxes [GRIN2B TSS region – green box, SETDB1 target site region – yellow box, 3C internal normalization control region – white box, enhancer regions 1,2 and 3 – red boxes]. Below is the GRIN2B transcript with exons shown as vertical lines and introns in between the exons. Note the ATG translation start site begins with exon 2 and is located 126Kb downstream of the TSS. Tracks below (top to bottom order) indicate CpG island concentrations, brain neuronal nuclei specific ChIP-sequence signals for histone 3 lysine 4 tri-methyl (h3k4me3), cell line specific ChIP-sequence signals for acetylated histone 3 lysine 27 (h3k27Ac) signal, cell line specific ChIP-sequence signals for mono-methyl histone 3 lysine 4 (h3k4me1) signal, RNA sequencing signal from brain neuronal nuclei (UCSC Genome Browser data).

Due to the fact that neighboring restriction fragments tend to show much higher interaction frequencies in 3C assays (Miele et al. 2006), DNA sequences positioned less than 25 Kb from the TSS showed, as expected, robust interactions with the 8Kb Hind III fragment containing the *GRIN2B* TSS that is used as an anchor fragment (**Figure 4.6**). Interestingly, there were also strong interactions between the *GRIN2B*-TSS containing restriction fragment with each of the 3 sites (red boxes 1-3 in **Figure 4.5**) harboring nucleosomes dually decorated with H3K4me1 and H3K27ac peaks in the peripheral cell lines (ENCODE) (**Figure 4.6**). These sites were positioned (i) 170Kb upstream (peak 1), and (ii) 350Kb downstream within intron 4 (peak 2) and (iii) 460 Kb (peak 3) downstream from the TSS 42 Kb downstream of the 3' transcript. These interactions were highly specific because no PCR product was observed in 3C assays from the same samples when processed without the critical DNA ligase step (which conjugates non-contiguous DNA elements) prior to phenol extraction and DNA purification. Furthermore, 3C assays on fibroblasts of two donors showed no evidence for physical interactions for fragments positioned > 50Kb from the GRIN2B TSS (**Figure 4.6)**, suggesting that the 3-dimensional GRIN2B conformations described here are specific for brain tissue expressing GRIN2B. In contrast to these tissue and cell-type specific differences at the GRIN2B locus on chromosome 12, the physical interaction (measured as PCR band intensities) of non-contiguous DNA elements across a 75Kb intergenic portion on chromosome 16 were similar between PFC tissue and cultured fibroblasts (mean ± S.E.M, PFC, 0.30± 0.02; fibroblasts 0.32 ± 0.01).

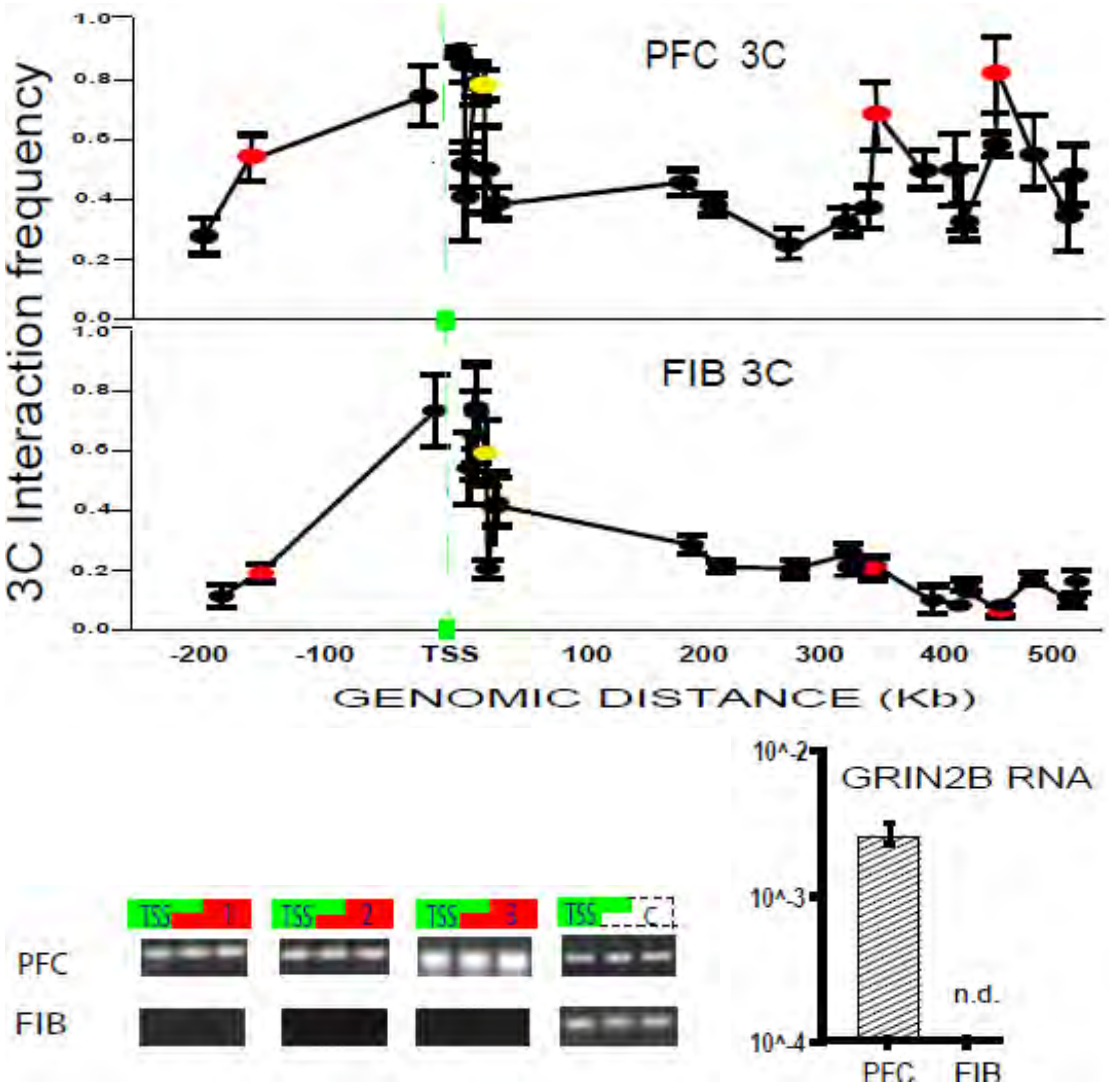
PFC 3C
FIB 3C
3C Interaction frequency
1.0
0.8
0.6
0.4
0.2
0.0
-200
-100
TSS
100
200
300
400
500
GENOMIC DISTANCE (Kb)
TSS 1
TSS 2
TSS 3
TSS C
PFC
FIB
GRIN2B RNA
10^-2
10^-3
10^-4
n.d.
PFC
FIB

Fig.4.6 Chromosome Conformation Capture (3C) at the human GRIN2B (Glutamate Receptor Ionotropic – 2B) gene reveals transcription specific long range significant physical interactions in human brain PFC (Prefrontal Cortex) nuclei
3C interaction frequency maps for PFC (prefrontal cortical nuclei) of human brain subjects (Table) and FIB (human keratinocyte derived fibroblasts). Note the striking increase in interaction frequency at active enhancer enriched h3k27Ac signal for regions 1, 2 and 3 (red dots). All interaction frequencies represented by circular data points are means +/- SEM and are measured by the average PCR product intensity (n=3) for primers amplifying across the ligation junctions of the specific interacting fragment with the TSS fragment. Each data point is an integral of interaction frequency measures from 4 human brain PFC and 3 FIB 3C libraries. PCR products for the 3 red fragments are shown in the gel below for PFC and FIB. Panel on the right shows GRIN2B RNA levels (N=3; mean +/- SD) normalized to 18S RNA for both PFC and FIB (undetectable).

GRIN2B Chromatin looping emerges during the course of neuronal differentiation

The above experiments suggest that physical interactions of open chromatin-associated DNA elements at the *GRIN2B* locus, including loop formations of the TSS with distal sequences dually decorated with enhancer-related markings, including H3K4me1 and H3K27ac, are tissue specific and readily detectable in PFC. Of note, PFC is defined by robust expression of GRIN2B RNA, in contrast to skin fibroblasts which lack detectable levels of gene expression and a tractable 3-dimensional chromosomal architecture at this locus (**Figure 4.6**). From this, one would predict that *GRIN2B* chromosomal loopings are associated with active gene expression and specific for differentiated brain tissue. To further test this hypothesis, we measured the physical interactions of intronic peak 2 and also the intergenic peak 3, both defined by robust physical interactions with *GRIN2B*'s TSS in the PFC (**Figure 4.6**), in two different stem cell lines (H9ESC and the W6 iPS) and their differentiated neural cultures primarily comprised of neurons and Nestin-immunoreactive precursor cells (**Figures 4.7, 4.8**). Indeed, both GRIN2B RNA levels and TSS-peak 3 interactions increased several-fold upon neuronal differentiation from each of the two stem cell lines (**Figures 4.7, 4.8**). These effects were consistently observed in 3/3 experiments. The observed increased TSS-peak 3 interactions were specific because PCR amplicons from TSS-peak 2 remained at very low levels in this differentiation assay (data not shown), and furthermore, the physical interaction (measured as PCR band intensities) of non-contiguous DNA elements across the 75kb intergenic portion on chromosome 16 (which remained unaffected by cellular differentiation in a previous study (Ferraiuolo et

al. 2010) were similar between stem cells (0.31 ± 0.01) and differentiated neural cultures (0.33± 0.01).

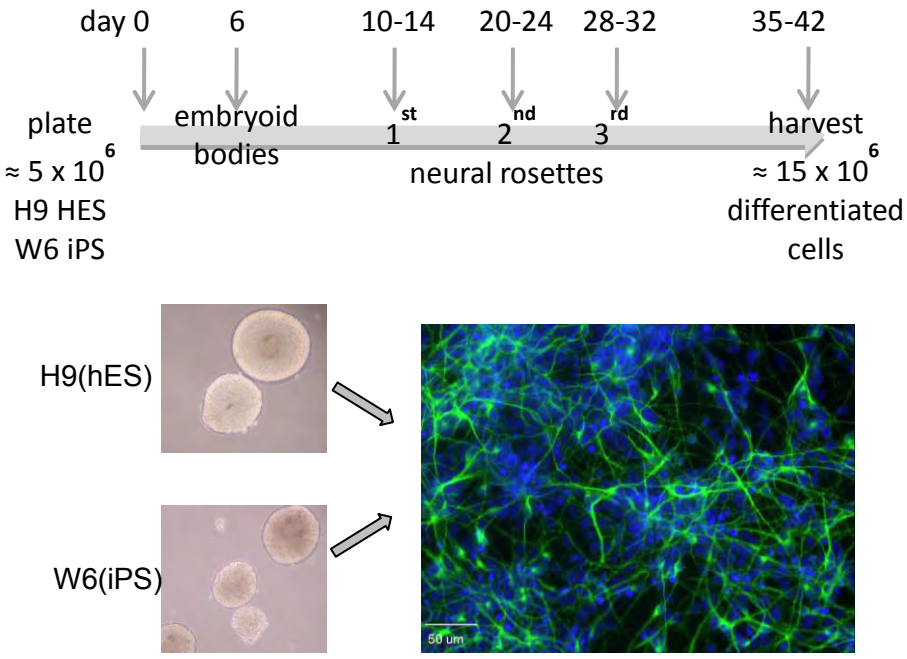

Cathy Whittle, Akbarian Lab

Fig.4.7. Characterization of GRIN2B mRNA level up-regulation in a cellular neurodevelopment model

Differentiation of iPS (Induced Pluripotent Stem) cells/ H9 HES (Human Embryonic Stem) cells to Neurons

On top is a schematic showing the timeline for the differentiation of H9 HES (Human Embryonic Stem) cells & iPS (Induced Pluripotent Stem) cells into neurons in culture. Below is an image depicting H9 HES and iPS cells in their embryoid body stage (day 6) and to the right is a fluorescence image of MAP-2 stained neuronal nuclei (green) counterstained against DAPI (blue). Presence of neuronal nuclei indicates successful differentiation (60 – 85%) although the types of neuronal nuclei present were not estimated in the differentiation assay. Samples were harvested from iPS, H9 HES and from neurons and processed for RNA quantification and 3C interaction data as mentioned in the protocols section.

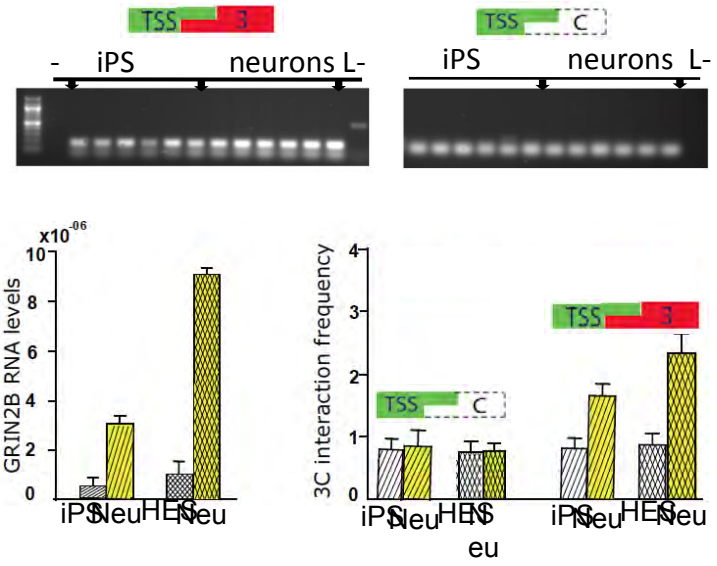
TSS
3
-
iPS
neurons
L-
TSS
C
iPS
neurons
L-
x10-06
GRIN2B RNA levels
10
8
6
4
2
0
iPS
Neu
HES
Neu
3C interaction frequency
4
3
2
1
0
TSS
C
TSS
3
iPS
Neu
HES
Neu
iPS
Neu
HES
Neu

Fig.4.8. **3C interaction pattern at GRIN2B gene locus shows an increase in interaction frequency correlating with GRIN2B mRNA up-regulation in mature neurons but not in their iPS or H9ESC counterparts**
On top is a gel with 3C PCR products run in triplicate from 2 different iPS 3C libraries, and their neuronal counterparts, as labeled, followed by the no ligase control (single last lane on the right). Gel image on the left is for the interaction between the GRIN2B TSS and region 3 while gel image on the right is for the interaction between the GRIN2B TSS and control region. Bar graph on the left shows GRIN2B mRNA normalized to 18S rRNA for iPS, H9 ESC and their differentiated neuronal counterparts. Bar graph on the right shows the interaction frequency change between iPS, H9 ESC and their differentiated neuronal counterparts between GRIN2B TSS with the control region (green GRIN2B TSS fragment with white control fragment) and GRIN2B TSS with H3K27Ac rich region 3 (green GRIN2B TSS fragment with red fragment). Bar graphs for RNA values and 3C interaction frequencies are plotted as means +/- SEM, N=3 batches per bar graph.

Non-coding sequences located within GRIN2B Higher Order Chromatin Facilitate Transcription

The results described above, including 3C assays encompassing 700kb of sequence at the site of the GRIN2B gene, indicate a subset of the chromosomal loopings that interact with the TSS in the adult PFC (**Figure 4.6**) are reproducible in the cell culture dish and emerge during the course of neural differentiation in association with a robust increase in *GRIN2B* gene expression (**Figure 4.8**). Therefore we hypothesized that DNA elements interacting with the *GRIN2B* TSS in a differentiation-dependent manner could play a role in facilitating transcription. To explore this, we focused on a 125 bp sequence (chr12:13683691-13683811, HG19) located in the center of the restriction fragment 3' from GRIN2B that interacts with the TSS (peak 3 in Figure 2) that was significantly enriched with 8 AP-1 (heterodimer of c-Jun and c-Fos) early response transcription factor motifs, which are thought to be highly regulated by neuronal activity both in human and rodent PFC (Covington et al. 2010). We fused the 125 bp DNA sequence, which showed a 10-fold higher AP-1 density compared to the rest of the restriction fragment, upstream of a minimal promoter sequence and explored changes in transcriptional activity with a luciferase assay in HEK-293 cells. Indeed, addition of the 125bp element resulted in a robust > 6-fold increase in luciferase expression and activity; compared to an AP-1 free 125bp control sequence, this effect was consistently observed in 3/3 experiments (**Figure 4.9**). These experiments strengthen the hypothesis that GRIN2B transcription is facilitated by physical interactions of the TSS with non-coding sequences positioned 500kb further downstream on a linear genome.

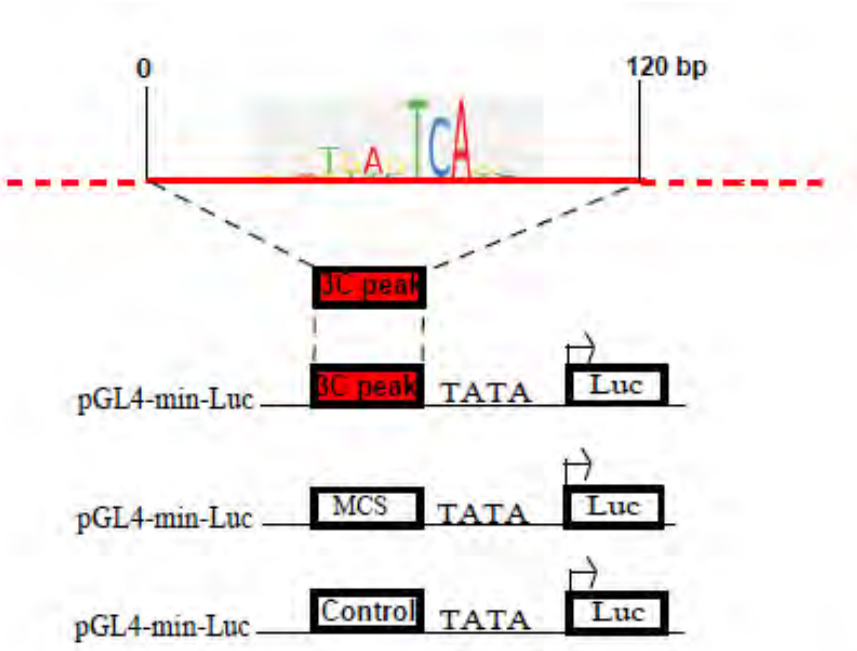
0
120 bp
3C peak
pGL4-min-Luc
3C peak
TATA
Luc
pGL4-min-Luc
MCS
TATA
Luc
pGL4-min-Luc
Control
TATA
Luc

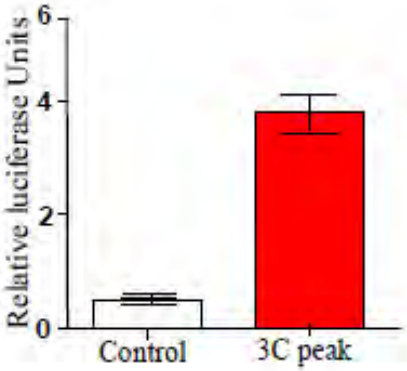
Relative luciferase Units
6
4
2
0
Control
3C peak

Fig 4.9. Luciferase reporter gene expression assay confirms enhancer potential of GRIN2B peak interacting region

Luciferase reporter gene assay schematic with the 120bp sequence within potential enhancer region 3 that is cloned into pGL4-min-Luc vector. Altogether, 3 clones were generated: 3C peak, empty vector and Control shown in order from the top to bottom for transfection assays. 3C peak region cloned has AP-1 transcription factor sites enriched in that sequence with the consensus binding site sequence for AP-1 represented in the cartoon above the 120bp red bar. Control region cloned in is a 125bp region from human GRIN2B intron 4, with no AP-1 sites. Transfection was performed in HEK cells using the lipofectamine transfection kit (Invitrogen). Selective media (200 ug/ml hygromycin) was used to propogate transfected cells which were harvested after 48hrs using the lysis protocol as described in the Promega luciferase assay kit. Firefly luciferase units were estimated in a luminometer for each of the 3 clones. In addition, the renilla luciferase vector was co-transfected into every experimental cell batch and renilla luciferase units were used for normalization in accordance with the Promega luciferase kit protocol. Luciferase units estimated were normalized for transfection efficiency and were normalized against the minimum TATA box driven luciferase to obtain relative luciferase units (RLU) plotted on the Y-axis of the bar graph (B) for control region and 3C peak region clones. Relative Luciferase Units are luciferase activity units plotted relative to the minimal promoter driven luciferase default vector system. Negative controls employed were a random plasmid vector with no luciferase gene and untransfected cell lysate (data not shown).

Opposing regulation of facilitative and repressive loopings at GRIN2B TSS in the context of repressive chromatin remodeling by SETDB1

Chromatin-associated protein complexes are of critical importance for the regulation of enhancer-TSS interactions and gene expression. For example, a protein complex comprised of the transcriptional co-activator, Mediator, together with Cohesin, a ring-shaped protein interconnecting disparate DNA elements, facilitiates enhancer-promoter loopings and active gene expression (Kagey et al. 2010). Repressive chromatin remodeling has also been implicated in higher order chromatin. For example, intronic sequences 28-31 Kb downstream from the TSS of human and mouse GRIN2B/GRIN2B show high levels of occupancy by the histone H3-lysine 9 (H3K9) specific methyltransferase KMT1E, also known as Set domain, bifurcated 1 (SETDB1). It is thought that these SETDB1-enriched intronic sequences associate with the TSS due to an interaction with the SETDB1 binding partner and transcriptional co-repressor, KRAB-associated Protein 1 (KAP-1) (Jiang et al. 2010). Consistent with this model, the density of the Krueppel-associated Box (KRAB) motif, the docking signal for KRAB-Zinc Finger Proteins (KRAB-ZNF) that act as recruitors for KAP-1 repressor, was highest at the *GRIN2B* TSS and the SETDB1 target site, in comparison to the surrounding 100kb. Therefore, we wanted to explore whether the SETDB1-mediated transcriptional downregulation of *GRIN2B* expression involves a dynamic interplay of repressive and facilitative chromatin loopings at the site of the TSS. To test this hypothesis, we generated a stable human embryonic kidney 293(HEK 293) cell line with tetracycline-inducible expression of full length human SETDB1 cDNA (**Figure 4.10**). Notably, 72

hours after induction with doxycycline, there was a robust increase in SETDB1 RNA and protein levels (which at baseline is expressed only at very low levels in HEK293), in conjunction with a several-fold decline in GRIN2B RNA, when compared to non-induced cells (**Figure 4.10**).

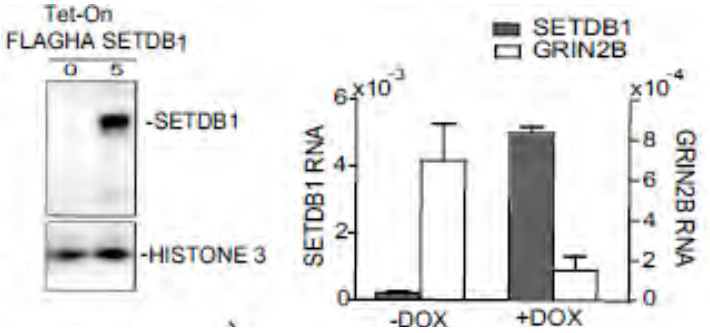

Cyril Peter, Akbarian Lab

Fig 4.10. GRIN2B RNA level is inversely related to SETDB1 expression in a SETDB1 inducible system in HEK (Human Embryonic Kidney) cells
Quality control Western Blot image for the doxycycline (DOX) induced FLAG-HA-SETDB1 vector with no SETDB1 expression detectable at 0 ug/ mL DOX and detectable SETDB1 protein (anti-FLAG antibody) upon treatment with 5 ug/ mL DOX. Histone 3 is the loading control. FLAG antibody dilution used was 1:1000 with secondary antibody dilution 1:2000 for detection by chemiluminescence.
Quantification of SETDB1 RNA normalized to 18S RNA on the left Y axis shows a 50 fold increase upon DOX (5ug/ mL) treatment with a corresponding 4-fold drop in GRIN2B RNA normalized to 18S RNA on the right Y axis. For further details on methodology and quantification, please refer to the protocols section.

As expected, and consistent with previous observations in transgenic mouse cerebral cortex and SETDB1-transfected human glioma cells (Jiang et al. 2010), upregulated SETDB1 expression and activity in HEK293 cells resulted in a strong, up to 3 fold increase in trimethylated H3K9 at the *GRIN2B* intronic SETDB1 target site (yellow box in **Figure 4.1**) and the TSS (**Figure 4.11**). Furthermore, there was a robust, approximately 5-10 fold increase in HP1 (Heterochromatin Protein 1) at the GRIN2B locus, which together with increased SETDB1 activity further contributes to heterochromatization and epigenetic silencing (**Figure 4.11**). These changes were specific, because no consistent changes were observed in levels of the open chromatin active enhancer mark, H3K27ac, across the *GRIN2B* sequences tested in this system (**Figure 4.11**). To explore whether this SETDB1-mediated downregulation in *GRIN2B* expression, and increased H3K9 trimethylation and HP1 occupancy is associated with changes in higher order chromatin at the *GRIN2B* locus, we employed 3C assays in doxycycline-induced and control HEK293. Indeed, in 3/3 experiments, doxycycline-induced cells showed a consistent, approximately 25% increase in physical interactions between the TSS and the SETDB1 target site, positioned 31Kb downstream from the 5'end of GRIN2B (**Figure 4.11**). Furthermore, after doxycycline induction, there was a corresponding decrease in TSS interactions with two of the three peak interacting fragments (peak 2, 3 in **Figure 4.11**) that had shown robust physical association with the TSS in (GRIN2B expressing) PFC and (peak 3) in neuronal cultures but not in fibroblasts or undifferentiated precursor cells that showed much lower, or undetectable levels of GRIN2B (**Figures 4.6 & 4.7**). These experiments, taken together, suggest that SETDB1-

mediated epigenetic downregulation of *GRIN2B* expression includes dynamic changes in higher order chromatin involving the *GRIN2B* TSS, including competing interactions with facilitative and repressive loop formations.

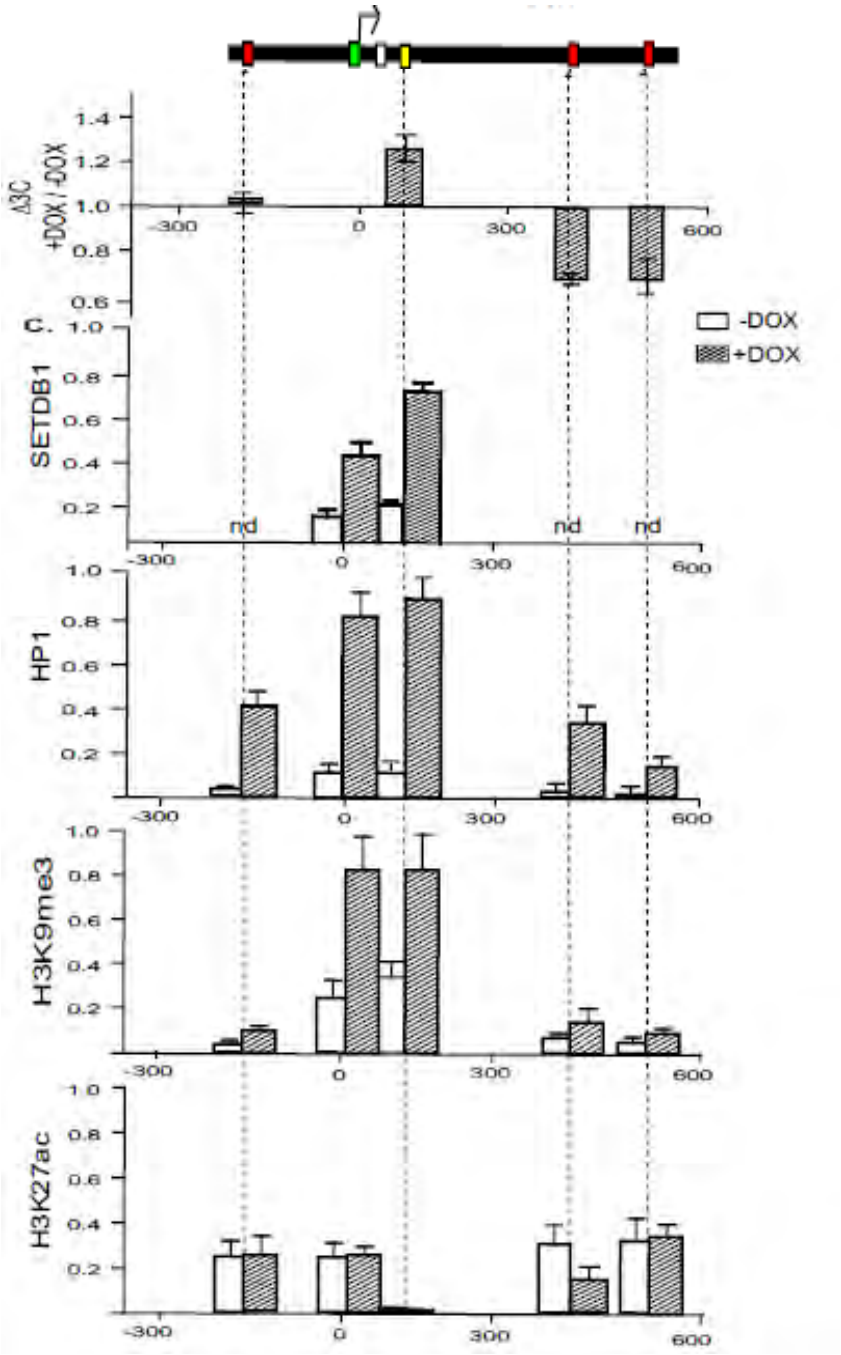
Δ3C
+DOX / -DOX
1.4
1.2
1.0
0.8
0.6
-300
0
300
600
C.
-DOX
+DOX
SETDB1
nd
nd
nd
HP1
H3K9me3
H3K27ac

Fig 4.11. SETDB1 induction leads to a change in epigenetic modifications and chromatin structure across 700 Kb of the human GRIN2B gene indicative of transcription repression

3C interaction frequency (Y-axis) is shown as a DOX (5ug/ mL)-induced fold increase (above the horizontal axis at y=1) or a fold decrease (below the horizontal axis) over vehicle treated HEK cell line culture. Data are shown for region 1, SETDB1 target site (yellow box), regions 2 and 3 from left to right. Each bar graph mean +/- SEM is an output of N=3 samples.

Below is ChIP/Input plotted on Y-axis versus genomic locations on X-axis for SETDB1, HP-1, H3K9me3 (tri-methyl Histone 3 Lysine 9) modification and H3K27Ac (acetylated Histone 3 Lysine 27) modification from top to bottom. DOX (5ug/ mL) induced HEK cell line is shaded while vehicle is shown as empty bar. Data are represented as bar graphs (N=3/ bar graph) +/- SEM shown for region 1, SETDB1 target site (yellow box), regions 2 and 3 from left to right. Where there is no signal detected, nd (none detected) is used instead of the bar. Vertical dotted lines indicate the same location they originate from on the horizontal bar shown on top to depict the GRIN2B gene including -200Kb upstream to +80Kb downstream. HP-1 antibody, Millipore, 1:1000 dilution of 1ug/ul; H3K27Ac and H3K4me3 antibodies, Abcam, 1:1000 dilution of 1ug/ul.

GRIN2B higher order chromatin in PFC of subjects with schizophrenia

Dysregulation of NMDA receptor-mediated neurotransmission plays a central role in many neurobiological models of schizophrenia and include alterations in GRIN2B/NR2B dependent glutamatergic signaling and trafficking in the PFC (Kristiansen et al. 2010). However, GRIN2B RNA levels show considerable variability between subjects and the transcript does not show a consistent disease-associated alteration (Akbarian et al. 1996; Kristiansen et al. 2006). We wanted to explore the molecular foundations for this inter-individual variability in the context of psychosis. To this end, we quantified *GRIN2B* RNA levels from the rostral PFC of 50 subjects from the Dallas Brain Collection, including 25 cases with schizophrenia and 25 controls. In agreement with earlier work with a California-based brain collection (Akbarian et al. 1996), GRIN2B levels were approximately 25% decreased in the clinical cohort, without reaching statistical significance. We then performed 3C assay on a subset of 10 schizophrenia cases with *GRIN2B* RNA levels below the 20th percentile (N=5) or above the 80th percentile (N=5) of the disease cohort. Similarly, 3C assays were conducted on the 10 (5+5) controls with RNA levels in the 1st or 5th quantile of the non-diseased group. Interestingly, schizophrenia subjects with low *GRIN2B* RNA levels showed a significant, 40% decrease in physical interaction frequencies between the TSS and the restriction fragment containing an enhancer element ('peak 3') (**Figure 4.12.A & B**). These subsets of cases

and controls showed no significant differences in age, or postmortem parameters including autolysis time and RNA Integrity Number (RIN). Therefore, we conclude that disorder and disorganization of 3-dimensional chromatin architectures at the *GRIN2B* locus may play a role in the molecular pathology of some cases on the psychosis spectrum.

4.12.A.

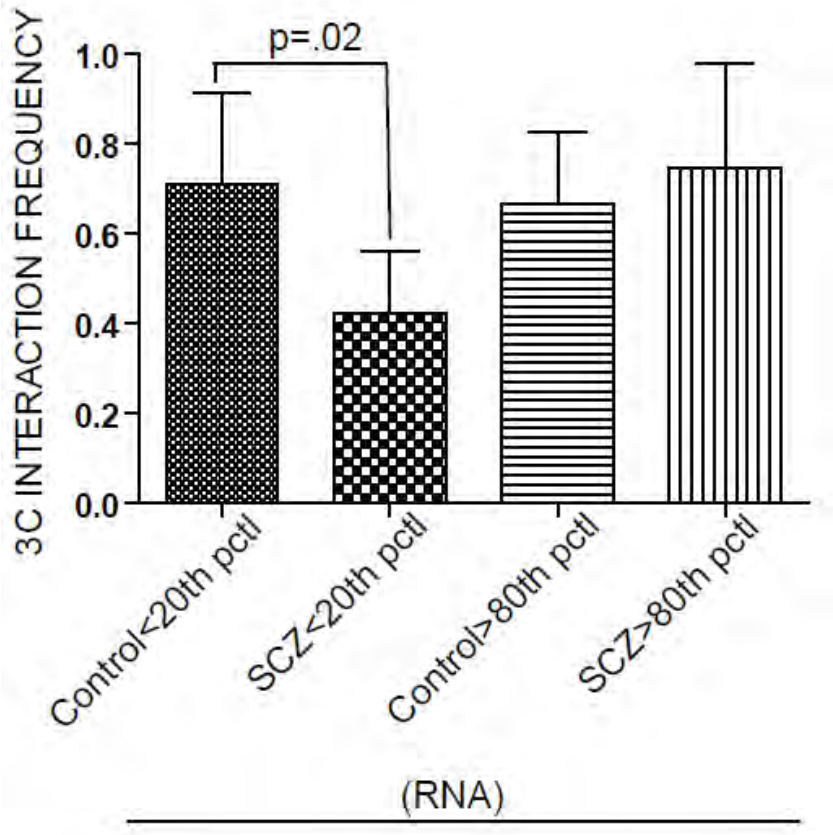
p=.02
3C INTERACTION FREQUENCY
1.0
0.8
0.6
0.4
0.2
0.0
Control<20th pctl
SCZ<20th pctl
Control>80th pctl
SCZ>80th pctl
(RNA)

4.12.B.

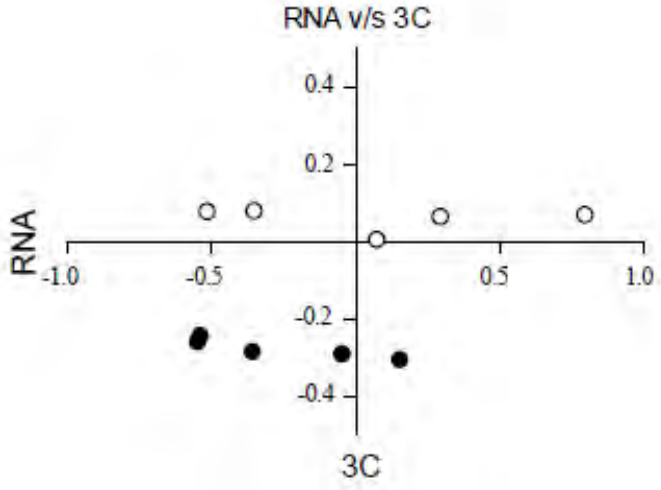
RNA v/s 3C
0.4
0.2
RNA
-1.0
-0.5
0.5
1.0
-0.2
-0.4
3C

Fig.4.12. 3C interaction frequency between enhancer region 3 and GRIN2B TSS is lower for low <20th percentile GRIN2B expressing schizophrenia brain subjects
A. 3C interaction frequency bar graphs (mean +/- SEM) for each of 4 groups left to right:<20th percentile GRIN2B expression control, <20th percentile GRIN2B expression schizophrenia, >80th percentile GRIN2B expression control, >80th percentile GRIN2B expression schizophrenia. Note the significant change in 3C interaction frequency only in the <20th percentile low GRIN2B expressing controls compared to schizophrenia groups (p=.0225 from t test, two tailed).
B. In the X-Y graph plotted below, 10 schizophrenia cases are represented by the extent of deviation of their RNA values from the mean control group RNA value (low and high considered together) on the Y axis and by the extent of deviation of their 3C interaction frequencies from the mean control group 3C interaction frequency value (low and high considered together) on the X axis. Each data point is a measure of the deviation from mean control group RNA value and mean control group 3C interaction frequency value on X and Y axes, respectively. White dots with black outlines are the 5 higher GRIN2B expression schizophrenia cases (>80th percentile). Black dots are the 5 lower GRIN2B expression schizophrenia cases (<20th percentile).

Discussion

Previous studies focused on the transcription regulation of GRIN2B have identified regulatory elements found immediately upstream of the human GRIN2B promoter but little is known about regulatory elements located several hundred Kb away (Dhar, S.S et al., 2010). Our work is a first attempt to identify where these regulatory elements might be located within a 700 Kb region surrounding the human GRIN2B TSS. Ours is also the first study to perform this chromatin architectural study in human brain using 3C, a technology that has been already established robustly, in yeast and mammalian cell cultures (Miele A et al., 2006), but not in the human brain. GRIN2B is a 418 Kb long gene and there are no genes for up to a distance of 350Kb upstream of the GRIN2B promoter, implying the strong possibility of the presence of regulatory elements in this and intronic regions of the GRIN2B gene. Besides the novelty of technology application to answer a biologically relevant question, we have also tried to explore a clinical angle for our chromatin structure findings. From the results, it is clear that there are three long range human brain specific chromosomal loops within the GRIN2B genetic region mapped. This finding is exciting, in that it is absent in the non-expressing fibroblasts, instantly suggesting that this may be an expression relevant chromosomal loop structure, relevant to the human brain. This result clearly does not imply a neuron specific looping structure, though, and it would also be important to look for this looping interaction in other tissues that express low levels of GRIN2B just to evaluate if there is any gradation observable in the level of interaction frequency across these tissues. This would give a clearer idea as to the robustness of 3C quantification done in human brain. While the

results from the neuronal cell culture offers evidence for the possible enrichment of GRIN2B chromosomal looping in neurons as compared to non-neuronal cells, it still does not clearly argue that the GRIN2B chromosomal loop detectable, is neuron specific, and only demonstrates that this loop may be developmentally up-regulated in correlation with the increase in GRIN2B RNA. The ideal experiment to perform should include a cell sorting experimental design followed by probing the neuronal and the non-neuronal fractions for GRIN2B RNA levels and 3C interactions at the GRIN2B genetic region to clearly answer the underlying question of neuronal specificity. However, the cross-linking part of the technique confounds the process of cell sorting, whereas, cell sorting without cross-linking may not preserve all the relevant chromatin architecture. Nevertheless, this approach should now be tried to see if these results can be duplicated. It must be mentioned that while chromosomal looping between peak3 and the GRIN2B TSS was robustly confirmed via sequencing, there was no detectable signal for looping between peak 1 and the GRIN2B TSS. Signal was detectable for peak2, albeit very faint, and no change in interaction frequency for peak2 was recorded between the iPS cells and neurons. The fact that the distance between peak3 and the TSS is much greater than peak1 or peak2 goes to show that there is chromosomal looping and higher order chromatin architecture across the genome that brings genetic regions located further apart on a linear scale in closer proximity so that the interaction frequency does not reflect or correlate with the linear distance factor. **Figure 4.9** is a shorter way of achieving a status of strong putative enhancer for the interacting region sequence cloned into the reporter gene assay, but needs much more experimentation before anything conclusive can be said

about the interacting region being an enhancer, relevant to GRIN2B gene expression. Firstly, there are AP-1 sites enriched in the cloned region from the interacting peak co-ordinates, but AP-1 factor is not specific to neurons only, and can also be active in HEK cells and drive reporter gene expression of luciferase. Also, the presence of AP-1 binding motifs in the sequence needs to be backed up with a chromatin immunoprecipitation experiment demonstrating the occupancy of AP-1 within the peak interacting region, around the AP-1 binding motifs. Lastly, if the peak interacting region acts as an enhancer, there is a strong possibility of detecting AP-1 signal in the GRIN2B TSS region too. Once these experiments are conducted, we can start to better understand the role that this region plays as an enhancer and if AP-1 is the transcription activator mediating enhancer function. This also then opens up new avenues of experimentation, including identifying binding partners for AP-1, or knocking down AP-1 to see if there is a decrease in GRIN2B expression, which would have to be done in a neuronal cell culture, ideally. The HEK SETDB1 inducible system is a good system to probe for SETDB1 overexpression mediated chromatin remodeling and is a great system to confirm some of the local chromatin findings from mouse GRIN2B, which include an increase in interaction frequency between the SETDB1 target site and the GRIN2B TSS coupled with an increase in HP1 signal and correlating with a decrease in GRIN2B expression. Again, there is no change in peak 1 interaction while peaks 2 and 3 show a decrease in interaction with SETDB1 overexpression. A couple of drawbacks to this experiment is the fact that there is no detectable SETDB1 signal at the far off regions and the absence of decreasing H3K27Ac signals with the overexpression of SETDB1. Finally, the clinical

data shown in figure 3.8 does explore a novel diagnostic area of clinically relevant chromatin signatures, with some serious factors that still need to be accounted for. Firstly, we need to perform these results in a greater number of schizophrenia samples to achieve better significance, and we need to establish a timeline in terms of the appearance of chromatin first that can influence GRIN2B RNA levels later. This would then be of true diagnostic significance with clinical chromatin serving a preventative purpose, since it may be manifest much earlier than the decrease observed in GRIN2B RNA levels. Secondly, schizophrenia is a polygenic illness, with many genes implicated in its etiology; therefore GRIN2B cannot be proposed forth as a sole molecular marker (Akbarian and Huang, 2006; Fung et al., 2010; Schmidt and Mirnics, 2012). Lastly, while these studies have evaluated the prefrontal cortical tissues of schizophrenia case and control subjects, there is a need to check and see if this finding is also manifest in other brain regions, known to be involved in the spectrum of symptoms seen with schizophrenia. The results presented in this study here are novel and innovative, albeit leaving a lot more work to be done, but setting a nice platform to explore chromatin architecture in the context of transcription regulation and clinical significance. There is also a dearth of appropriate disease models when it comes to schizophrenia and many other polygenic illnesses like some cancers, but the complexity of a cognitive disease is special in that it is nearly impossible to design a disease model capable of simulating the cognitive makeup and connectivity resembling the human brain. The closest animal disease model to explore would be primates, which is difficult to handle and treat and process, for emotional, technical and data validity reasons. In the absence of the right

disease models and protein pathological hallmarks, the best way to explore transcription regulation mechanism based diseases might be cellular developmental models as presented here, in this study, with confirmation of the results in diseased tissue. At this point in time, the results of such a study can purely have an impact on diagnosis and not cure, but can biologically give insight into disease mechanism and may shed some light by way of preventative care.

Summary

This is the first study of its kind performed to evaluate chromatin architecture at the human GRIN2B genetic region in brain cortex. Findings have relevance to GRIN2B transcription on account of its absence in non GRIN2B expressing human fibroblasts. The study also advances the notion that epigenetic modifications combine with higher order chromatin to influence gene regulation. This is the first attempt using a combinatorial approach of histone modification signals, chromosome interaction frequency and RNA quantification to better understand transcription regulation mechanism. Also, the fact that we have tried to explore transcription regulation from a facilitative and repressive chromatin angle, makes our study interesting. The most biologically significant result would be the decrease in interaction frequencies at far-off peaks 2 and 3, with the over-expression of SETDB1 and concurrent decrease in GRIN2B expression from the inducible HEK cell culture model. Our results here also show that there is a strong possibility that there could be an extension of histone modifications to regulatory elements from far off that come in physical contact with the gene TSS region or that histone modifications occur at regulatory elements located far off from the gene TSS. This makes us wonder if there could be pre-determined epigenetic signals at specific regulatory elements or if the regulatory elements are in constant interaction with gene TSS upon transcription and therefore is subject to histone modifications by virtue of the spatial proximity. In addition, what decides which regulatory elements come in contact with the gene TSS and what conformations are more favorable in the cell nucleus at a specific genetic region? The redundancy of regulatory elements makes this a

complicated question to answer. We must first start to map regulatory elements that play a functional role in gene transcription using chromatin techniques like 3C, ChIP-seq and RNA quantitation. Next, we should confirm enhancer potential of these elements in reporter gene assays. This is always complicated when it comes to negative regulatory elements. Once the most significant regulatory elements have been identified, targeted deletion studies must be performed to confirm the relevance or exclusivity of a particular element/s for a given gene. Identification of significant elements is critical since these may hold the key to epigenetic diagnostic tests for disease susceptibility. The presence of SNPs (Single Nucleotide Polymorphisms) within any of these functional regulatory elements is also an added degree of clinical relevance to any regulatory element mapped especially with respect to a candidate risk gene such as GRIN2B. These are exciting times in the field of chromatin dynamics analysis and understanding the relevance of higher order chromatin in a transcriptional and clinical context.

CHAPTER V

PROTOCOLS, MATERIALS AND METHODS

3C (Chromosome Conformation Capture) protocol for post-mortem human brain nuclei (1-5 million nuclei)

I. Crosslinking

1. Dounce homogenize completely, up to 0.5 gm of brain tissue in sterile 1X PBS (Phosphate Buffered Saline) containing 1.5% formaldehyde for 15 mins at RT.
2. Add glycine to a final concentration of .125M and keep at RT for 5 min.
3. Centrifuge at 4000 rpm --- 10 min at 4ºC.
4. Resuspend the cell pellet in 2mL of lysis buffer and incubate at RT for 45 min. Observe the pellet swell.
5. Pipette up and down (~50 times) with constant force taking care to see no air bubbles develop.
6. Spin down at 5000 rpm --- 5 min and remove the supernatant.
7. Resuspend pellet in 1mL 1X NEB buffer (check buffer compatibility with restriction enzyme of choice) centrifuge at 5000 rpm at RT --- 5 min – Repeat once.
8. Resuspend pellet in 3mL of 1X NEB buffer to ensure that there are no clumps.

II. Digestion

9. Distribute 362 µl of the cell pellet to each microcentrifuge tube (~8 tubes).

10. Add 38 µl of 1% SDS per tube and mix well by inverting the tube.
11. Incubate at 65ºC --- 10 min (this will remove the proteins that are not crosslinked to the DNA)
12. Add 44 µl of 10% Triton X-100 to each tube and mix well by inverting to avoid air bubbles (to quench SDS)
13. Add 20 µl of Hind III (400U) per tube, mix well and incubate at 37ºC overnight. Incubate with gentle shaking to maximize enzymatic action.
14. Add 86 µl of 10% SDS and incubate at 65ºC --- 30 min to inactivate the enzyme

III. Ligation and reverse crosslink

15. Prepare the ligation cocktail according to the table below and distribute ~7.6ml (assuming an approximate volume of 400µl of restriction digested sample) of cocktail to a cold 15 ml conical tube

Ligation cocktail	*per reaction*
10% Triton X-100	800 µl
10X Ligation buffer	800 µl
10 mg/ml BSA (100X, NEB)	80 µl
100 mM ATP	80 µl
water	5840 µl (assuming a 400ul sample vol.)

16. Transfer restriction digested sample from Step 14 into each 15 ml conical tube.
17. Add 40µl of T4 DNA ligase (Invitrogen, 1 U/ µl) per tube
18. Incubate at 16ºC --- 6 hrs with intermittent inverting of tubes every hour.
19. Add 50 µl of 10 mg/ ml proteinase K per tube
20. Incubate at 65ºC overnight.

IV. Purification

21. Add 50 µl of 10 mg/ ml proteinase K per tube and incubate at 65ºC --- 2hr
22. Transfer ligated sample into clean 250 ml centrifuge tube (max 100mL in 1 tube).
23. Add equal volume of phenol (pH 8.0) per tube, vortex well for 2 min and then spin at 4000 rpm --- 15 min
24. Transfer supernatant to fresh 250 ml centrifuge tubes (most of the DNA is close to the interphase; supernatant is a bit cloudy). Note that no part of the organic phase should be transferred. If this occurs, repeat step.
25. Add equal volume of phenol: chloroform (1:1; pH 8.0) per tube, vortex well for 1 min and spin at 4000 rpm --- 15 min
26. Transfer aqueous phase into a 250-ml conical centrifuge tube (supernatant should be clear). Note that no part of the organic phase should be transferred. If this occurs, repeat step.
27. Add 1X TE buffer (about 10% total volume of aqueous phase), pH 8.0 per tube (dilution might help to prevent DTT precipitation)

28. Add 3M sodium acetate, pH 5.2 (10% total volume), vortex briefly and add, 2.5 times the total volume, 100% ice-cold ethanol, mix gently by inverting the tube.
29. Incubate at -80ºC overnight.
30. Spin at 6500 rpm --- 30 min at 4ºC
31. Dissolve pellet in 1mL of 1X TE buffer, pH 8.0 and transfer to a RNase/DNase free 2mL tube.

(if dissolving is difficult, put samples at 70ºC for 10 minutes.)

32. Add an equal volume of phenol, pH 8.0, to each tube and vortex well for 1 min; then spin at full speed (benchtop centrifuge) for 5 min
33. Transfer the upper aqueous phases to fresh 2mL autoclaved tubes
34. Add an equal volume of phenol:chloroform (1:1, pH 8.0), vortex well for 30 sec and spin at full speed (benchtop centrifuge) for 5 min

    Note that there is the possibility to also perform a single chloroform reaction to remove last traces of phenol in case the supernatant is turbid.
35. Transfer the aqueous phases into a 15mL centrifuge tube.
36. Add 1/10 volume of 3M NaAc, pH 5.2, vortex briefly
37. Add 2.5 volumes of 100% ice-cold ethanol, mix gently by inverting the tube.
38. Incubate at -80ºC for at least 3 hrs.
39. Transfer into 2mL autoclaved tubes and centrifuge at top speed in a refrigerated benchtop centrifuge for 30 min

40. Wash the pellets in 1 ml of room temperature (RT) 70% ethanol and spin at RT, full speed on a benchtop centrifuge for 10 min
41. Repeat ethanol wash several times until pellets "collapse" (~7 times)

    Note that RT washes will wash off more salt due to higher solubility. Pellet volume decreases and general consistency is crisper after each wash which is essential for superior 3C library quality.

42. Dissolve a single pellet in a volume of up to 250µl of 1X TE buffer, pH 8.0
43. Add 1µL of 10 mg/mL of DNase-free, RNase A and incubate at 37ºC for 15 min
44. Load 1 µL and 2 µL of 10X diluted template on 1% agarose/1X TAE gel, along with 1Kb DNA ladder; quick run to check quality and quantity of the template
45. Store this 3C template up to 2 years at -20ºC

3C-PCR set up:

46. Primers for a 3C PCR reaction are designed in the same orientation (5'-3', 30 – 32 nucleotides in length, Tm = 60C, within 200 base pairs of the restriction site). These parameters offer a certain level of consistency for every PCR product generated from a 3C library. In addition, to account for the differences in the quantification of PCR products due to primer pair efficiency variations, a control 3C template library including the region from the genomic template you are probing for 3C interactions is generated from a BAC (Bacterial Artificial Chromosome) clone. The specific protocol with

materials and reagents used to generate a BAC 3C control template is as mentioned in the 3C methodology paper (Miele A et al., 2006).

Table generated for 1 reaction tube:

10x PCR	2.5
50mM $MgSO_4$	2
25mM Dntp	0.2
100µM primer 1	0.1
100µM primer 2	0.1
Taq	0.2
Water	15.9
Total	21

Add 4µL of 3C library template to bring the total volume of the PCR reaction mix to 25 µL.

Materials:

Buffer solutions:

1X TE pH8.0

10 mM Tris-HCl pH8.0

1 mM EDTA pH8.0

Use autoclaved water.

Store at 4°C.

10X Ligation buffer

500 mM Tris-HCl pH7.5

100 mM $MgCl_2$

100 mM DTT

Autoclaved MQ

Store at -80°C

100 mM ATP

Dilute in autoclaved water. Store 1mL aliquots at -80°C

1X Lysis buffer (50 ml)

10 mM Tris-HCl pH8.0

10 mM NaCl

0.2% Ige cal CA630 (NP40)

Dilute with autoclaved water

Store at 4°C

Proteinase K

Dissolve Proteinase K in 1X TE buffer, pH 8.0, at a concentration of 10 mg/ml. Aliquot and store at -20°C.

10X PCR buffer

600 mM Tris–H_2SO_4 (pH 8.9)

180 mM ammonium sulfate (Sigma Aldrich, A-4915)

Reagents

- MilliQ autoclaved water to be used in all solutions

- Chemical hood station approved for work with human tissue samples
- 37% (vol/vol) formaldehyde solution (Sigma Aldrich, 533998-500ML)

  Make sure that the formaldehyde solution is not older than 6 months to 1 year. If the reagent is older than 1 year, crosslinking efficiency is lower.
- Glycine (Fisher, cat. no. BP381-1)
- Protease inhibitor cocktail (Sigma Aldrich, P8340)
- 10 X restriction enzyme buffer (New England Biolabs – please choose according to your restriction enzyme of choice)
- 10% (wt/vol) SDS (Biorad, 161-0418)
- 10% (vol/vol) Triton X-100 (VWR, cat. no. VW3929-2)
- 10X T4 ligation buffer: 500 mM Tris–HCl (pH 7.5), 100 mM magnesium chloride (Fisher, cat. no. BP214-500), 100 mM DTT (Fisher, cat. no. BP172-25)

  Aliquot ligation buffer into 15mL BD falcon tubes and freeze at −80 °C. Avoid repeated freeze–thaw cycles.
- BAC clones (Invitrogen, http://clones.invitrogen.com; CHORI, http://bacpac.chori.org)
- 10 mg ml^{-1} BSA (NEB, cat. no. B9001S)
- ATP (Sigma, cat. no. A9187-1G)
- T4 DNA ligase (Invitrogen, cat. no. 15224-090)
- 10 mg ml^{-1} Proteinase K in 1 × TE buffer, pH 8.0 (Invitrogen, cat. no. 25530-031)
- Phenol (pH 6.6; Fisher, cat. no. BP1750-400).

  Please note that it is necessary to add the 1M Tris buffer supplied with the

phenol to the bottle, mix well and stand for 1 hour prior to use. This will ensure that phenol pH is 8.0 which is necessary for the extraction of ligated DNA fragments. Store at 4ºC.

Caution: Toxic and corrosive material. Wear protective gear in a chemical fume hood when handling.

- Phenol Chloroform - 1:1, pH 8.0 (Fisher, cat. no. BP1752-400). **Please note that it is necessary to add the 1M Tris buffer supplied with the phenol chloroform bottle, mix well and stand for 1 hour prior to use. This will maintain the reagent at a pH of 8.0 for longer storage periods.**

  Caution: Toxic and corrosive material. Wear protective gear in a chemical fume hood when handling. Store at 4ºC.
- 3 M sodium acetate (pH 5.2; Fisher, cat. no. BP333-500)
- Absolute ethanol 200 proof
- 10 mg ml^{-1} RNase A (DNase-free) in H_2O (Sigma, cat. no. R6513-50MG)
- Agarose (Invitrogen, cat. no. 15510-027)
- Large-construct DNA purification kit for generation of BAC library (Qiagen, cat. no. 12462)
- 5 U μl^{-1} *Taq* DNA polymerase (NEB, cat. no. M0267L)
- dNTP mix (25 mM each; Invitrogen, cat. no. 10297-018)
- 50 mM magnesium sulfate (Sigma, cat. no. M2773-500G)
- 1-kb DNA marker of known concentration (e.g., 1-kb DNA ladder; NEB, cat. no. N3232L)

- Low-molecular-weight DNA markers of known concentration (e.g., 100-bp DNA ladder; NEB, cat. no. N3231L)
- MinElute PCR purification kit (Qiagen, cat. no. 28004)
- Ethidium bromide 10mg/mL

Equipment

- Glass homogenizer
- Automated thermal cycler
- UVP Bioimaging gel documentation system featuring a 12-bit digital camera coupled to the LabWorks 4.5 computer software for quantifying PCR products

4C (Chromosome Conformation Capture coupled with Chromatin Immunoprecipitation) protocol for post-mortem human brain nuclei (1-5 million nuclei)

I. Crosslinking

1. Dounce homogenize completely, up to 0.5 gm of brain tissue in sterile 1X PBS containing 1.5% formaldehyde for 15 mins at RT.

2. Add glycine to a final concentration of .125M and keep at RT for 5 min.

3. Centrifuge at 4000 rpm --- 10 min at 4ºC.

4. Resuspend the cell pellet in 2mL of lysis buffer and incubate at RT for 45 min. Observe the pellet swell.

5. Pipette up and down (~50 times) with constant force taking care to see no air bubbles develop.

6. Spin down at 5000 rpm --- 5 min and remove the supernatant.

7. Resuspend pellet in 1mL 1X NEB buffer (check buffer compatibility with restriction enzyme of choice) centrifuge at 5000 rpm at RT --- 5 min – Repeat once.

8. Resuspend pellet in 3mL of 1X NEB buffer to ensure that there are no clumps.

II. Digestion

9. Distribute 362 µl of the cell pellet to each microcentrifuge tube (~8 tubes).

10. Add 38 µl of 1% SDS per tube and mix well by inverting the tube.

11. Incubate at 65ºC --- 10 min (this will remove the proteins that are not crosslinked to the DNA)

12. Add 44 µl of 10% Triton X-100 to each tube and mix well by inverting to avoid air bubbles (to quench SDS)

13. Add 20 µl of Hind III (400U) per tube, mix well and incubate at 37ºC overnight. Incubate with gentle shaking to maximize enzymatic action.

14. Incubate at 65ºC --- 20 min to inactivate the enzyme

15. Place samples on ice immediately. Proceed to set up samples for Antibody treatment to immunoprecipitate restriction digested chromatin.

16. Add 200µL of 10X FSB (FACS sorting buffer) to the restriction digested chromatin fragments followed by the addition of 1µL of 0.1mM benzamidine, 1uL of 0.1mM PMSF (Phenyl methyl sulfonyl fluoride) and 1µL of 3 mM DTT (Di-ThioThreitol) and make up the volume with milliQ autoclaved H_2O.

17. Add up to 1µg of specific chromatin protein antibody that you wish to pull down associated fragments of.

18. Rotate in a 15mL conical tube at 4ºC O/N to achieve sufficient immunoprecipitation.

19. Prepare Protein G agarose beads for pull down of antibody chromatin complexes.

(Always remember to pipette beads using pipette tips with a large orifice so that the beads do not get damaged or loose their spherical conformation. We use only 1mL or 200μL tips with the heads cut off for this purpose)

20. Pipette out 250μL of beads for use with each rotating tube of sample. Spin down beads in suspension at 1000 rpm for 30 seconds. Wash with 1X FSB buffer and spin down at 1000 rpm for 30 seconds. Repeat.

21. Add the entire amount of beads to the tube and rotate at 4ºC for 2 hours.

22. Centrifuge sample at 1000 rpm for 2 minutes. Preserve supernatant for later quality control analysis.

23. Resuspend beads on ice in 1X ligation buffer and proceed to perform 3C ligation according to the table from the 3C protocol treating the beads equivalent to the restriction digested sample in the 3C protocol.

24. Ligation can be performed overnight or for 6 hours at least.

25. Centrifuge at 1000 rpm for 1 minute. Remove supernatant. Proceed to wash the beads with different wash buffers (compositions provided at the end of the protocol).

26. Wash beads from each tube with 1mL of each washing buffer.

27. Rotate for a specific time which is different for different buffers:

Low salt washing buffer (3 min), High salt washing buffer (1 min), lithium chloride solution (1 min), 1X TE buffer (3 min).

28. After rotation with each buffer, centrifuge at 1000 rpm for 1 min. Discard supernatant carefully and proceed to the next wash buffer in the sequence above.

29. Make fresh elution buffer and add 250µL of elution buffer for beads from 1 tube.

30. Rotate for 15 mins. Centrifuge at 2000 rpm for 1 min. Transfer supernatant to a 2mL O-ring centrifuge tube.

31. Add another 250µL of elution buffer to the beads and vortex vigorously for about 15 mins. Centrifuge at top speed in a benchtop centrifuge for 10 mins. Transfer supernatant to the same 2mL tube from above.

32. Proceed to add 10µL Proteinase K (10mg/mL) to the eluted mixture and incubate at 65ºC for 4 hours with intermittent shaking in between.

33. Perform phenol followed by phenol chloroform extractions as described in the 3C protocol in accordance with the pH and buffer compositions.

34. Proceed to perform ethanol extraction as described in the 3C protocol above.

35. Incubate at -80ºC for at least 2 hours.

36. Ethanol washes are to be performed as in the 3C protocol least 8 times even after the pellets collapse since the degree of sensitivity by PCR detection should allow for the detection of fragments with very low interaction frequencies.

37. Proceed to detect using PCR according to the 3C-PCR conditions and buffers.

38. Controls:

A. No antibody control that is essentially a 4C library prepared with the entire protocol but without an antibody. Ideally, this control should not yield a product.

B. No ligation control that is essentially a 4C library prepared with the entire protocol with no ligase added in the ligation step. This control should definitely not yield any product.

Materials:

Buffer solutions:

All buffers included here are specifically for the 4C (3C-ChIP) protocol. Buffers for the 3C protocol are included in the materials section from 3C above.

1 X FSB Buffer:

20mM Tris.Cl [pH 7.5]

5mM EDTA

50mM NaCl

Low Salt Washing Buffer 1X

[2mM EDTA/20mM Tris.Cl [pH 8.0]/500mM NaCl/0.1% sodium

dodecyl sulfate (SDS)/1% Triton X-100]

High Salt Washing Buffer 1X

[2mM EDTA/20mM Tris.Cl [pH 8.0]/500mM NaCl/

1% sodium dodecyl sulfate (SDS)/1% Triton X-100]

Lithium Chloride Wash Solution 1X

(250mM LiCl/1mM EDTA/10mM Tris.Cl [pH 8.0]/1%

IGEPAL-CA360/1% deoxycholic acid)

Elution Buffer 1X

100mM $NaCO_3$

1% SDS

Dilute with milliQ autoclaved H_2O to the desired volume.

Materials& Reagents:

Materials and Reagents provided here are specifically for the chromatin immunoprecipitation, bead mediated immune complex pull down and elution of complexes part of the 4C protocol and do not include the reagents for the chromosome conformation capture part. Please refer to the previous 3C protocol materials section for a complete list of required materials.

1. Benzamidine (0.1mM stock aliquots)

2. Phenylmethylsulfonyl fluoride (PMSF) (0.1mM stock aliquots)

3. 1,4-dithio-DL-threitol (DTT) (3 mM stock aliquots)

4. Protein G agarose slurry (Qiagen)

5. Antibody of choice (1µg/µL stock concentration)

Cross-linked Chromatin Immunoprecipitation (ChIP) coupled with quantitative PCR for mammalian cell culture, neuronal cells, human brain & mouse brain tissue

All ChIP experiments were performed according to the protocol specified in the Akbarian Lab publication by Hsien-Sung Huang:

Journal of Neuroscience Methods 156 (2006) 284–292

Lysis for the human brain, mouse brain and HEK cell samples were done using the 3C lysis protocol since that worked consistently well for all samples processed. There were minor modifications made to the sonication step with regards to the microtip output and the number of cycles of sonication used for a specific sample. That variation was made after running sonicated sample (5μL) on a 1% agarose gel in TAE (Tris-Acetate EDTA) buffer to look at the degree of sonication achieved, which can vary between sample to sample processed.

RNA isolation and quantification using reverse transcription real time PCR for mammalian cell culture & human brain tissue samples

Total RNA was isolated and purified from brains by using RNeasy Lipid Tissue Mini kit (Qiagen, Valencia, CA). Samples were treated with DNase I to avoid DNA contamination and further processed using the 1-step RT-RTPCR kit from Applied Biosystems using SYBR® Green to quantify RNA levels from samples. All RNA levels quantified were quantified as mean Ct values and corrected for differences in primer pairs using the equation: RNA level = (1+E)^Ct, where E = E max/ E primer pair with E max =

1.443 (1/ln 2) that corresponds to a maximum primer efficiency of the theoretical 2-fold increase with a single cycle of amplification. RNA levels were then normalized to 18S rRNA levels calculated using the same equation from above.

Fluorescence Activated Cell Sorting (FACS) for mouse brain nuclei

FACS sorting for CamII-H2B-GFP involves the following steps- (1) extraction of nuclei from the tissue, (2) ultracentrifugation, (3) immunolabeling and (4) fluorescence-activated sorting and these steps were performed exactly as outlined in the protocol mentioned in the publication : BMC Neurosci. 2008 Apr 28;9:42. doi: 10.1186/1471-2202-9-42.

Enhancer expression using the luciferase reporter gene expression assay system

Luciferase reporter gene assays were performed using the minimal promoter (TATA box) luciferase vector (pGL4.23 [luc2/minP] Vector; Promega-E8411) in HEK-293 cell cultures. Human genomic sequence was cloned into the multiple cloning site (MCS) of the luciferase vector. Sequence verified clones were transfected into HEK-293 cells using the Invitrogen Lipofectamine-2000 transfection kit. Renilla luciferase vector (Prl-TK; Promega-E2241) was co-transfected into every well to control for variations in transfection efficiency. Cells were harvested and lysed 48h post transfection using lysis buffer from the Promega luciferase assay kit (catalog no. E1910). Firefly luciferase units were quantified (kit luciferase substrate) using Biorad luminometer followed by measurement of Renilla luciferase units by chemiluminescence (kit Stop& Glo reagent)

according to the kit protocol. Relative Luciferase Units (RLU) were calculated (post transfection efficiency normalization) relative to minimal TATA box driven luciferase units. Data were then plotted to demonstrate enhancer potential of cloned regions to drive luciferase expression over that of minimum TATA box driven luciferase expression.

Protocol for the differentiation of Induced Pluripotent Stem (iPS) Cells to mixed neuron cultures

Below is outlined a very detailed protocol with images to assist the description.

<u>W6 iPS cells</u>: Generated from human fibroblast by Dr Rasmussen's Laboratory, University of Connecticut.

W6 induced Pluripotent Stem Cells were grown feeder free on 0.33mg/ml Matrigel (BD#356231) coated 6 well plates. 6 well plates were coated with 0.33mg/ml Matrigel in DMEM/F12 media for 30 mins at room tempreture. The Matrigel was then aspirated and replaced with media. Before splitting, W6 cells were weeded to remove any sign of differentiating cells. W6 iPS colonies were split by scoring colonies in a hatched pattern, rinsing plates with DMEM/F12 media then 1mg/ml dispase (a protease suited for the gentle dissociation of a wide variety of tissue) for 2-3 minutes. Then aspirate the dispase, wash twice with DMEM/F12, add 1ml mTeSR (maintains pluripotency of cells for prolonged periods) media and scrape off the colonies with a 10ml glass pipet. Spin down the colonies and resupend in fresh mTeSR media (Stem cell technologies Inc #05851), splitting one well into one 6 well plate. Cells were split approx every 5-7 days.

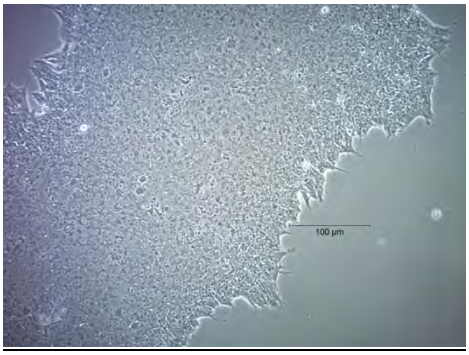

Fig 5.1. W6-iPS (Induced Pluripotent Stem) colony ready to make embryoid bodies.

Formation of Embryoid bodies from W6 iPS: We found it difficult to make good embryoid bodies by the method used for H9 embryonic stem cells as the iPS cells were less sticky and tended to fall apart and not form good embryoid bodies. We used AggreWell 400 plates (AggreWell plates promote the formation of uniform embryoid bodies from iPS and ES cells; stem cell technologies #27845). One 6 well plate of W6 iPS colonies was rinsed with PBS and Accutase (proteolytic agent similar in action to trypsin but is less harmful to cells and purer; Invitrogen#07920) 0.75ml/well added and incubated 37 2-5 mins. The dissociated iPS colonies were titrated to separate cells and collected into a 15ml centrifuge tube. The wells were washed with DMEM/F12 and the washings added to the tube. The cells were spun at RT for 5 mins and re-suspended in AggreWell media (stem cell technologies #05893) and counted. 1.2x 10^6 cells were added per well in 2mls of AggreWell media with 10μM Y-27632 Rock inhibitor(stem cell technologies #07171) on the AggreWell Plate as per the directions from stem cell technologies. The plates were incubated for 24-48hours until embryoid bodies could be clearly seen changing 50% of media after 24 hours without disturbing the cells.

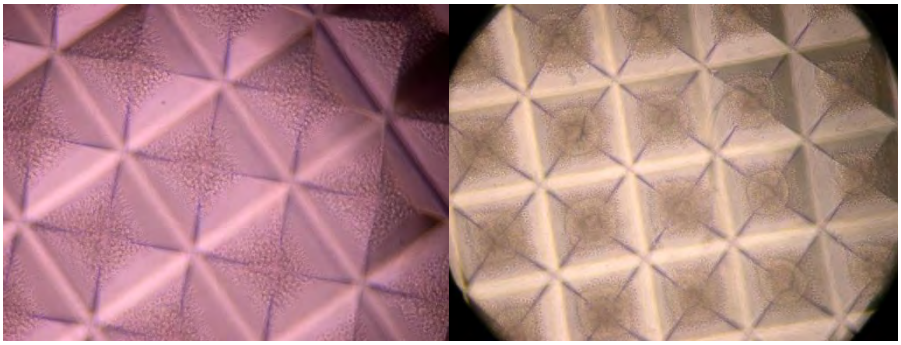

AggreWell 0hours **AggreWell 48hours**

Fig 5.2 Embryoid body formation 48 hours post addition into Aggrewell plates

After the embryoid bodies have formed they are washed out of the well using a 1ml pipet tip and DMEM/F12 media. Strained through a 40μM Cell strainer (stem cell technologies #27305) and cultured in AggreWell media in a low adherence T25 for 2 more days, changing the media daily. Day 4 the media was changed to 50% Neural Induction media/ 50% AggreWell media and day 5-6 100% Neural Induction media (serum free media that stimulates the formation of neural progenitor cells/ neural rosettes) +10ng/ml bFGF.

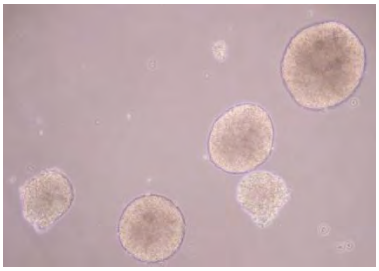

Fig 5.3. Day 6 iPS Embryoid Bodies

iPS Differntiation:

On Day 6 the embryoid bodies from iPS are collected, re-suspended in fresh Neural Induction media+10ng/ml bFGF (basic Fibroblast Growth Factor) and plated on 10cm tissue culture plates which have been treated with 15µg/ml Poly-l-ornithine (Sigma #P3655) for 2 hours, then washed with PBS twice for 30 mins at 37°C, then coated with 3mls of 20ug/ml Laminin(invitrogen #23017-015)/DMEM-F12 for 2 hours to overnight. The media is changed every other day.

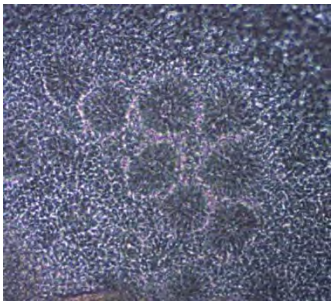

Fig 5.4 iPS Embryoid bodies Day 10

Around Day 10-14 (4-8 days after plating on laminin) the primary neural tube like rosettes are harvested. The plate is washed with warm DMEM/F12 and then 0.5mg/ml Dispase sterile filtered in DMEM/F12 is added for 2-5 minutes at 37°C. This just loosens the rosettes, but does not detach them. The plate is gently washed twice with DMEM/F12 then 5 ml fresh DMEM/F12 added and the rosettes are pushed off the plate using a 10µl tip under the microscope. The collected rosettes are spun for I minute low speed and then resuspended in Neural Induction media + 10ng/ml bFGF in a low adherence flask.

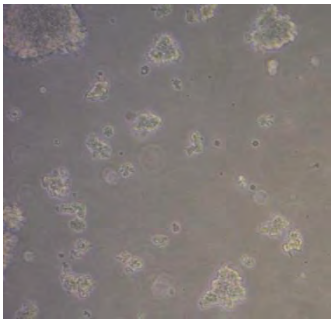

Fig 5.5 Floating neural rosettes observable 1 day post plating in neural induction media in a low adherence flask

The neural rosettes are grown for 2 days in suspension, changing the media daily by allowing the rosettes to settle and removing 90% of the media and replacing with fresh media. After 2 days (approx 12-14 days from starting the protocol) the primary neural rosettes are plated on laminin coated plates in Neural Induction media +10ng/ml bFGF. After 24 hours the media is changed to Neural Proliferation Media (Dhara et al., 2008) but with added N2 Supplement. (475mls Neurobasal Media (Invitrogen#21103), 5mls L-glutamine/glutamax mix (Invitrogen#45000-676 and 35050-061),10 ml B27 supplement (Invitrogen#17504-044), 5 ml N2 supplement (invitrogen#17502-048) and 5 ml Pen/strep with 20ng/ml bFGF and 10ng/ml LIF (Recombinant Human Leukemia Inhibitory Factor R alpha - a lymphoid factor which promotes long-term maintenance of embryonic stem cells by suppressing spontaneous differentiation., R&D systems #249-LR-050/CF.) This was found to be the best media for neural proliferation.

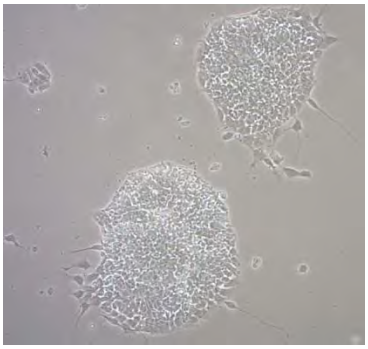

Primary neural rosettes one day after plating on laminin. The N2 supplemented Neural Proliferation Media was changed every other day.

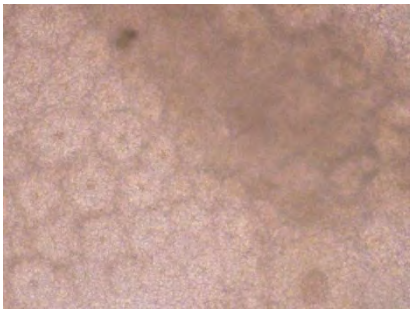

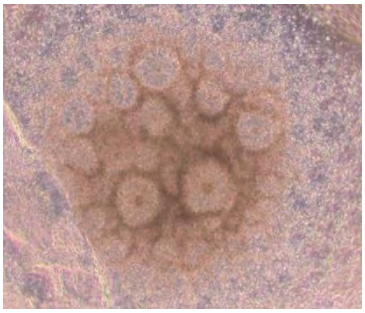

Secondary neural rosettes 12 days after plating- day 24.

Fig.5.6 Neural rosettes post plating on laminin in neural proliferation media

Collection of Secondary Neural Rosettes: After 6-12 days, much more prominent neural rosettes can be seen under the microscope (approximately 24-26 days into the protocol). These are collected by rinsing the plate with HBSS solution (25 ml 10xHBSS (Invitrogen #14185-52), 0.86 ml 45% glucose solution (Sigma #G-8769), 3.55 ml 10x HEPES (Invitrogen#15630-080) in 250 sterile water-all sterile filtered. Add fresh warm HBSS to the plate and scrape the secondary rosettes into the HBSS. Then spin the rosettes for 1min and re-suspend in fresh N2 Neural proliferation media in a low adherence flask. If the neural rosettes are in less defined areas you can gently pipette the HBSS over the entire plate several times and this will dislodge the neural rosettes whilst leaving the majority of the flat unwanted cells behind.

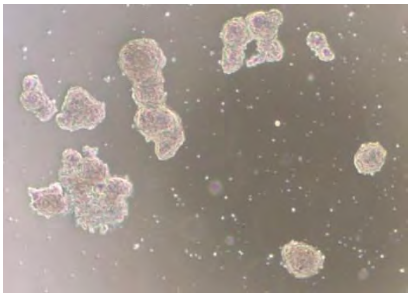

Fig. 5.7 Secondary neural rosettes 1 day in suspension in neural proliferation media in a low adherence flask

After 2 days in suspension, the secondary neural rosettes are plated on fresh laminin coated plates in N2 supplemented neural proliferation media as above but with the addition on 200ng/ml SHH for 24-48 hours (Recombinant Human Sonic Hedgehog, R&D Systems #1314-SH/CF). Without the addition of the SHH, the survival rate of the re-plated neural rosettes is much reduced. The media is changed every other day. The secondary neural rosettes expand, some start to become neural stem cells and others form tertiary neural rosettes.

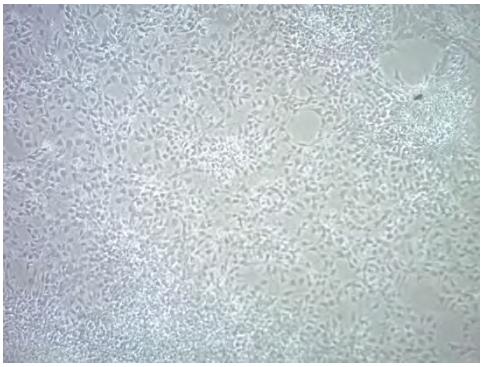

Fig. 5.8 Day 30 neural stem cells growing out from the plated secondary neural rosettes on laminin in neural proliferation media, N2 supplemented with 200ng/ml SHH (Sonic Hedgehog)

Collection of tertiary neural rosettes and human neural stem cells:

At this stage, some cultures are almost all neural stem cells. If this was the case, the plates were weeded to remove unwanted cell types, rinsed with PBS and then cells collected with Accutase, titrated to ensure a single cell suspension, diluted with media and spun for 5 min in a bench top centrifuge. The cells live were counted and the suspension re-plated on laminin plates at approx 3.5 $x10^6$ cells per 10cm plate in N2 supplemented neural proliferation media with the addition on 200ng/ml SHH for 24-48 hours.

If the culture is more mixed with pockets of neural stem cells and pockets of tertiary neural rosettes, these would be collected in HBSS as above. The tertiary neural rosettes are grown in suspension for 1 day, this allows them to round up and be separated from contaminating cells types which were growing around them. After 1 day in suspension the neural rosettes are filtered through a 40μM cell strainer, treated with Accutase for 10 minutes at 37°C, then titrated to a single cell suspension, diluted with media and spun and counted as above, then plated at approx 3.5 $x10^6$ cells per 10cm plate. Finally areas of neural stem cells were collected in HBSS and treated as above with Accutase and plated.

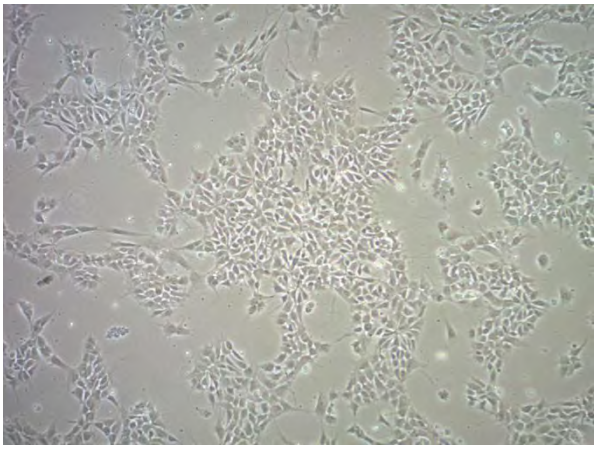

Fig. 5.9 Human neural stem cells ready for neural differentiation.

Differentiation of Neural stem cells to mixed neuronal cultures:

When the single cell cultures of tertiary neural rosettes or neural stem cells are 60-70% confluent differentiation is induced by changing to neural differentiation media (485 ml Neurobasal Media (Invitrogen#21103), 5mls N2 Supplement (Invitrogen#17502-048), 5 ml 1xNEAA(Invitrogen#11140-050) and 5ml Pen/strep (Li XJ et al., 2005). This media has no added growth factors. The cells are allowed to differentiate for 7-10 days and are then harvested for RNA, 3C analysis, slides are fixed for immunocytochemistry. From 4X6 well plates of starting iPS cells we can generate approximately 50 million neurons.

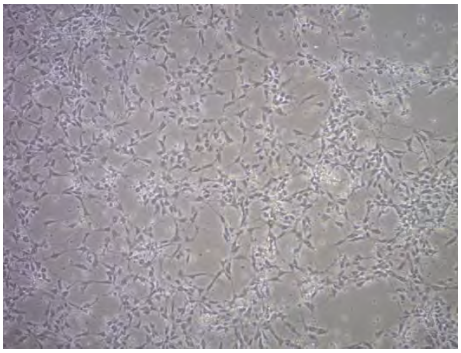

Differentiated neurons at harvest.

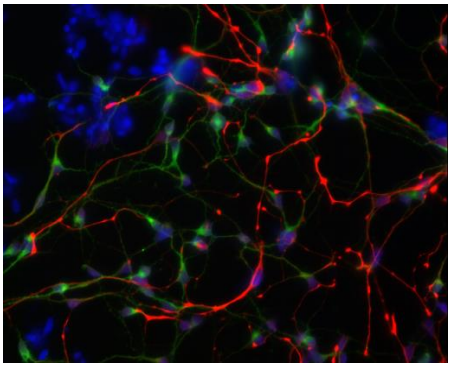

200X MAP2 (green)/Nestin(red)/ DAPI (blue)

Fig. 4.10 Differentiated neurons ready for harvest.

(Above) unstained 50X neuron image. (Below) Green – MAP2 stained neurons, Red – Nestin stained neuronal precursors, Blue – DAPI stained cells.

REFERENCES

Abdolmaleky HM, Cheng KH, Russo A, Smith CL, Faraone SV, Wilcox M, Shafa R, Glatt SJ, Nguyen G, Ponte JF, Thiagalingam S, and Tsuang MT. (2005).
Hypermethylation of the reelin (RELN) promoter in the brain of schizophrenic patients: a preliminary report. Am J Med Genet B Neuropsychiatr Genet 134B: 60-66.

Addington AM, Gornick M, Duckworth J, Sporn A, Gogtay N, Bobb A, Greenstein D, Lenane M, Gochman P, Baker N, Balkissoon R, Vakkalanka RK, Weinberger DR, Rapoport JL, Straub RE. (2005).
GAD1 (2q31.1), which encodes glutamic acid decarboxylase (GAD67), is associated with childhood-onset schizophrenia and cortical gray matter volume loss. Mol Psychiatry 10(6): 581-8.

Akbarian S, Sucher NJ, Bradley D, Tafazzoli A, Trinh D, Hetrick WP, Potkin SG, Sandman CA, Bunney WE Jr, Jones EG. (1996)
Selective alterations in gene expression for NMDA receptor subunits in prefrontal cortex of schizophrenics. The Journal of neuroscience : the official journal of the Society for Neuroscience 16, 19-30

Akbarian S. (2010).
Epigenetics of schizophrenia. Curr Top Behav Neurosci. 4:611-28

Akbarian, S. and H. S. Huang (2006).
Molecular and cellular mechanisms of altered GAD1/GAD67 expression in schizophrenia and related disorders. Brain Res Rev 52(2): 293-304.

Alaminos M, Davalos V, Ropero S, Setien F, Paz MF, Herranz M, Fraga MF, Mora J, Cheung NK, Gerald WL, and Esteller M. (2005)
EMP3, a myelin-related gene located in the critical 19q13.3 region, is epigenetically silenced and exhibits features of a candidate tumor suppressor in glioma and neuroblastoma. Cancer Res 65: 2565-2571.

Asada H, Kawamura Y, Maruyama K, Kume H, Ding RG, Kanbara N, Kuzume H, Sanbo M, Yagi T, Obata K. (1997).
Cleft palate and decreased brain gamma-aminobutyric acid in mice lacking the 67-kDa isoform of glutamic acid decarboxylase. Proc Natl Acad Sci U S A 94(12): 6496-9

Ayalew M, Le-Niculescu H, Levey DF, Jain N, Changala B, Patel SD, Winiger E, Breier A, Shekhar A, Amdur R, Koller D, Nurnberger JI, Corvin A, Geyer M, Tsuang MT, Salomon D, Schork NJ, Fanous AH, O'Donovan MC, Niculescu AB. (2012)
Convergent functional genomics of schizophrenia: from comprehensive understanding to genetic risk prediction. Molecular psychiatry 17, 887-905

Bártová E, Krejcí J, Harnicarová A, Galiová G, Kozubek S. (2008).
Histone modifications and nuclear architecture: a review. J Histochem Cytochem. 56(8):711-21.

Benes FM, Berretta S. (2001).
GABAergic interneurons: implications for understanding schizophrenia and bipolar disorder. Neuropsychopharmacology. Jul;25(1):1-27.Review.

Benes FM. (1997).
The role of stress and dopamine-GABA interactions in the vulnerability for schizophrenia. J Psychiatr Res. Mar-Apr;31(2):257-75.Review.

Bharadwaj R, Peter C, Akbarian S. (2012).
The Mind and its Nucleosomes – Chromatin (dys) regulation in major psychiatric diseases. Elsevier Publishing: Epigenetics of the Nervous System, D. Sweatt .

Brown AS, and Derkits EJ. Prenatal infection and schizophrenia: a review of epidemiologic and translational studies. (2010).
Am J Psychiatry 167: 261-280.

Canitano R, and Scandurra V (2011).
Psychopharmacology in autism: an update. Prog Neuropsychopharmacol Biol Psychiatry 35: 18-28.

Cedar H, Bergman Y. (2009).
Linking DNA methylation and histone modification: patterns and paradigms. Nat Rev GenetMay;10(5):295-304.

Chen CY, Morris Q, Mitchell JA. (2012).
Enhancer identification in mouse embryonic stem cells using integrative modeling of chromatin and genomic features. BMC Genomics. Apr 26;13:152

Cheung I, Shulha HP, Jiang Y, Matevossian A, Wang J, Weng Z, Akbarian S. (2010)
Developmental regulation and individual differences of neuronal H3K4me3 epigenomes in the prefrontal cortex. Proceedings of the National Academy of Sciences of the United States of America 107, 8824-8829

Cichon S, Craddock N, Daly M, Faraone SV, Gejman PV, Kelsoe J, Lehner T, Levinson DF, Moran A, Sklar P, and Sullivan PF (2009). Genomewide association studies: history, rationale, and prospects for psychiatric disorders. Am J Psychiatry 166: 540-556.

Clark SJ, Harrison J, Paul CL, Frommer M.(1994).
High sensitivity mapping of methylated cytosines. Nucleic Acids Res. Aug11;22(15):2990-7.

Colantuoni C, Lipska BK, Ye T, Hyde TM, Tao R, Leek JT, Colantuoni EA, Elkahloun AG, Herman MM, Weinberger DR, and Kleinman JE.(2011).
Temporal dynamics and genetic control of transcription in the human prefrontal cortex. Nature 478: 519-523.

Costa E, Davis JM, Dong E, Grayson DR, Guidotti A, Tremolizzo L, and Veldic M. (2004).
A GABAergic cortical deficit dominates schizophrenia pathophysiology. Crit Rev Neurobiol 16: 1-23.

Covington HE 3rd, Lobo MK, Maze I, Vialou V, Hyman JM, Zaman S, LaPlant Q, Mouzon E, Ghose S, Tamminga CA, Neve RL, Deisseroth K, Nestler EJ. (2010) Antidepressant effect of optogenetic stimulation of the medial prefrontal cortex. The Journal of neuroscience : the official journal of the Society for Neuroscience 30, 16082-16090

Daskalakis ZJ, Fitzgerald PB, Christensen BK. (2007).
The role of cortical inhibition in the pathophysiology and treatment of schizophrenia. Brain Res Rev. Dec;56(2):427-42.Review.

Dekker J. (2008).
Gene regulation in the third dimension. Science. Mar 28;319(5871):1793-4.

Dhar, S.S. & Wong-Riley, M.T. (2010)
Chromosome conformation capture of transcriptional interactions between cytochrome c oxidase genes and genes of glutamatergic synaptic transmission in neurons. Journal of neurochemistry 115, 676-683

Dhara SK, Hasneen K, Machacek DW, Boyd NL, Rao RR, Stice SL. (2008).
Human neural progenitor cells derived from embryonic stem cells in feeder-free cultures. Differentiation. May;76(5):454-64.

Dong E, Guidotti A, Grayson DR, Costa E. (2007).
Histone hyperacetylation induces demethylation of reelin and 67-kDa glutamic acid decarboxylase promoters. Proc Natl Acad Sci U S A. 2007 Mar 13;104(11):4676-81.

Dostie J, Dekker J. (2007).
Mapping networks of physical interactions between genomic elements using 5C technology. Nat Protoc. (4):988-1002.

Duan Z, Andronescu M, Schutz K, McIlwain S, Kim YJ, Lee C, Shendure J, Fields S, Blau CA, Noble WS. (2010).
A three-dimensional model of the yeast genome. Nature, 465(7296):363-7.

Esclapez M, Tillakaratne NJ, Kaufman DL, Tobin AJ, Houser CR. (1994).
Comparative localization of two forms of glutamic acid decarboxylase and their mRNAs

in rat brain supports the concept of functional differences between the forms. J Neurosci 14(3 Pt 2): 1834-55.

Ferraiuolo MA, Rousseau M, Miyamoto C, Shenker S, Wang XQ, Nadler M, Blanchette M, Dostie J. (2010)
The three-dimensional architecture of Hox cluster silencing. Nucleic acids research 38, 7472-7484

Fung, S.J., Webster, M.J., Sivagnanasundaram, S., Duncan, C., Elashoff, M., and Weickert, C.S. (2010).
Expression of interneuron markers in the dorsolateral prefrontal cortex of the developing human and in schizophrenia. The American journal of psychiatry 167, 1479-1488

Buttice, G., Quinones, S., and M Kurkinen (1991)
The AP-1 site is required for basal expression but is not necessary for TPA-response of the human stromelysin gene. Nucleic Acids Res. July 11; 19(13): 3723–3731.

Gao, L., Sun, C., Qiu, H. L., Liu, H., Shao, H. J., Wang, J., Li, W. X. (2004).
Cloning and characterization of a novel human zinc finger gene, hKid3, from a C(2)H(2)-ZNF enriched human embryonic cDNA library. Biochem Biophys Res Commun 325 (4) 1145-52.

Gaszner, M. & Felsenfeld, G.
Insulators: exploiting transcriptional and epigenetic mechanisms. Nat Rev Genet 7, 703-713 (2006)

Gavin DP, Akbarian S. (2012).
Epigenetic and post-transcriptional dysregulation of gene expression in schizophrenia and related disease. Neurobiol Dis. 2012 May;46(2):255-62.

Ge S, Goh EL, Sailor KA, Kitabatake Y, Ming GL, Song H. (2006).
GABA regulates synaptic integration of newly generated neurons in the adult brain. Nature 439(7076): 589-93.

Gertz J, Varley KE, Reddy TE, Bowling KM, Pauli F, Parker SL, Kucera KS, Willard HF, and Myers RM. (2011).
Analysis of DNA methylation in a three-generation family reveals widespread genetic influence on epigenetic regulation. PLoS Genet 7: e1002228.

Gheldof N, Smith EM, Tabuchi TM, Koch CM, Dunham I, Stamatoyannopoulos JA, Dekker J. (2010).
Cell-type-specific long-range looping interactions identify distant regulatory elements of the CFTR gene. Nucleic Acids Res. Jul;38(13):4325-36.

Goff DC, Evins AE. (1998).
Negative symptoms in schizophrenia: neurobiological models and treatment response. Harv Rev Psychiatry. Jul-Aug;6(2):59-77.Review.

Gupta S, Kim SY, Artis S, Molfese DL, Schumacher A, Sweatt JD, Paylor RE, Lubin FD. (2010).
Histone methylation regulates memory formation. J Neurosci. Mar 10;30(10):3589-99.

Hallmayer J, Cleveland S, Torres A, Phillips J, Cohen B, Torigoe T, Miller J, Fedele A, Collins J, Smith K, Lotspeich L, Croen LA, Ozonoff S, Lajonchere C, Grether JK, and Risch N. (2011)
Genetic heritability and shared environmental factors among twin pairs with autism. *Arch Gen Psychiatry* 68: 1095-1102.

Habl G, Schmitt A, Zink M, von Wilmsdorff M, Yeganeh-Doost P, Jatzko A, Schneider-Axmann T, Bauer M, Falkai P. (2012).
Decreased reelin expression in the left prefrontal cortex (BA9) in chronic schizophrenia patients. Neuropsychobiology. 66(1):57-62.

Heckers, S., Stone, D., Walsh, J., Shick, J., Koul, P., Benes, F.M., (2002).
Differential hippocampal expression of glutamic acid decarboxylase 65 and 67 messenger RNA in bipolar disorder and schizophrenia. Arch. Gen. Psychiatry 59, 521–529.

Houston I, Peter CJ, Mitchell A, Straubhaar J, Rogaev E, Akbarian S. (2013)
Epigenetics in the human brain. Neuropsychopharmacology : official publication of the American College of Neuropsychopharmacology 38, 183-197

Huang HS, Akbarian S. (2007).
GAD1 mRNA expression and DNA methylation in prefrontal cortex of subjects with schizophrenia. PLoS One. Aug 29;2(8):e809.

Huang HS, Matevossian A, Jiang Y, Akbarian S. (2006)
Chromatin immunoprecipitation in postmortem brain. J Neurosci Methods. Sep 30;156(1-2):284-92.

Hyde, T.M., Lipska, B.K., Ali, T., Mathew, S.V., Law, A.J., Metitiri, O.E., Straub, R.E., Ye, T., Colantuoni, C., Herman, M.M., et al. (2011).
Expression of GABA signaling molecules KCC2, NKCC1, and GAD1 in cortical development and schizophrenia. The Journal of neuroscience : the official journal of the Society for Neuroscience 31, 11088-11095.

International Human Genome Sequencing Consortium (2004).
"Finishing the euchromatic sequence of the human genome.". *Nature* **431** (7011): 931–45.

Ibrahim HM, and Tamminga CA (2010)

Schizophrenia: Treatment Targets Beyond Monoamine Systems. Annu Rev Pharmacol Toxicol.

Iwamoto K, Bundo M, Yamada K, Takao H, Iwayama-Shigeno Y, Yoshikawa T, and Kato T. (2005).
DNA methylation status of SOX10 correlates with its downregulation and oligodendrocyte dysfunction in schizophrenia. J Neurosci 25: 5376-5381.
Jacobs KM, Donoghue JP (1991).
Reshaping the cortical motor map by unmasking latent intracortical connections. Science. Feb 22;251(4996):944-7.

Jarskog LF, Miyamoto S, and Lieberman JA (2007). Schizophrenia: new pathological insights and therapies. *Annu Rev Med* 58: 49-61.

Jiang Y, Jakovcevski M, Bharadwaj R, Connor C, Schroeder FA, Lin CL, Straubhaar J, Martin G, Akbarian S. (2010).
Setdb1 histone methyltransferase regulates mood-related behaviors and expression of the NMDA receptor subunit NR2B. J Neurosci. May 26;30(21):7152-67.

Jiang Y, Langley B, Lubin FD, Renthal W, Wood MA, Yasui DH, Kumar A, Nestler EJ, Akbarian S, Beckel-Mitchener AC. (2008).
Epigenetics in the nervous system. J Neurosci. 28(46):11753

Kagey MH, Newman JJ, Bilodeau S, Zhan Y, Orlando DA, van Berkum NL, Ebmeier CC, Goossens J, Rahl PB, Levine SS, Taatjes DJ, Dekker J, Young RA. (2010)
Mediator and cohesin connect gene expression and chromatin architecture. Nature 467, 430-435

Katarova Z, Mugnaini E, Sekerková G, Mann JR, Aszódi A, Bösze Z, Greenspan R, Szabó G. (1998).
Regulation of cell-type specific expression of lacZ by the 5'-flanking region of mouse GAD67 gene in the central nervous system of transgenic mice. Eur J Neurosci 10(3): 989-99

Kobayashi T, Ebihara S, Ishii K, Kobayashi T, Nishijima M, Endo S, Takaku A, Sakagami H, Kondo H, Tashiro F, Miyazaki J, Obata K, Tamura S, Yanagawa Y. (2003).
Structural and functional characterization of mouse glutamate decarboxylase 67 gene promoter. Biochim Biophys Acta 1628(3): 156-68.

Kristiansen, L.V., Bakir, B., Haroutunian, V. & Meador-Woodruff, J.H. (2010)
Expression of the NR2B-NMDA receptor trafficking complex in prefrontal cortex from a group of elderly patients with schizophrenia. Schizophrenia research 119, 198-209

Kristiansen, L.V., Beneyto, M., Haroutunian, V. & Meador-Woodruff, J.H. (2006)
Changes in NMDA receptor subunits and interacting PSD proteins in dorsolateral

prefrontal and anterior cingulate cortex indicate abnormal regional expression in schizophrenia. Molecular psychiatry 11, 737-747, 705

Kuo, Min-Hao; Allis, C. David. . (1999).
In Vivo Cross-Linking and Immunoprecipitation for Studying Dynamic Protein:DNA Associations in a Chromatin Environment. Methods vol. 19 issue 3 November, p. 425-433

Lewis, D. A. (2000).
GABAergic local circuit neurons and prefrontal cortical dysfunction in schizophrenia. Brain Res Brain Res Rev 31(2-3): 270-6

Li G, Fullwood MJ, Xu H, Mulawadi FH, Velkov S, Vega V, Ariyaratne PN, Mohamed YB, Ooi HS, Tennakoon C, Wei CL, Ruan Y, Sung WK. (2010).
ChIA-PET tool for comprehensive chromatin interaction analysis with paired-end tag sequencing. Genome Biol. 11(2):R22.

Li XJ, Du ZW, Zarnowska ED, Pankratz M, Hansen LO, Pearce RA, Zhang SC. (2005).
Specification of motoneurons from human embryonic stem cells. Nat Biotechnol. Feb;23(2):215-21.

Lundorf MD, Buttenschøn HN, Foldager L, Blackwood DH, Muir WJ, Murray V, Pelosi AJ, Kruse TA, Ewald H, Mors O. (2005).
Mutational screening and association study of glutamate decarboxylase 1 as a candidate susceptibility gene for bipolar affective disorder and schizophrenia. Am J Med Genet B Neuropsychiatr GenetMay 5;135B(1):94-101.

Marenco S, Savostyanova AA, van der Veen JW, Geramita M, Stern A, Barnett AS, Kolachana B, Radulescu E, Zhang F, Callicott JH, Straub RE, Shen J, and Weinberger DR. (2010)
Genetic modulation of GABA levels in the anterior cingulate cortex by GAD1 and COMT. Neuropsychopharmacology 35: 1708-1717.

Martucci L, Wong AH, De Luca V, Likhodi O, Wong GW, King N, Kennedy JL. (2006).
N-methyl-D-aspartate receptor NR2B subunit gene GRIN2B in schizophrenia and bipolar disorder: Polymorphisms and mRNA levels. Schizophr Res. Jun; 84(2-3):214-21.

Maston, G.A., Landt, S.G., Snyder, M. & Green, M.R.(2012)
Characterization of enhancer function from genome-wide analyses. Annual review of genomics and human genetics 13, 29-57

Melgar MF, Collins FS, Sethupathy P (2011)
Discovery of active enhancers through bidirectional expression of short transcripts. Genome Biol. 2011 Nov 14;12 (11):R113

Middleton FA, Strick PL. (2002).

Basal-ganglia 'projections' to the prefrontal cortex of the primate. Cereb Cortex. (9):926-35.

Miele A, Dekker J. (2009).
Mapping cis- and trans- chromatin interaction networks using chromosome conformation capture (3C). Methods Mol Biol.464:105-21.

Miele, A., Gheldof, N., Tabuchi, T.M., Dostie, J. & Dekker, J. (2006)
Mapping chromatin interactions by chromosome conformation capture. Current protocols in molecular biology / edited by Frederick M. Ausubel ... [et al.] Chapter 21, Unit 21 11

Mill J, Tang T, Kaminsky Z, Khare T, Yazdanpanah S, Bouchard L, Jia P, Assadzadeh A, Flanagan J, Schumacher A, Wang SC, and Petronis A. (2008).
Epigenomic profiling reveals DNA-methylation changes associated with major psychosis. Am J Hum Genet 82: 696-711.

Mukai J, Dhilla A, Drew LJ, Stark KL, Cao L, MacDermott AB, Karayiorgou M, Gogos JA (2008)
Palmitoylation-dependent neurodevelopmental deficits in a mouse model of 22q11 microdeletion. Nat Neurosci 11:1302–1310.

Münzel M, Globisch D, Brückl T, Wagner M, Welzmiller V, Michalakis S, Müller M, Biel M, Carell T. (2010).
Quantification of the sixth DNA base hydroxymethylcytosine in the brain. Angew Chem Int Ed Engl. Jul 19;49(31):5375-7.

Need AC, Attix DK, McEvoy JM, Cirulli ET, Linney KL, Hunt P, Ge D, Heinzen EL, Maia JM, Shianna KV, Weale ME, Cherkas LF, Clement G, Spector TD, Gibson G, Goldstein DB.(2009)
A genome-wide study of common SNPs and CNVs in cognitive performance in the CANTAB. Hum Mol Genet. Dec 1;18(23):4650-61.

O'Roak BJ, Vives L, Fu W, Egertson JD, Stanaway IB, Phelps IG, Carvill G, Kumar A, Lee C, Ankenman K, Munson J, Hiatt JB, Turner EH, Levy R, O'Day DR, Krumm N, Coe BP, Martin BK, Borenstein E, Nickerson DA, Mefford HC, Doherty D, Akey JM, Bernier R, Eichler EE, Shendure J. (2012)
Multiplex targeted sequencing identifies recurrently mutated genes in autism spectrum disorders. Science 338, 1619-1622

Ong CT, Corces VG. (2011)
Enhancer function: new insights into the regulation of tissue-specific gene expression. Nat Rev Genet. 2011 Apr;12(4):283-93.

Represa, A. and Y. Ben-Ari (2005).
Trophic actions of GABA on neuronal development. Trends Neurosci 28(6): 278-83.

Sanyal, A., Bau, D., Marti-Renom, M.A. & Dekker, J.
Chromatin globules: a common motif of higher order chromosome structure? Curr Opin Cell Biol 23, 325-331 (2011).

Schmidt, M.J., and Mirnics, K. (2012).
Modeling interneuron dysfunction in schizophrenia. Developmental neuroscience 34, 152-158

Schultz DC, Ayyanathan K, Negorev D, Maul GG, Rauscher FJ 3rd. (2002).
SETDB1: a novel KAP-1-associated histone H3, lysine 9-specific methyltransferase that contributes to HP1-mediated silencing of euchromatic genes by KRAB zinc-finger proteins. Genes Dev. Apr 15;16(8):919-32.

Sebat J, Levy DL, and McCarthy SE.(2009).
Rare structural variants in schizophrenia: one disorder, multiple mutations; one mutation, multiple disorders. Trends Genet 25: 528-535.

Sharma RP, Grayson DR, Gavin DP. (2008).
Histone deactylase 1 expression is increased in the prefrontal cortex of schizophrenia subjects: analysis of the National Brain Databank microarray collection. Schizophr Res. Jan;98(1-3):111-7.

Shulha HP, Crisci JL, Reshetov D, Tushir JS, Cheung I, Bharadwaj R, Chou HJ, Houston IB, Peter CJ, Mitchell AC, Yao WD, Myers RH, Chen JF, Preuss TM, Rogaev EI, Jensen JD, Weng Z, Akbarian S (2012)
Human-specific histone methylation signatures at transcription start sites in prefrontal neurons. PLoS biology 10, e1001427

Silbersweig DA, Stern E, Frith C, Cahill C, Holmes A, Grootoonk S, Seaward J, McKenna P, Chua SE, Schnorr L, et al. (1995).
A functional neuroanatomy of hallucinations in schizophrenia.
Nature. 378(6553):176-9.

Straub RE, Lipska BK, Egan MF, Goldberg TE, Callicott JH, Mayhew MB, Vakkalanka RK, Kolachana BS, Kleinman JE, Weinberger DR. (2007).
Allelic variation in GAD1 (GAD67) is associated with schizophrenia and influences cortical function and gene expression. Mol Psychiatry 12(9): 854-69

Talkowski ME, Rosenfeld JA, Blumenthal I, Pillalamarri V, Chiang C, Heilbut A, Ernst C, Hanscom C, Rossin E, Lindgren AM, Pereira S, Ruderfer D, Kirby A, Ripke S, Harris DJ, Lee JH, Ha K, Kim HG, Solomon BD, Gropman AL, Lucente D, Sims K, Ohsumi TK, Borowsky ML, Loranger S, Quade B, Lage K, Miles J, Wu BL, Shen Y, Neale B, Shaffer LG, Daly MJ, Morton CC, Gusella JF. (2012)
Sequencing chromosomal abnormalities reveals neurodevelopmental loci that confer risk across diagnostic boundaries. Cell 149, 525-537

Tang, B., Dean, B., and Thomas, E.A. (2011).
Disease- and age-related changes in histone acetylation at gene promoters in psychiatric disorders. Translational psychiatry 1, e64

Thorne AW, Myers FA, Hebbes TR. (2004).
Native chromatin immunoprecipitation. Methods Mol Biol.287:21-44.

Tozuka Y, Fukuda S, Namba T, Seki T, Hisatsune T (2005).
GABAergic excitation promotes neuronal differentiation in adult hippocampal progenitor cells." Neuron 47(6): 803-15.

Vakoc CR, Letting DL, Gheldof N, Sawado T, Bender MA, Groudine M, Weiss MJ, Dekker J, Blobel GA. (2005).
Proximity among distant regulatory elements at the beta-globin locus requires GATA-1 and FOG-1. Mol Cell.Feb 4;17(3):453-62.

Volk, D.W., Matsubara, T., Li, S., Sengupta, E.J., Georgiev, D., Minabe, Y., Sampson, A., Hashimoto, T., and Lewis, D.A. (2012).
Deficits in Transcriptional Regulators of Cortical Parvalbumin Neurons in Schizophrenia. The American journal of psychiatry.

Weinberger, DR. (1987).
Implications of normal brain development for the pathogenesis of schizophrenia. Arch Gen Psychiatry 44:660-669.

Weiss LA. Autism genetics: emerging data from genome-wide copy-number and single nucleotide polymorphism scans. (2009).
Expert Rev Mol Diagn 9: 795-803.

Wood, A.J., Severson, A.F. & Meyer, B.J. (2010)
Condensin and cohesin complexity: the expanding repertoire of functions. Nat Rev Genet 11, 391-404

Zhang TY, Hellstrom IC, Bagot RC, Wen X, Diorio J, and Meaney MJ. (2010).
Maternal care and DNA methylation of a glutamic acid decarboxylase 1 promoter in rat hippocampus. J Neurosci 30: 13130-13137.

Zhu J, Adli M, Zou JY, Verstappen G, Coyne M, Zhang X, Durham T, Miri M, Deshpande V, De Jager PL, Bennett DA, Houmard JA, Muoio DM, Onder TT, Camahort R, Cowan CA, Meissner A, Epstein CB, Shoresh N, Bernstein BE. (2013).
Genome-wide Chromatin State Transitions Associated with Developmental and Environmental Cues. Cell